Understanding the Influence of the Atmosphere and Land Surface Conditions on Flood Risk using Probabilistic Hydrology in the Context of Mechanistic Hydrologic Models

A Dissertation

Presented to the Faculty of the Graduate School

of Cornell University

In Partial Fulfillment of the Requirements for the Degree of

Doctor of Philosophy

by

James O'Neil Knighton

May, 2019

UNDERSTANDING THE INFLUENCE OF THE ATOSPHERE AND LAND SURFACE ON FLOOD RISK USING PROBABILISTIC HYDROLOGY IN THE CONTEXT OF MECHANSTIC HYDROLOGIC MODELS

James O'Neil Knighton

Cornell University 2019

The emergence of large-scale hydrologic datasets, data analytic techniques, and mechanistic hydrologic models has supported the advancement of flood risk analysis. Traditionally, the study of hydrologic extremes has centered on observations made within the stream channel. Recent research has highlighted the importance of understanding the aspects of the atmosphere, land surface, and river network that impart their unique fingerprint on floods. In this dissertation I first review the critical aspects of sub-daily precipitation in the context of a stochastic weather generator. Next, we consider the direction of influence of the land surface on hydrologic extremes in conjunction with changes to climatic forcing. Finally, we propose a framework for flood risk analysis from the perspective of flood inducing meteorological events.

BIOGRAPHICAL SKETCH

James Knighton is a PhD student interested in using stochastic approaches applied to physically-based hydrologic models to study a diverse range of environmental issues. James' research is currently focused on riverine nutrient and sediment load estimation, reframing riverine flooding risk from an atmospheric perspective, and describing unsaturated zone dynamics through simulation of stable water isotopes. James previously worked as a professional engineer studying coastal flood risks posed for US nuclear facilities and urban flooding risk in Philadelphia, PA.

If you’re reading this, it’s for you.

ACKNOWLEDGMENTS

I would like to acknowledge the contributions of Dr. Todd Walter, Dr. Scott Steinschneider, and Dr. Arthur DeGaetano for contributing to each of these chapters.

TABLE OF CONTENTS

LIST OF FIGURES

LIST OF TABLES

PREFACE

Extreme precipitation and associated riverine discharge extremes have major social and economic impacts across the US and globally. A review of US insurance claims exceeding one billion dollars from 1980 – 2011 shows that the most severe economic losses are dominated by large-scale storm events that induce riverine flooding [NCDC, 2018]. Advances in flood risk analysis and research can yield opportunities for the development of more resilient communities. Accurate appraisals of hydrologic extremes is conditional on our ability to understand of influence of atmospheric forcing and the role of the catchment in translating atmospheric extremes into discharge.

Hydrologic forecasts have long served our need for an understanding of risks of hydrologic extremes (i.e. floods, droughts, ecological disturbance, and degraded water quality events) and for developing a working understanding of future conditions. Mechanistic models used in concert with stochastic hydrometeorology have proven useful for constraining hydrometeorological forecasts such as refined flooding risks, refined downscaling of GCM predictions, and predicting erosion dynamics, among many other topics. The advent of mechanistic hydrologic models in parallel with data analytic techniques such as Bayesian approaches for numerical model calibration, model averaging techniques (e.g. Bayesian Model Averaging), and data assimilation (e.g. Ensemble Kalman Filtering) broaden the reach of mechanistic models to data-limited problems. The development of distributed hydrometeorological datasets which facilitate distributed hydrometeorological predictions (e.g. general circulation models [GCMs]) has further encouraged researchers to merge the divergent classic branches of hydrology with

evolving data-analytic approaches to develop more robust hydrologic insights over larger spatial and temporal scales.

Mechanistic approaches attempt to describe hydrology from a physical perspective. Physically-based and empirical relationships both leverage our knowledge of physics (with varied degrees of complexity) to constrain hydrologic predictions which may be challenging to observe. While theoretically sound, mechanistic model applications tend to outpace their own data requirements for model forcing and parameterization. Deterministic approaches and overly-trained mechanistic models may neglect our true uncertainty in a projection, yielding potentially misleading or overly-confident results. Applications of mechanistic hydrologic models therefore benefit by incorporating emerging stochastic techniques to properly leverage the physical underpinnings of these models.

Identification of the appropriate model structure or simplifying assumptions is often a difficult and subjective choice. Model averaging techniques such as BMA in particular may provide the most robust path towards the development of meaningful hydrologic predictions in the face of structural uncertainty of mechanistic models and down-scaled climate products. The emerging reality of climate induced changes to risk profiles has lead researchers to focus on issues with transferability of mechanistic hydrologic models and model averaging techniques with respect to hydrologic forecasts within a changing climate.

The research presented in this dissertation centers on utilizing stochastic approaches within a physically-based hydrologic modeling framework to constrain water resources predictions, focusing on hydrologic extremes. This forward modeling approach allows us to incorporate knowledge of physical processes observed at convenient scales (e.g. soil infiltration rates) to inform our knowledge of infrequent events that are challenging to observe (e.g. floods) by constraining these predictions with a mechanistic model. In this research I have attempted to demonstrate how shifting hydrologic state variables and atmospheric conditions respectively could result in changes to the flood regime of a riverine system. It is generally accepted that global climate change will result in thermodynamic intensification of the hydrologic cycle, which will increase the frequency and magnitude of precipitation extremes. Somewhat more uncertain though is the impact that climate change will have on extremes related to shifting atmospheric dynamics, i.e., how the atmospheric circulation and storm tracks will change under warming and the implications for the frequency of extreme storms in different regions. Further, the response of the land surface to changes in the atmospheric boundary may result in substantial modification of hydrologic extremes.

In this dissertation the role of atmospheric forcing and land surface feedbacks are examined in the context of hydrologic extremes:

Chapter 1: Recent advances have been made to modernize estimates of probable precipitation scenarios; however, researchers and engineers often continue to assume that rainfall events can be described by a small set of event statistics, typically average

intensity and event duration. Given the easy availability of precipitation data and advances in desk-top computational tools, we suggest that it is time to rethink the "design storm" concept. Design storms should include more holistic characteristics of flood-inducing rain events, which, in addition to describing specific hydrologic responses, may also be watershed or regionally specific. We present a sensitivity analysis of nine precipitation event statistics from observed precipitation events within a 60 year record for Tompkins County, NY USA. We perform a two-sample Kolmogorov-Smirnov test to objectively identify precipitation event statistics of importance for two related hydrologic responses: (1) peak outflow from the Six Mile Creek watershed and (2) peak depth within the reservoir behind the Six Mile Creek Dam. We identify the total precipitation depth, peak hourly intensity, average intensity, event duration, interevent duration, and several statistics defining the temporal distribution of precipitation events to be important rainfall statistics to consider for predicting the watershed flood responses. We found that the two hydrologic responses had different sets of statistically significant parameters. We demonstrate through a stochastic precipitation generation analysis the effects of starting from a constrained parameter set (intensity and duration) when predicting hydrologic responses as opposed to utilizing an expanded suite of rainfall statistics. In particular, we note that the reduced precipitation parameter set may underestimate the probability of high stream flows and therefore underestimate flood hazard.

Chapter 2: Watershed flooding is a function of meteorological and hydrologic catchment conditions. Climate change is anticipated to affect air temperature and precipitation patterns such as altered total precipitation, increased intensity, and shorter event durations in the northeast USA. While significant work has been done to estimate future

meteorological conditions, much is currently unknown about future changes to distributions of hydrologic state variables. We perform high resolution hydrologic simulations of Fall Creek (Tompkins County, NY USA), a small temperate watershed (324 km2) with seasonal snowmelt, to evaluate future climate change may impacts on flood hydrology. We isolate the effects of hydrologic state and environmental variables on river flood stage, and demonstrate the importance of groundwater elevation, unsaturated soil moisture, snowpack and air temperature. We demonstrate that the temporal persistence of these hydrologic state variables allows for an influence on watershed flood hydrology for up to twenty days. Finally we simulate six hypothetical climate change forcing scenarios to estimate the influence of catchment conditions on the watershed runoff response. We simulate the possibility of drier summers and wetter springs with a reduced winter snowpack in the Northeast USA. These hydrologic changes influence flood discharge in the opposite direction as climate effects due to a reduced snowpack accumulation and melt time. Strong hydrologic state influence on flood discharge may be most attributable to increased air temperature and decreased precipitation. Hydrologic state variables may change both the location and shape of seasonal flood discharge distributions despite expected consistency in the shape of precipitation statistic distributions.

Chapter 3: There is a chronic disconnection among purely probabilistic flood frequency analysis of flood hazards, flood risks, and hydrological flood mechanisms, which hamper our ability to assess future flood impacts. We present a vulnerability-based approach to estimating riverine flood risk that accommodates a more direct linkage between decision-

relevant metrics of risk and the dominant mechanisms that cause riverine flooding. We adapt the conventional peaks-over-threshold (POT) framework to be used with extreme precipitation from different climate processes and rainfall-runoff based model output. We quantify the probability that at least one adverse hydrologic threshold, potentially defined by stakeholders, will be exceeded within the next N years. This approach allows us to consider flood risk as the summation of risk from separate atmospheric mechanisms, and supports a more direct mapping between hazards and societal outcomes. We perform this analysis within a bottom-up framework to consider the relevance and consequences of information, with varying levels of credibility, on changes to atmospheric patterns driving extreme precipitation events. We demonstrate our proposed approach using a case study for Fall Creek in Ithaca, NY, USA, where we estimate the risk of stakeholder-defined flood metrics from three dominant mechanisms: summer convection, tropical cyclones, and spring rain and snowmelt. Using downscaled climate projections, we projected how flood risk associated with a subset of mechanisms may change in the future, and the resultant shift to annual flood risk. The flood risk approach we propose can provide powerful new insights into future flood threats.

CHAPTER 1

CRITICAL RAINFALL STATISTICS FOR PREDICTING WATERSHED FLOOD RESPONSES: RETHINKING THE DESIGN STORM CONCEPT

1. Introduction

Riverine flood hazard and risk analysis generally relies on estimates of precipitation and the land surface runoff response to precipitation. A critical question facing hydrologists, especially hydrological engineers, is how to best describe probable precipitation events for decision making, analysis and input into hydrologic models. Rainfall event statistics (e.g. depth, duration, intensity) have proven to be a useful tools for simplifying our characterization of precipitation events. For example, Wu et al. (2015) propose a flash flood warning system based on real time analysis of several precipitation event statistics that are related to flooding potential. Berg et a.l (2013), Mirhosseini et al. (2013), Muschinski and Katz (2013) and Madsen (2014) among others have used precipitation event statistics to demonstrate that our climate is non-stationary with respect to the frequency of high intensity storms. While recent advances have been made to modernize estimates of probable future precipitation based on event statistics (e.g. Huard et al., 2009; Genest and Favre, 2007; Vernieuwe et al., 2015), it is still common practice to describe a precipitation event with two or three event statistics, often referred to as a "design storm. " This is especially common in hydrologic engineering to estimate a runoff flow-rate or volume for some specified frequency of occurrence (return period). However, the design storm concept is based on some possible problematic assumptions.

In its broadest sense, a design storm is an artificial hyetograph developed for use in engineering design. The standard formulation for a design storm is a reduction of precipitation to a bivariate distribution of intensity and duration defined for various

exceedance thresholds, commonly presented as Intensity, Duration, Frequency (IDF) curves. The temporal distribution of precipitation is sometimes included to characterize design storms, especially for long-duration storms. The Natural Resources Conservation Service (NRCS) 24-hour hyetographs (USDA-NRCS 1986) and the more flexible NOAA Atlas 14 temporal distributions of precipitation (NOAA, 2015a) are two commonly used for distribution a design storm over its duration. The NOAA Atlas 14 also provides IDF information and is a widely used to construct design storms in the USA. For a review of the development and hydrologic applications of the design storm approach see Watt and Massalak (2013).

The design storm approach has well documented shortcomings in characterizing complex interactions within hydraulic and hydrologic systems (e.g. Guo and Adams, 1999; Wang et al., 2010; Grimaldi et al., 2012; Rogger et al., 2012; Watt and Massalak, 2013). The event statistics used to describe the classic design storm (IDF) may not fully describe precipitation responses of more complicated systems. For example, a contributing watershed that generates runoff can act as a reservoir with some storage capacity and a non-linear recovery rate. The design storm concept does not properly inform us on how the non-linear retention of rainfall resulting from watershed storage affects watershed outflow. The dynamically varying hydrologic state of watersheds must be considered when translating precipitation return periods into system response return periods (Shaw and Walter, 2009; Camici et al., 2011; Pathiraja et al., 2012; Rogger et al., 2012; Chapi et al., 2015). Watershed surface depression storage retains some portion of the total precipitation where runoff is only generated once this reservoir is filled. Similarly, the soils of a watershed have some storage capacity and will only contribute runoff when either the soil storage capacity (as a saturation-excess process) or infiltration potential (as an infiltration-excess process) of the watershed are exceeded. Under infiltration-excess conditions, the

infiltration potential of watershed soils varies through time as a function of the current soil moisture content (Rossman, 2010).

We may consider additional complexity by engineering systems to purposefully store and release water, e.g., stormwater retention basins or flood control reservoirs. Guo and Markus (2011) and Salvadori et al. (2011) demonstrate that the computation of return periods for reservoir stress is a complex relationship between flow, volume and the antecedent water level. A relief drain or weir on the system may be overwhelmed by a large inflow rate; however, this only presents a problem when the storage capacity of the system is also exceeded. The memory of the system presents itself in the form of the antecedent water level within the reservoir as well as the water retained within the contributing watershed, essentially behaving as two reservoirs in series.

To overcome the complex interactions described, return periods for responses of a system (i.e. runoff, reservoir water level, etc.) may be estimated through analysis of continuous observed streamflow records. In the absence of streamflow records, continuous precipitation records may be translated into streamflow through continuous simulation with a rainfall-runoff model (for a comparison of these methods see Rogger et al., 2012 and Grimaldi et al., 2012). The primary advantage of this approach is that epistemic uncertainties associated with defining precipitation event statistics are removed. Rather than distilling a precipitation record down to a representative design event, continuous simulations utilize observed precipitation data to force a hydrologic model. A statistical analysis of the resulting flow estimates is then performed. The disadvantage of this approach is that it relies heavily on a sufficiently long precipitation record length to reproduce the full range of aleatory variations or variations originating from a truly stochastic process. For example, Balistrocchi and Bacchi (2011) demonstrate that possible combinations of precipitation event statistics

may be inferred from historical precipitation records within which they have not necessarily occurred.

Stochastic rainfall generation attempts to merge concepts from design storms and continuous simulation to provide a more complete estimate of potential future precipitation patterns (e.g. Wang et al., 2010; Vandenberghe et al., 2010; Balistrocchi and Bacchi, 2011; Haberlandt and Radtke, 2014). Through the stochastic rainfall generation approach one may derive probable combinations of precipitation event statistics and precipitation timing based on observed precipitation patterns. While this approach has evolved significantly with time, it still relies on careful selection of which event statistics should be considered much like in the development of design storms. The selection of important precipitation event statistics shows inconsistency among recent research. Table 1.1 summarizes precipitation event statistics analyzed in several recent publications.

Different combinations of event statistics are considered in the literature (Table 1.1). We think some of these studies may have imposed an artificial restraint on the development of design storms or stochastically generated precipitation records by considering limited sets of possible event statistics to describe precipitation events. For example, Watt and Massalak (2013), Paschalis et al. (2014), Terranova et al. (2015) and Vernieuwe et al. (2015) discuss the importance of considering the temporal distribution of a precipitation event for design hyetograph construction or runoff response, yet not all studies consider the temporal distribution as a random variable (or variables) with a probability of occurrence less than unity. We propose that recent studies may potentially under- or overestimate the aleatory uncertainties of precipitation and system response return frequencies to extreme precipitation due to a constricted set of rainfall statistics. Epistemic uncertainties in rainfall event statistics that were avoided with the continuous simulation approach (e.g. the effects of

interevent timing, antecedent soil conditions, and temporal structure of precipitation events) are potentially reintroduced to the stochastic rainfall approach unnecessarily.

We propose that critical rainfall characteristics for the hydrologic response of interest should be determined objectively before developing design storms or a stochastic precipitation generation methodology. Considering all critical precipitation characteristics when studying responses of a hydrologic system may improve the accuracy of flow-frequency predictions and better define the overall uncertainty in these predictions.

We present a case study of the rainfall-runoff response resulting in simulated flood flows in Six Mile Creek and resulting in flood water storage behind the Six Mile Creek Dam. We first evaluate an expanded suite of rainfall statistics to objectively identify which statistics of a rainfall event are important for both watershed peak runoff and peak depth within the reservoir above the Six Mile Creek Dam, NY USA. We speculate that the relevant rainfall statistics will be dependent on the hydrologic response of interest. Next we utilize these important rainfall event statistics to stochastically generate a large number of artificial rainfall records. We use these synthetic rainfall records to simulate a suite of synthetic continuous streamflow and reservoir water surface elevation time series. We then compare our proposed methodology to a stochastic rainfall generation approach utilizing only the intensity and duration of precipitation events. We will demonstrate that the use of all critical precipitation characteristics in a stochastic precipitation methodology produces a better estimate of watershed outflow and reservoir depth and provides a better understanding of hydrologic response uncertainty.

2. Methodology

2.1 Study Site Description

The contributing area to Six Mile Creek Dam is a 120 km2 forested watershed within Tompkins County, NY USA (Figure 1). The soil profile consists primarily of silt loam and silty clay loam with a shallow confining layer at a depth of approximately 0.5 to 1 m (USDA NRCS, 2015). We estimate the time of concentration (TC) of the watershed to be approximately 4 hours based on methods presented in USDA (1986).

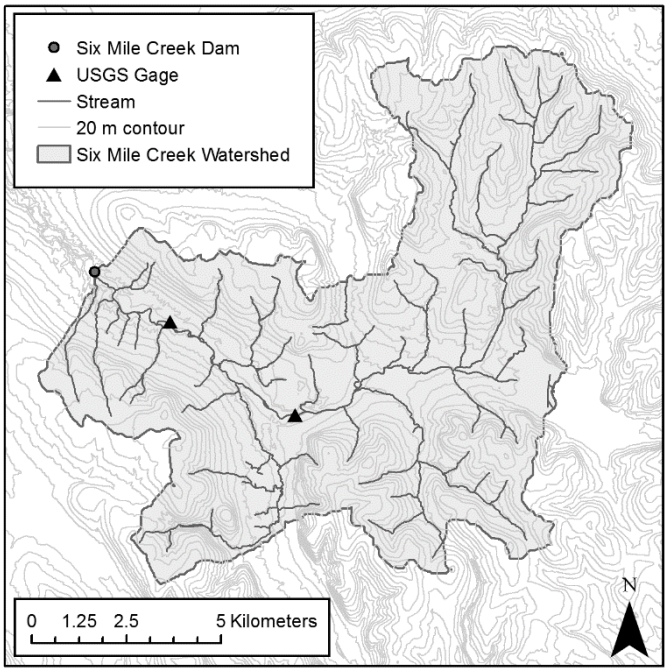

Figure 1 – Six Mile Creek watershed to the Six Mile Creek Dam (USGS, 2015b)

Six Mile Creek Dam (Tompkins County, NY) is a 10.9 m dam downstream of a reservoir that used to be the water supply for Ithaca, NY (Figure 1). The city is interested in dredging and repurposing it for potential flood control. If all the accumulated sediment were removed, it can retain approximately 4.89 × 〖10〗 ^5 m^3 at peak capacity. At the base of the dam is a 1.52 m diameter orifice that we assume can act as a slow release for the purposes of this study. The dam has a 19.8 m

wide spillway at elevation 178 m NAVD-88. Although we could construct a virtual dam, this one offers a realistic situation. We evaluate a proposed future scenario where the slow drain orifice is replaced with a 0.22 m diameter orifice to maximize the use of storage within the reservoir.

2.2 SWMM Subcatchment and Dam Modeling

We simulate all rainfall-runoff and reservoir routing with the Environmental Protection Agency (EPA) Storm Water Management Model (SWMM) model (build 5.0.022) (Rossman, 2010). SWMM integrates a hydrologic rainfall-runoff model with a 1-dimensional dynamic wave flow routing model which may be used to simulate overland and riverine flow. The hydrologic model of SWMM used in this research maintains the water balance through simulation of precipitation, infiltration, evaporation and watershed outflow. Although the governing equations are physically-based, the SWMM watershed is idealized as an inclined rectangle where the velocity of overland flow is solved with Manning's equation. The hydrologic computations of the SWMM model of the Six Mile Creek watershed are carried out at a 5 minute time step. We simulate the Six Mile Creek Dam slow drain as a submerged circular orifice and the emergency spillway as a weir element. The Six Mile Creek reservoir is simulated as a storage node (i.e. no sediment accumulation of scour) using the full dynamic wave approximation of the St. Venant equations. Flood routing is computed at a 5 second time step to meet the Courant-Friedrichs Lewey (CFL) condition of the SWMM model explicit solution technique.

This modeling approach introduces several simplifying assumptions. First, we assume that the runoff response of the land surface behaves as an infiltration-excess process. It has been suggested by Easton et al. (2007) that the Tompkins County, NY USA region may behave with more of a saturation excess response to smaller precipitation events, although here we focus exclusively on extreme events, which are

more likely to involve infiltration excess (Walter et al., 2003). Second, we assume that the entire watershed area may be considered as one uniform subcatchment with mean estimates for soil properties, slope, roughness and representative width. Third, we consider precipitation to occur uniformly across the watershed. We apply the appropriate depth-area scaling relationships to translate the point estimates of precipitation to areal estimates. Fourth, we do not simulate processes related to snow.

We test the impact of these simplifying assumptions on the predictions of peak flows through comparison of the simulated and observed flow return periods. We scale the 20 year flow time series from USGS Gage 04233300 (USGS, 2015) to the flow at the Six Mile Creek Dam based on contributing area (Figure 1). We estimate return periods for observed peak flows by fitting the annual maxima series to a Log-Pearson Type III distribution. We tested the efficacy of our model structure and parameters by comparing the instantaneous peak flow return periods estimated through continuous simulation to those estimated from observed stream flow data as in Haberlandt and Radtke (2014); return periods are calculated using the Weibull plotting position.

In assessing our rainfall runoff model we do not examine return periods above 10 years for three reasons. First a large amount of uncertainty accompanies return period estimates for flows beyond the 10 return period derived from 20 years of stream flow data. This uncertainty in the fit of the theoretical statistical distribution may overwhelm the uncertainty related to model parameter estimates. Second, three large precipitation events occurred in 1962, 1976 and 1981 which were significantly larger than the storms occurring during the stream gage period of record. Third, streamflow estimates are computed from stream depth measurements and a rating curve. At present, the streamflow gage rating curve has only been developed up to a flow of 125 m3/s (approximately the 10 year storm as estimated by the Log-Pearson Type III distribution) through field measurements (USGS, 2015).

2.3 Determination of Important Rainfall Event Statistics

We consider a 60 year record (January 1, 1954 – January 1, 2014) of hourly precipitation depths recorded in Tompkins County, NY USA (Latitude: 42° 27' N Longitude: 76° 27' W) at an elevation of 292 m NAVD88 (NRCC, 2015). Unique precipitation events were identified by applying a minimum precipitation threshold of 0.25 cm and a minimum interevent time of 6 hours. Nine precipitation event statistics are computed: total precipitation depth, peak hourly intensity, average intensity, duration, interevent duration, time to peak (TP), and time to 25%, 50% and 75% volume passing (respectively called T25%, T50%, and T75%). Instead of using Huff curves as in Paschalis et al. (2014) and Vernieuwe et al. (2015), we describe the temporal distribution of loading at discrete intervals and through the TP. We normalize the TP, T25%, T50%, and T75% parameters to exist on the interval from (0, 1) to remove the effects of event duration from the statistics describing the temporal structure of precipitation. These statistics are the accumulation of the statistics that previous researchers have identified as important to large storm runoff events with the addition of peak hourly intensity.

To determine rainfall statistic importance we apply the general sensitivity methodology first described by Spear and Hornberger (1980). We determine two subsets of behavioral precipitation events which resulted in: 1) peak flow above the bankfull discharge of 50 m3/s and 2) an increase in the reservoir depth above 4.6 m (40% full). We compute the Kolmogorov-Smirnov two-sample test-statistic (KS) for each precipitation event statistic (null hypothesis H0: behavioral events are drawn from the same underlying distribution as non-behavioral events; KS close to zero indicate a high degree of significance). The KS provides an objective ranking of parameter importance. We accept parameter sensitivity at the $\alpha \leq 0.1$ threshold. In this way we may determine objectively which precipitation event statistics are most

relevant to the design and evaluation of the Six Mile Creek watershed and dam.

Next, we determine the 2-dimensional KS-test for combinations of dependent precipitation event statistics. We employ the n-dimensional KS-test proposed by Fasano and Franceschini (1987) to determine the significance of bivariate combinations of the sensitive precipitation event statistics.

2.4 Stochastic Precipitation Flood Frequency Analysis

Synthetic records of precipitation may be created through copula modeling of the dependence of precipitation event statistics (e.g. Haberlandt and Radtke, 2014; Paschalis et al., 2014; Rogger et al., 2012; Vandenberghe et al., 2010; Wang et al., 2010). For a thorough review of the theory behind copulas and their application to hydrologic data refer to Genest and Favre (2007). Vandenberghe et al. (2010) presents significant discussion of the theory on the application of copulas to precipitation datasets.

We first determine the rainfall event statistics of interest (as described in Section 2.3). Next, we compute Spearman's ranked correlation coefficient (Spearman's Rho, ρ) and Kendall's Tau (τ) for each bivariate combination of event sensitive statistics to determine where parameter dependencies exist for our dataset. We then make a somewhat subjective choice about which parameters to include in the copula model based on demonstrated dependence and sensitivity similar to the methodology presented by Vandenberghe et al. (2010).

Vandenberghe et al. (2010) demonstrate that the fit of a copula for precipitation data is somewhat imprecise and state that a wide selection of copula families may be considered. We test the fit of the observed seasonal precipitation event statistics to the normal, t-copula, and the Archimedean Joe, Frank, Gumbel, and Clayton theoretical copula models. We translate selected rainfall statistics to the unit square using a kernel estimator (within Matlab R2014b) of the underlying cumulative

distribution. We formally evaluate the seasonal fit of each copula using the Sn estimator as in Genest et al. (2009). We informally review the fit of each copula through scatter plots generated by each copula model as recommended by Genest and Favre (2007).

We fit the selected copula using the maximum likelihood estimate of the best fit copula (C) based on ρ using the observed 60 years of precipitation data as a learning dataset. We estimate the joint exceedance probability of two random variables (X, Y) with a copula (Equation 1) where C is the copula model, x and y are threshold values and F() and G() are the respective marginal distributions of the random variables.

$$P(X > x, Y > y) = C(F(X > x), G(Y > y)) \qquad \text{(Equation 1)}$$

Where,

X, Y – random variable

x, y- threshold value

C – copula model

F(), G() – marginal distributions of random variables X and Y

P(X > x, Y > y) – joint probability of exceedance for random variables X and Y

We then generate random samples from the copula (with Matlab R2014b) to create unique precipitation event statistics on the unit square. These random samples are translated back to the scale of the original event statistics. Because the copula model may return physically unrealistic event statistics (e.g. negative event depths, peak hourly intensities greater than total depth), we include several filters that resample the copula if unrealistic results are obtained. Random samples for sensitive

parameters not included in the copula are determined from the empirical marginal distributions.

Random event statistics are used to generate synthetic years of precipitation. In constructing hyetographs we consider the structure of observed precipitation events for Tompkins County, NY. The temporal distribution of the past 60 years of precipitation events was evaluated by binning the precipitation data by month. The time to reach the cumulative volume threshold for each unique precipitation event is presented in Figure 2 at 10% intervals. This result demonstrates that in general precipitation occurs fairly uniformly for all seasons. The temporal structure breaks down somewhat in late summer as demonstrated by an increased variance; however, the median estimates are in line with all other months. We therefore propose a theoretical hyetograph shape based on the starting assumption that precipitation can be uniform.

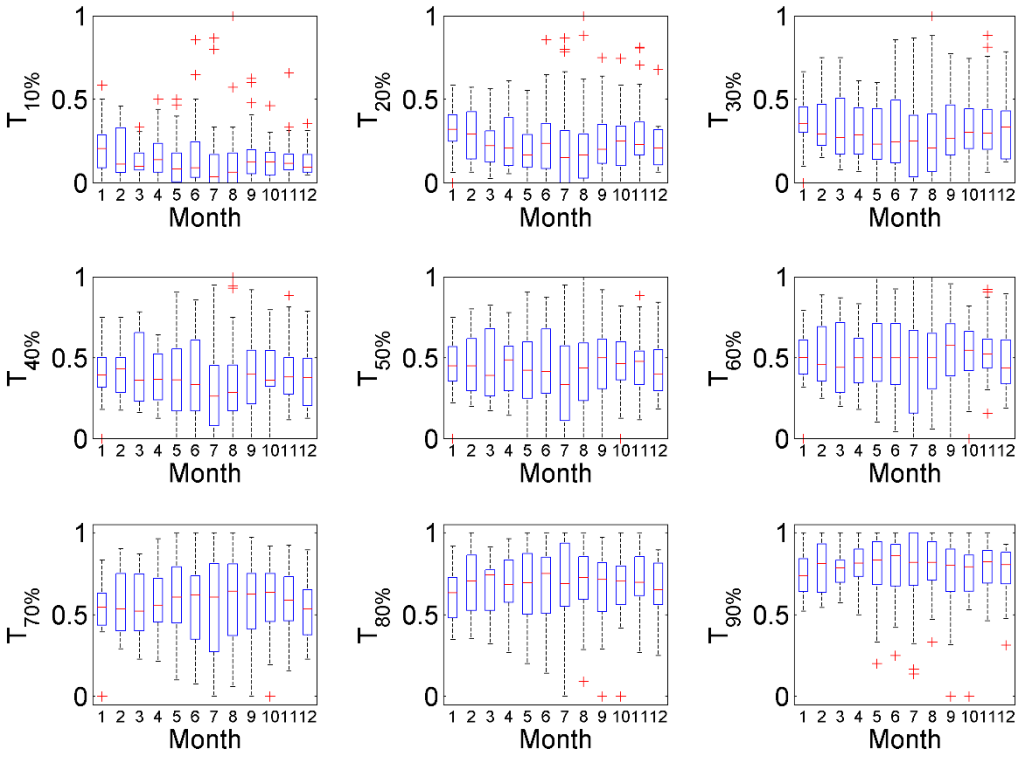

Figure 2 – Temporal distribution of individual precipitation events (>0.25 cm) by month

The purpose of the first set of synthetic precipitation records is to preserve the most important precipitation event statistics (determined in Sections 3.2 and 3.3) when resampling. We do not include the T50% parameter because it is contained within the T75% parameter and T50% was less sensitive when considering reservoir depth. We construct the first set of synthetic hyetographs through the following steps (presented graphically in Figure 3):

- Determine the event total depth, duration, interevent time and T75% by sampling the copula function and marginal distributions.
- Precede each event with zero precipitation for a duration equal to the interevent time.

- Place the peak intensity at the median TP of 0.65. As TP will be shown to be non-sensitive (Sections 3.2 and 3.3) we may neglect the true variability of this parameter without affecting the result.
- Determine the timing of the first 75% of the volume based on T75% and the event duration. Rescale this volume depending on the location of peak intensity. Distribute this volume uniformly from 0 to T75%.
- Distribute the remaining 25% of the volume uniformly from T75% to the event duration.

We then create a second set of synthetic precipitation records considering only the traditional intensity and duration event statistics for comparison. We estimate the average interevent time to be 117 hours. We construct the second set of synthetic events through the following steps:

- Determine the event total precipitation depth and duration by resampling the copula function best fit to these statistics.
- Precede each event with zero precipitation for the average interevent time of 117 hours.
- Construct a uniform hyetograph based on the event average intensity.

We then simulate runoff annual time series by forcing the SWMM model with each stochastic annual precipitation time series. We compute return periods for extreme flows using a partial duration series of peak flows and reservoir depths. We estimate the annual probability of exceedance for each peak flow or reservoir depth (X) with the Weibull plotting position (equation 2), where x is the threshold value determined from simulated peak flow values, and m(x) is the rank of the observed value.

$$P(X > x) = \frac{1}{m(x)+1} \qquad \text{(Equation 2)}$$

Where,

X – observed value

x – threshold value

m(x) – rank of x

2.5 Continuous Simulation and Design Storm Flood Frequency Estimates

We compare the empirical flood frequency curves for watershed peak flow and reservoir depth as determined from design storms, continuous simulation of observed precipitation, continuous simulation of stochastic rainfall generation based on all critical storm characteristics and continuous simulation of stochastic rainfall generation based only on intensity and duration. This comparison informs us on the shortcomings of the design storm approach and stochastic precipitation generation when a constrained set of rainfall event statistics is considered.

The design storm estimates of flood frequency are generated by simulating a series of precipitation events (1yr, 2yr, 5yr, 10yr, 25yr and 50yr) as defined by Soil Conservation Survey (SCS) design storms (Hershfield, 1961). We initialize each simulation with a soil moisture content of 0.3 and an empty reservoir.

Continuous simulations are performed for the observed period of record (1954 – 2014) by forcing the calibration SWMM model with the observed precipitation data. We then analyze the resulting flow and depth data using a partial duration series to develop an empirical flood frequency distribution. We develop uncertainty estimates for continuous simulation by bootstrapping the partial duration series 10,000 times and analyzing the distribution of the resulting flood frequency curves.

3. Results and Discussion

3.1 Model Corroboration

We test our rainfall-runoff model through comparison of return period flow rates from flow data scaled from USGS Gage 04233300 to the Six Mile Creek Dam (Figure 4). We fit observed annual peak flow rates from 1995 through 2014 to a Log-Pearson Type 3 distribution to estimate flow return periods. We perform a continuous simulation of precipitation from 1954 – 2014. We compare the empirical distribution of model estimated annual peak flows to the empirical distribution from observed annual peak flow data as an indicator of the model's ability to accurately estimate runoff from infrequent flood inducing precipitation events.

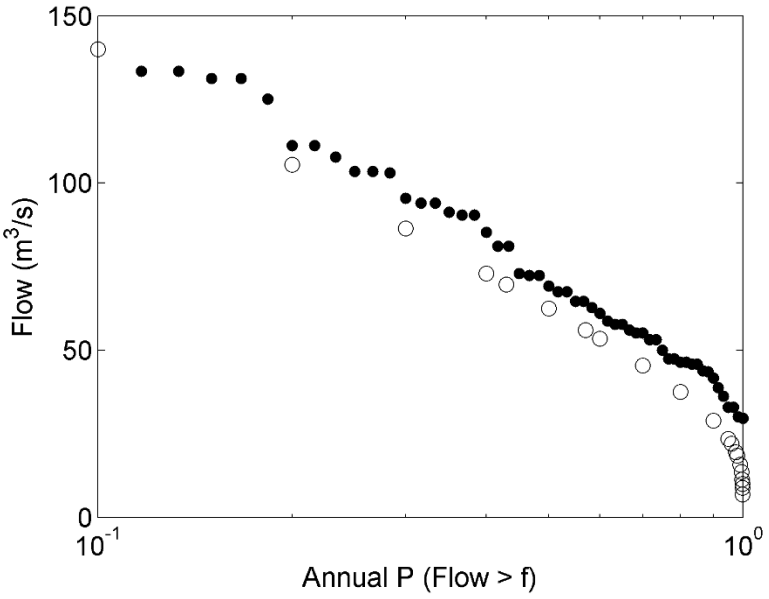

Figure 3 – Corroboration of SWMM model (solid) with return period flows estimated from USGS streamflow gage 04233300 (open)

Our model provides a reasonable estimate of runoff from intense precipitation events relevant to this study. The model accuracy is valid for testing hypothesis about extreme precipitation response. The simplifying assumptions introduced into the model do not impose any obvious artificial distortions of the extreme-event hydrology.

3.2 Precipitation Event Statistics for Peak Flow

The observed 60 year precipitation record yielded 7,045 unique precipitation events that met the minimum event volume and interevent spacing criteria. The KS statistics demonstrate that peak flow is sensitive to the precipitation event statistics of total depth, peak hourly intensity, average intensity, interevent time, T50% and T75% (Figure 5). Table 1.2 presents a summary of all KS-test statistics.

The total event depth (KS = 0.000) and peak hourly intensity (KS = 0.000) are strong predictors of whether or not a precipitation event will produce above bankfull peak flow for Six Mile Creek (Figure 5a, b); however, these parameters alone do not sufficiently describe all runoff potential. There is some overlap in total depth and peak intensity for events producing above and below the bank full discharge. This result suggests that the traditional IDF approach oversimplifies the description of precipitation events.

The precipitation event duration had no significant effect on peak flow (KS = 0.986) (Figure 5d). Watershed engineers commonly assume that the precipitation event controlling a given runoff frequency is directly related to the TC of the watershed and therefore proceed by holding precipitation duration constant. Alternately, one may consider that a "critical duration" of a storm event exists (Lau and Gali, 2010; Kang et al., 2013). Through the "critical duration" concept we choose the intensity-duration design event combination which maximizes runoff at a given frequency. We propose that both of these approaches oversimplify flood hazard estimation. For a fixed design storm duration, we could be under or overestimating the hazard by considering the probability of a given duration as 1. We agree generally that the "critical duration" approach of considering different durations is a good idea; however, researchers should also consider critical characteristics of other event

statistics, and in turn, their joint probability of occurrence when computing event frequency.

Events producing above the bank full discharge occurred at durations less than and greater than the estimated Tc (Figure 5d). The increased complexity of considering event duration in stochastic rainfall generation (e.g. Vernieuwe et al., 2015) is not necessarily justified in all cases. Researchers may be able to take a more parsimonious approach to estimating probable future rainfall runoff responses by removing this event statistic from consideration if it proves non-sensitive.

Average intensity is similarly as important to total depth and peak intensity (KS = 0.000) (Figure 5c). Average intensity is a combination of the total depth and duration statistics. As event duration provided significantly less information (KS = 0.986) (Figure 5d) than the total depth (KS = 0.000) (Figure 5a), the average intensity likely carries a similar information content as the total precipitation depth.

The interevent time of precipitation was shown to be a sensitive parameter for peak flow (KS = 0.001) (Figure 5e). We show that runoff is a function of precipitation as well as the antecedent conditions of the watershed soils. Our result is similar to findings presented in Chapi et al., (2015), Paschalis et al. (2014), Pathiraja et al. (2012) and Camici et al. (2011), Shaw and Walter (2009) who show that the antecedent soil moisture content has a significant effect on watershed runoff and floods.

The significance of the T50% (KS = 0.000) (Figure 5h) and T75% parameters (KS = 0.000) (Figure 5i) demonstrates the importance of the event temporal distribution when defining design hyetographs or stochastic rainfall generation as in Watt and Massalak (2013), Paschalis et al. (2014), Terranova and Ianquinta (2011), and Ruiz-Villanueva et al. (2012). We note two important differences found here. First, the temporal loading of the flood inducing precipitation events is skewed

towards the front of the storm (Figures 5h, i). For approximately 60% of the flood producing events, 75% of the event volume occurred before the halfway point of the storm. This result is somewhat counterintuitive as land surfaces saturate during precipitation. Precipitation volume occurring towards the end of precipitation events would be expected to generate larger runoff volumes per unit rainfall. This result suggests that for Tompkins County, the temporal distribution of intense storms is more commonly front-loaded and that neglecting the temporal distribution though design hyetograph construction (i.e. assuming center or end-loaded design hyetographs) or stochastic precipitation generation would tend to overestimate runoff for given return period precipitation intensities. As the temporal distribution has some effect on the peak runoff, it would be incorrect to prescribe a probability of 1 to any particular hyetograph shape. Second, we show that the TP parameter showed no significant sensitivity (KS = 0.350). While the location of the peak has been a parameter of interest in previous research on precipitation events (Yen and Chow, 1983) it was objectively less important than statistics describing the cumulative mass curve.

3.3 Precipitation Event Statistics for Reservoir Depth

The KS values demonstrate that peak reservoir depth is sensitive to the precipitation event statistics of total rainfall depth, peak hourly intensity, average intensity, duration, T50%, and T75% (Figure 6). Unlike our analysis for peak discharge, here duration is significant (KS = 0.000) (Figure 6d) and interevent time is less so (KS = 0.127) (Figure 6e), i.e., results suggest that the reservoir behind Six Mile Creek Dam has a different response to precipitation than does the watershed peak flow. The results also reinforce the belief that traditional IDF relationships may not provide a universally sufficient basis for hydrologic studies.

There logically exist some values for rainfall statistics of total rainfall depth and peak intensity above which these rainfall characteristics would tend to drive the

results. For example above approximately 7 cm, the total rainfall depth of an event appears to overwhelm the storage capacity of the watershed and reservoir rendering all other rainfall statistics non-sensitive (Figure 6a). Similarly, above approximately 3 cm/hr the peak intensity appears to overwhelm the watershed losses and reservoir drain (Figure 6b). Events with lower total volume and less intense precipitation may also result in high reservoir levels; however, they must occur jointly with other precipitation characteristics favorable to runoff generation.

The interevent time (KS = 0.127), which showed near-sensitive results, represents a composite measure of the importance of memory within the system (Figure 6e). The Six Mile Dam reservoir water level responds somewhat differently to the peak watershed flow rate with respect to this statistic. While the peak watershed flow is sensitive to antecedent conditions (Figure 5d, e), the reservoir responds to events maximizing total runoff volume over longer durations (Figure 6d, e).

Event duration demonstrated sensitivity (KS = 0.000) (Figure 6d); however, flood conditions existed across a wide range of observed event durations (6 to 40 hours). This result suggests that event duration is important only with respect to second level interactions with other rainfall event statistics. For example shorter event durations may only lead to flooding conditions above a certain precipitation depth or intensity.

The results of these two sensitivity analysis demonstrate that precipitation parameters of interest will vary depending on the system response considered, in this case peak discharge versus water height behind a flood control dam. We recommend an iterative approach where important precipitation characteristics are identified and then carried through to design hyetograph construction, or for use in stochastic precipitation generation.

Table 1 – Two-sample KS-test statistics for behavioral and non-behavioral precipitation event statistics as measured by bankfull discharge and reservoir depth

Parameter	Discharge	Reservoir Depth
Total Depth	0.000	0.000
Peak Intensity	0.000	0.000
Avg. Intensity	0.000	0.000
Duration	0.986	0.000
Interevent Time	0.001	0.127
T_P	0.350	0.642
$T_{25\%}$	0.357	0.974
$T_{50\%}$	0.000	0.044
$T_{75\%}$	0.000	0.000

3.3 Multi-variate Precipitation Event Statistics

The scatter plots of the significant precipitation event statistics show the complex response of the watershed outflow (Figure 7). While the significant peak depth and intensity tended to trigger a rise in the reservoir water surface elevation, this was not the case for all of the most intense events. Similarly, the shorter interevent times tended to result in significant increases in reservoir water level, but not exclusively. The joint probability of total precipitation depth, peak intensity, interevent time and temporal distribution must therefore be considered to properly determine the reservoir precipitation-runoff response.

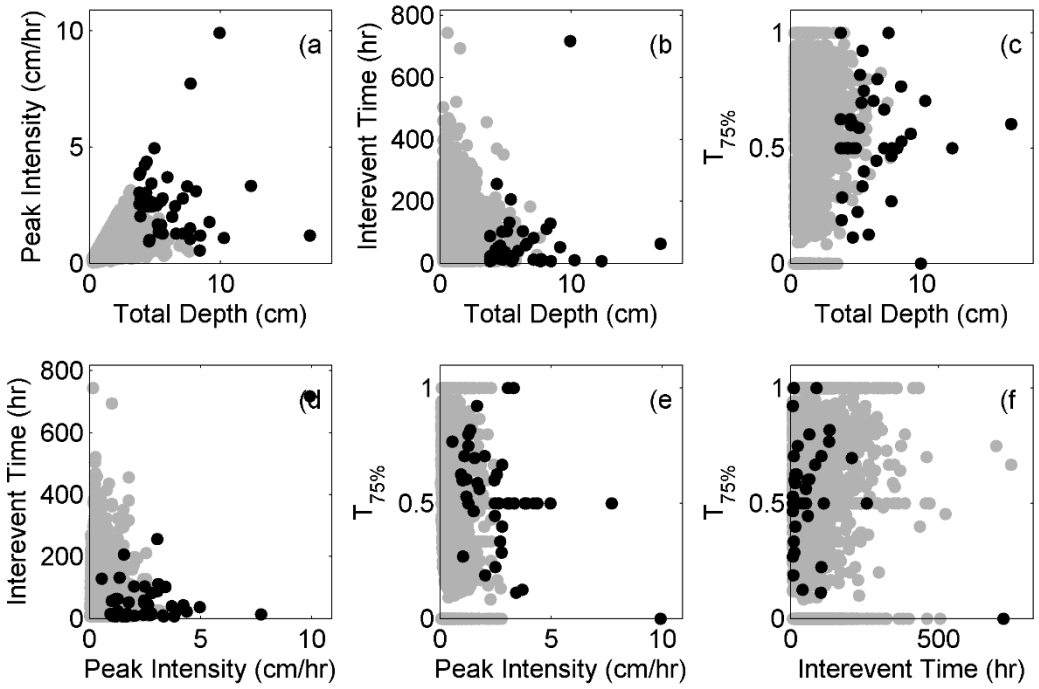

Figure 4 – Scatter plots of event statistics showing all events (gray) and behavioral events (black) for peak reservoir depth

This result is similar to the secondary return period concept discussed in Vandenberghe et al. (2010) and Salvadori et al. (2011); however, we note that the precipitation frequency identified by the secondary return period methodology would not necessarily identify flood event frequencies. As discussed in Serinaldi (2014, 2015) the concept of return periods for multivariate models can be somewhat misleading. Infinite combinations of precipitation event statistics exist for a fixed probability of exceedance; however, we cannot expect all such combinations to produce the same hazard as we have demonstrated that different variables contribute more than others (Figures 5 and 6; Table 1.2). It is therefore simpler and perhaps more meaningful to perform a hazard analysis in a univariate setting (i.e. streamflow) as opposed to the highly dimensional analysis of precipitation event statistics. We note that the univariate case of streamflow return periods while avoiding some of the

trappings of multivariate analysis is still subject to some poor assumptions in treating peak stream flows as identically distributed independent random variables as described in Serinaldi (2014, 2015).

Next we formally evaluate the sensitivity of bivariate combinations of the sensitive precipitation event statistics through a 2-dimensional KS-test (Table 1.3). We show that all behavioral bivariate combinations of the sensitive event statistics are drawn from significantly different distributions than those derived from the non-behavioral events.

Table 2 – 2-dimensional KS-test values for bivariate empirical distributions of precipitation event statistics of behavioral and non-behavioral events for the bankfull discharge and reservoir depth cases

Parameters	**Discharge**	**Reservoir Depth**
(Depth, Intensity)	0.0000	0.0000
(Depth, Duration)	0.0000	0.0000
(Depth, Interevent Time)	0.0000	0.0000
(Depth, $T_{75\%}$)	0.0000	0.0000
(Intensity, Duration)	0.0000	0.0000
(Intensity, Interevent Time)	0.0000	0.0000
(Intensity, $T_{75\%}$)	0.0000	0.0000
(Duration, Interevent Time)	0.0077	0.0021
(Duration, $T_{75\%}$)	0.0002	0.0004
(Interevent Time, $T_{75\%}$)	0.0000	0.0084

3.4 Flood Frequency Estimates for Flood Flow and Reservoir Depth

First, we determine the dependency of event statistics through Kendall's Tau and Spearman's Rho (Table 1.4). We observe correlation between the event statistics depth, intensity, duration and T75%. Interevent timing and T75% of precipitation events demonstrate somewhat less correlation than depth, intensity, and duration and were therefore not included in the copula model. Our subjective choice is somewhat similar to decisions presented by Vandenberghe et al. (2010).

Table 3 – Measured dependence of observed precipitation event statistics as Kendall's Tau (τ) and Spearman's Rho (ρ)

Parameters	τ	ρ
(Depth, Intensity)	0.44	0.60
(Depth, Duration)	0.49	0.64
(Depth, Interevent Time)	0.05	0.07
(Depth, $T_{75\%}$)	0.27	0.40
(Intensity, Duration)	-0.05	-0.07
(Intensity, Interevent Time)	0.03	0.04
(Intensity, $T_{75\%}$)	0.05	0.07
(Duration, Interevent Time)	0.02	0.03
(Duration, $T_{75\%}$)	0.20	0.29
(Interevent Time, $T_{75\%}$)	0.04	0.05

We evaluate the fit of several theoretical 3-dimensional copulas using the Sn estimator as in Geneste et al. (2009) (Table 1.5). The t-copula provides the most consistent fit through formal measures for all seasons (Table 1.5), though we

acknowledge that the normal copula provides a slightly better fit for some seasons. Informally the t-copula best represents dependence (Figures 8 and 9). We therefore select the t-copula to model the 3-dimensional dependence of event depth, peak intensity and duration.

Table 4 –Seasonal goodness-of-fit S_n values for theoretical copula models

Copula	Winter	Spring	Summer	Fall
Gumbel	0.490	0.430	0.286	0.238
Joe	0.554	0.582	0.342	0.277
Clayton	0.631	0.405	0.426	0.338
Frank	0.468	0.353	0.265	0.236
t-copula	0.375	0.280	0.225	0.233
Normal	0.415	0.248	0.199	0.222

We generate a total of 6,000 synthetic years of precipitation through copula modeling of depth, peak intensity, and duration and resampling of marginal rainfall characteristic distributions of interevent time and T75%. One potential shortcoming of this approach is that events exceeding the maximum values of the original distribution will not be reproduced as our approach maintains the marginal histograms of the learning dataset (Figures 8 and 9).

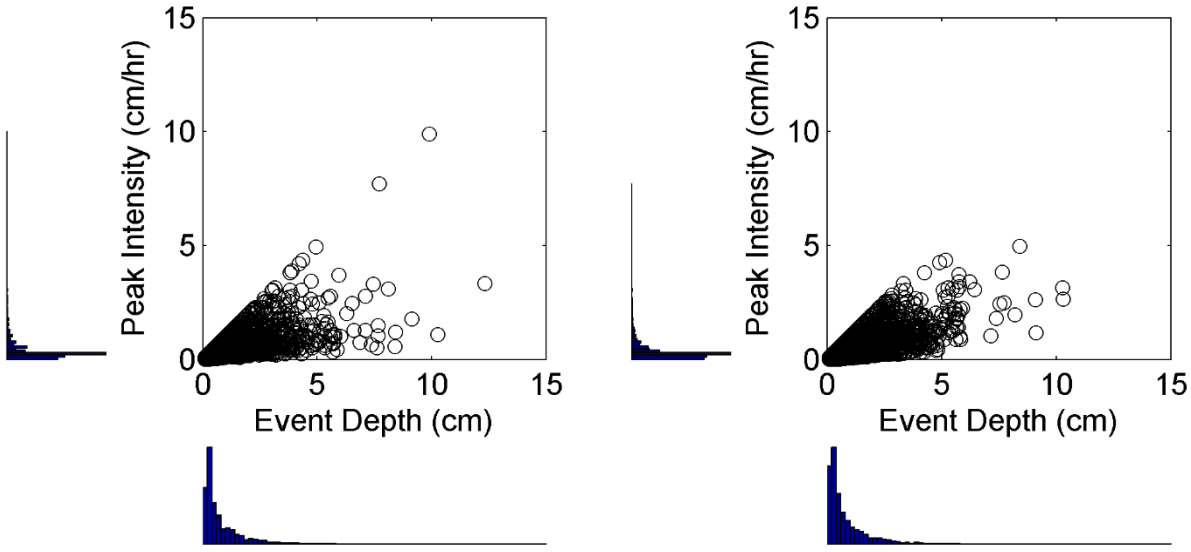

Figure 5 – Scatter plots and marginal histograms for 7,045 observed precipitation events (left) and 6,000 synthetic events resampled from the best fit copula (right) for event depth and peak intensity

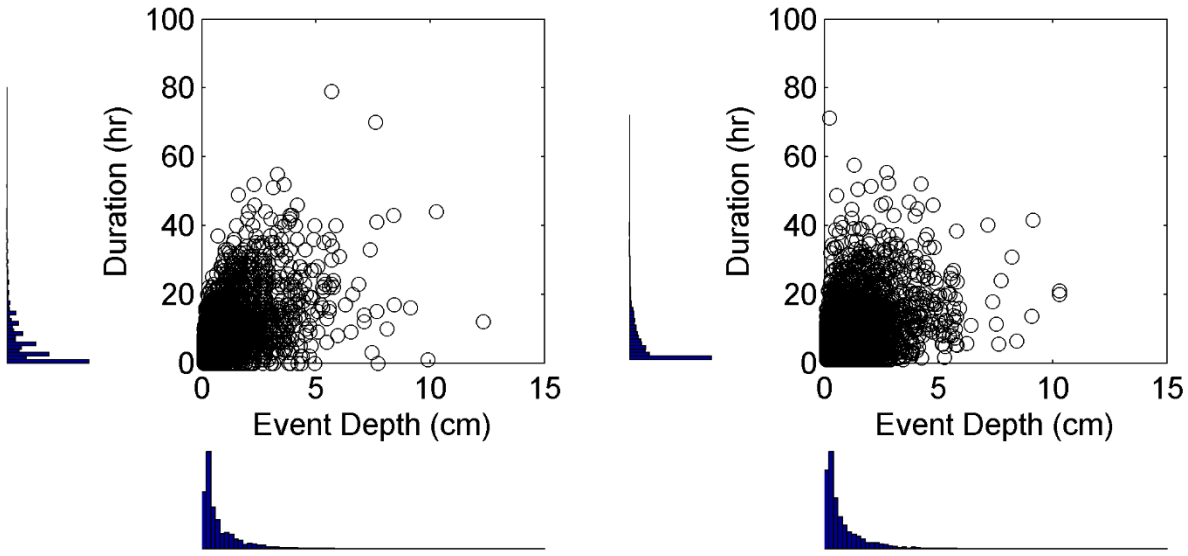

Figure 6 – Scatter plots and marginal histograms for 7,045 observed precipitation events (left) and 6,000 synthetic events resampled from the best fit copula (right) for event depth and duration

Each of the 6,000 years of precipitation data is simulated with the calibrated SWMM model to generate 6,000 years of Six Mile Creek flow and reservoir depth data. We then generate 60,000 unique sets of 60 year record sets by bootstrapping the 6,000 synthetic years of simulated flow and reservoir depth data. We repeat this sampling procedure for the precipitation dataset based only on average intensity and duration rainfall characteristics. We then compute the empirical frequency curve of the simulated peaks for the 60,000 record sets.

Figure 10 presents the annual exceedance probability for event peak watershed flow and peak reservoir depth at the Six Mile Creek Dam based on continuous simulation as well as stochastic precipitation generation considering all significant precipitation event statistics. Figure 11 presents the annual exceedance probabilities for the same analysis with a stochastic precipitation methodology considering only precipitation intensity and duration.

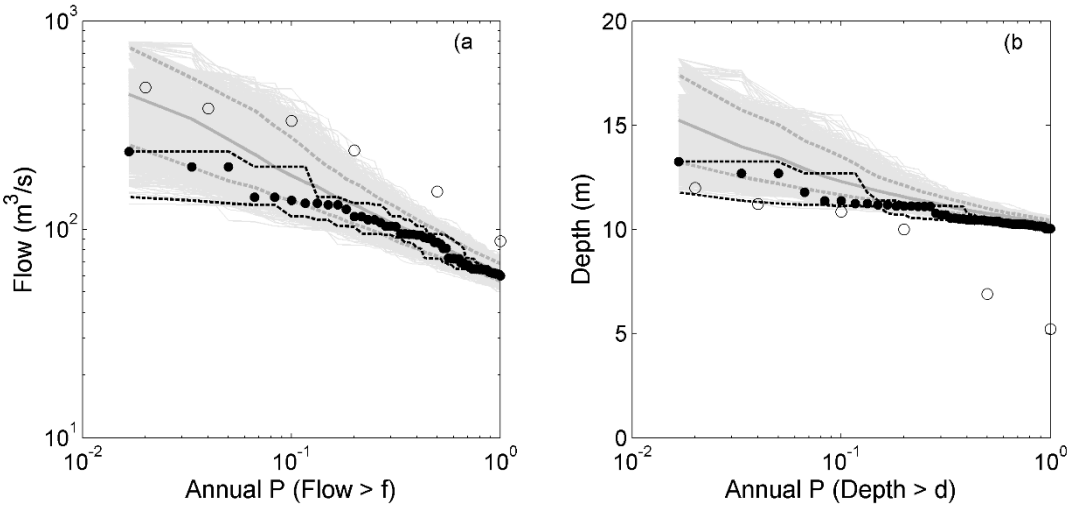

Figure 7 – Return period flow rates (a) and reservoir water depths (b) as determined by design storm (open), continuous simulation (black, 5% and 95% confidence bounds – dashed black) and stochastic rainfall generation considering the precipitation parameters total depth, peak intensity, duration, T_P, interevent timing and $T_{75\%}$ as random variables (median – solid gray, 5% and 95% confidence bounds – dashed gray)

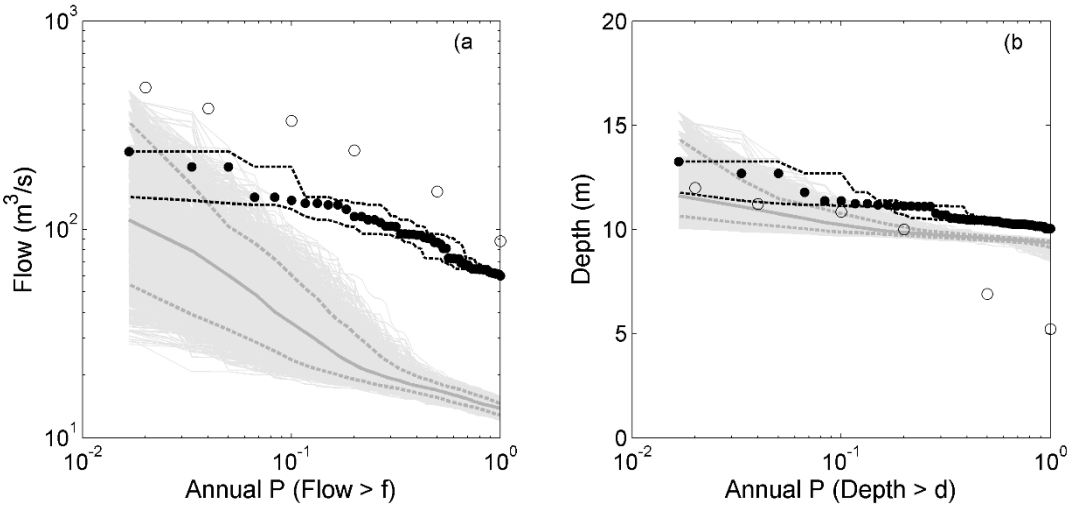

Figure 8 - Return period flow rates (a) and reservoir water depths (b) as determined by design storm (open), continuous simulation (black, 5% and 95% confidence bounds – dashed black) and stochastic rainfall generation considering the precipitation parameters total depth and duration (IDF) as random variables (median – solid gray, 5% and 95% confidence bounds – dashed gray)

The IDF stochastic precipitation scenario examined significantly oversimplifies the problem of flood inducing rainfall frequency by considering only rainfall intensity and duration. The return periods estimated do not agree well with those estimated through continuous simulation across a wide range of frequencies (Figure 11). The most significant difference is the potentially underestimated peak discharges. As we assumed a mean value for interevent times, neglected the peak hourly intensity and removed all information on the temporal distribution for each hyetograph, we have limited the ability of the precipitation to be maximized.

Design storm estimates of flow return periods are perhaps adequate estimates of the Six Mile Creek peak flow (Figure 10a); however, they are not useful for determining the response of the Six Mile Creek reservoir which exhibits a more complicated hydrologic response to precipitation (Figure 10b). Similar to the stochastic precipitation generation methodology considering only depth and duration, the design storm method significantly underestimates the depth within the reservoir for

more frequent events (Figure 10b). This result is likely due to the design storm method neglecting information on hyetograph structure, duration, and antecedent hydrologic conditions.

3.5 Discussion of Aleatory Uncertainties Associated with Precipitation

The stochastic precipitation generation methodology presents an improvement over continuous simulation and design storms in that we can propose and simulate probable precipitation events which have not yet been observed. We predict flows of up 700 m3/s as being probable (within the 90% confidence bounds) at the 60 year return interval whereas bootstrapping the continuous simulation results potentially produces an underestimate of the aleatory uncertainty associated with runoff events (Figure 10a, b). These results suggest that the past 60 years of precipitation within Tompkins County, NY has experienced fewer large flood causing precipitation events than we might experience on average over a significantly longer period. Based on the structure of the observed events and a stochastic resampling of the rainfall event characteristics, we predict higher flows at return periods above 10 years than we estimate through continuous simulation.

The average flood hazard estimates of the scenario considering all sensitive rainfall characteristics agrees well with the continuous simulation records below 10 years. The strong agreement is likely due to preservation of the significant rainfall characteristics, but also because the random samples drawn for stochastic precipitation were generated from a copula function trained on the 60 years of observed precipitation, which were used to force the continuous simulation.

While the methodology represents an improvement, we must acknowledge that we are still reliant on any limitations present within the observed precipitation dataset. The occurrence of hurricanes and tropical depressions within the Tompkins County, NY region is likely under-represented within our observed precipitation dataset. Only

one storm of this strength (Tropical Storm Frederic, 1979) has passed within 50 km of the Six Mile Creek watershed within the past 100 years (NOAA, 2015b). Recent research by Donnelly et al. (2001, 2004) suggests the frequency of land-falling intense tropical storms may be higher between New Jersey and Rhode Island, USA than our recent history suggests. We must therefore conclude that the true aleatory variability represented in Figure 10 may underestimate the true long term precipitation and runoff response for Six Mile Creek.

Further, extrapolation using the copula model developed herein beyond the 60 year return period (Figure 10) is likely not appropriate. Shin et al. (2015) and Smith et al. (2011) propose that regions experiencing multiple precipitation generating phenomena should employ mixture distributions to describe independently distributed (and physically different) precipitation sources. Within Tompkins County, extreme precipitation may be the result of a convective, orographic, tropical or extra-tropical system (Smith et al., 2011). Our study dataset provides us with extremely limited information on tropical system extreme precipitation events. We expect that higher return period precipitation events will be related to tropical systems and therefore conclude that the stochastic rainfall model developed herein should only be utilized to estimate frequent (return period < 50 years) precipitation and flooding events.

4. Conclusions

1. Traditional event statistics used in design storm construction and more recently stochastic precipitation generation may be too limiting to properly describe precipitation for estimating the rainfall-runoff responses of hydrologic systems. We demonstrate significant sensitivity to six rainfall characteristics for peak watershed outflow (total depth, peak intensity, average intensity, interevent time, T50%, and T75%) and six characteristics for reservoir depth (total depth, peak intensity, average intensity, duration, T50%, and T75%). We note that the sets of significant

characteristics differed for the two hydrologic systems considered. This result suggests that no global set of important rainfall statistics exists and that we are best served by determining this on a case by case basis.

2. We show that high flow responses of the Six Mile Creek watershed may be the result of high intensity events, or moderately intense events occurring simultaneously with other rainfall characteristics which are favorable to runoff. This result is similar to the concept of secondary return periods as discussed in Vandenberghe et al. (2010) and Salvadori et al. (2011). We note that flood triggering events would not necessarily be identified through secondary return period analysis of precipitation events as some combinations of extreme precipitation event statistics did not result in a flood event. As discussed in Serinaldi (2014, 2015) the concept of defining return periods for multivariate models (such as our case of precipitation event statistics) can be somewhat misleading. Infinite combinations of precipitation event statistics occur for a fixed probability of exceedance; however, we cannot expect all such combinations to produce the same hazard.

3. We demonstrate that the validity of the stochastic rainfall generation approach is highly dependent on the selection of appropriate rainfall characteristics. We may over- or underestimate the watershed precipitation response for a given frequency through selection of improper statistics. Our proposed methodology considers an expanded set of precipitation event statistics to better represent the true variability in flood inducing precipitation events. Stochastic precipitation records were able to produce a similar flood frequency curve as those derived through continuous simulation. Above the ten year flow the methods agree less. This is likely due to an under-sampling of the true stochastic rainfall processes for extreme events within the continuous observed record.

4. Stochastically generated precipitation datasets based on the significantly important rainfall event statistics and continuous simulation with a hydrologic model may be

used to quantify the aleatory uncertainty in watershed and reservoir flood response to precipitation. As expected, the aleatory uncertainty associated with precipitation increases with increasing return period for peak flow within Six Mile Creek watershed and the peak reservoir depth. We demonstrate that bootstrapping continuous simulation results may underestimate the aleatory uncertainty. The stochastic precipitation methodology is reliant on the original training data we must acknowledge any potential shortcomings contained in the original record may carry through to the final estimates.

REFERENCES

Balistrocchi, M., & Bacchi, B. 2011. Modelling the statistical dependence of rainfall event variables through copula functions. Hydrology and Earth System Sciences, 15(6): 1959-1977. doi: 10.5194/hess-15-1959-2011

Berg, P., Moseley, C., & Haerter, J. O. 2013. Strong increase in convective precipitation in response to higher temperatures. Nature Geoscience, 6(3): 181-185. doi: 10.1038/ngeo1731

Camici, S., Tarpanelli, A., Brocca, L., Melone, F., & Moramarco, T. 2011. Design soil moisture estimation by comparing continuous and storm-based rainfall-runoff modeling. Water Resources Research, 47(5). doi: 10.1029/2010WR009298

Cardoso, C. O., Bertol, I., Soccol, O. J., & Sampaio, C. A. D. P. 2014. Generation of intensity duration frequency curves and intensity temporal variability pattern of intense rainfall for Lages/SC. Brazilian Archives of Biology and Technology, 57(2), 274-283. doi: 10.1590/S1516-89132013005000014

Ceresetti, D., Anquetin, S., Molinié, G., Leblois, E., & Creutin, J. D. 2012. Multiscale evaluation of extreme rainfall event predictions using severity diagrams. Weather and Forecasting, 27(1), 174-188. doi: 10.1175/WAF-D-11-00003.1

Chapi, K., Rudra, R. P., Ahmed, S. I., Khan, A. A., Gharabaghi, B., Dickinson, W. T., & Goel, P. K. 2015. Spatial-Temporal Dynamics of Runoff Generation Areas in a Small Agricultural Watershed in Southern Ontario. Journal of Water Resource and Protection, 7(01), 14. doi: 10.4236/jwarp.2015.71002

Donnelly, J. P., Smith Bryant, S., Butler, J., Dowling, J., Fan, L., Hausmann, N. , Newby, P., Shuman, B., Stern, J., Westover, K., & Webb III, T. 2001. 700 yr sedimentary record of intense hurricane landfalls in southern New England, Geological Society of America Bulletin, 113(6), 714-727. doi: 10.1130/0016-7606

Donnelly, J. P., Butler, J., Roll, J., Wengren, S., and Webb, T. 2004. A backbarrier overwash record of intense storms from Brigantine, New Jersey, Marine Geology, 210(1), 107-121. doi:10.1016/j.margeo.2004.05.005

Easton, Z.M., Gérard-Marchant, P., Walter, M.T., Petrovic, A.M., & Steenhuis T.S. 2007. Hydrologic assessment of an urban variable source watershed in the Northeast United States. Water Resources Research 43(3): Art. No. W03413. doi: 10.1029/2006WR005076

Ebtehaj, M., & Foufoula-Georgiou, E. 2010. Orographic signature on multiscale statistics of extreme rainfall: A storm-scale study. Journal of Geophysical Research: Atmospheres (1984–2012), 115(D23).

Fasano, G., & Franceschini, A. 1987. A multidimensional version of the Kolmogorov–Smirnov test. Monthly Notices of the Royal Astronomical Society, 225(1), 155-170.

Froehlich, D. C. 2010. Short-duration rainfall intensity equations for urban drainage design. Journal of Irrigation and Drainage Engineering, 136(8), 519-526. Doi: 10.1061/(ASCE)IR.1943-4774.0000250

Froidevaux, P., Schwanbeck, J., Weingartner, R., Chevalier, C., & Romppainen-Martius, O. 2014. Does antecedent precipitation play a role for floods in (small) Swiss catchments?. In EGU General Assembly Conference Abstracts (Vol. 16, p. 4113).

Garambois, P. A., Larnier, K., Roux, H., Labat, D., & Dartus, D. 2014. Analysis of flash flood-triggering rainfall for a process-oriented hydrological model. Atmospheric research, 137, 14-24. doi:10.1016/j.atmosres.2013.09.016

Garambois, P. A., Roux, H., Larnier, K., & Dartus, D. 2012. Relations between streamflow indices, rainfall characteristics and catchment physical descriptors for flash flood events. IAHS-AISH publication, 581-586.

Genest, C., & Favre, A. C. 2007. Everything you always wanted to know about copula modeling but were afraid to ask. Journal of hydrologic engineering, 12(4), 347-368. Doi: 10.1061/(ASCE)1084-0699(2007)12:4(347)

Genest, C., Rémillard, B., & Beaudoin, D. 2009. Goodness-of-fit tests for copulas: A review and a power study. Insurance: Mathematics and economics, 44(2), 199-213.

Grimaldi, S., Petroselli, A., & Serinaldi, F. 2012. Design hydrograph estimation in small and ungauged watersheds: continuous simulation method versus event-based approach. Hydrological Processes, 26(20), 3124-3134. doi: 10.1002/hyp.8384

Guo, Y., & Adams, B. J. 1999. An analytical probabilistic approach to sizing flood control detention facilities. Water Resources Research, 35(8), 2457-2468. doi: 10.1029/1999WR900125

Guo, Y., & Markus, M. 2011. Analytical probabilistic approach for estimating design flood peaks of small watersheds. Journal of Hydrologic Engineering, 16(11), 847-857.

Haberlandt, U., & Radtke, I. 2014. Hydrological model calibration for derived flood frequency analysis using stochastic rainfall and probability distributions of peak flows. Hydrology and Earth System Sciences, 18(1), 353-365. doi:10.5194/hess-18-353-2014

Hershfield, D. M. 1961. Rainfall frequency atlas of the United States. Technical Paper 40. US Department of Commerce. Weather Bureau.

Spear, R. C., & Hornberger, G. M. 1980. Eutrophication in Peel Inlet—II. Identification of critical uncertainties via generalized sensitivity analysis. Water Research, 14(1), 43-49. doi:10.1016/0043-1354(80)90040-8

Huard, D., Mailhot, A., & Duchesne, S. 2010. Bayesian estimation of intensity–duration–frequency curves and of the return period associated to a given rainfall event. Stochastic Environmental Research and Risk Assessment, 24(3), 337-347. doi: 10.1007/s00477-009-0323-1

Kang, M. S., Goo, J. H., Song, I., Chun, J. A., Her, Y. G., Hwang, S. W., & Park, S. W. 2013. Estimating design floods based on the critical storm duration for small watersheds. Journal of Hydro-environment Research, 7(3), 209-218. doi:10.1016/j.jher.2013.01.003

Lau, D. and Gali, S. 2010. How "Critical" is Critical Duration in Determining Flood Risk, Flood Damages, and Stormwater Management Solutions?. Watershed Management 2010: pp. 1214-1225. doi: 10.1061/41143(394)109

Lee, C. H., Kim, T. W., Chung, G., Choi, M., & Yoo, C. 2010. Application of bivariate frequency analysis to the derivation of rainfall–frequency curves. Stochastic Environmental Research and Risk Assessment, 24(3), 389-397. doi: 10.1007/s00477-009-0328-9

Madsen, H., Lawrence, D., Lang, M., Martinkova, M., & Kjeldsen, T. R. 2014. Review of trend analysis and climate change projections of extreme

precipitation and floods in Europe. Journal of Hydrology, 519, 3634-3650. doi:10.1016/j.jhydrol.2014.11.003

Mirhosseini, G., Srivastava, P., & Stefanova, L. 2013. The impact of climate change on rainfall Intensity–Duration–Frequency (IDF) curves in Alabama. Regional Environmental Change, 13(1), 25-33. doi:10.1007/s10113-012-0375-5

Muschinski, T., & Katz, J. I. 2013. Trends in hourly rainfall statistics in the United States under a warming climate. Nature Climate Change, 3(6), 577-580. doi:10.1038/nclimate1828

National Oceanic and Atmospheric Administration (NOAA) 2015a. Precipitation Frequency Data Server (PFDS). Available Online: http://hdsc.nws.noaa.gov/hdsc/pfds/

National Oceanic and Atmospheric Administration (NOAA) 2015b. HURDAT2. Available Online: http://www.aoml.noaa.gov/hrd/hurdat/Data_Storm.html

Northeast Regional Climate Center (NRCC). 2015. NRCC Hourly Precipitation Database. Available Online: http://www.nrcc.cornell.edu/page_databases.html

Nguyen, V., Desramaut, N., & Nguyen, T. 2010. Optimal rainfall temporal patterns for urban drainage design in the context of climate change. Water Science & Technology, 2010, doi:10.2166/wst.2010.295

Paschalis, A., Fatichi, S., Molnar, P., Rimkus, S., & Burlando, P. 2014. On the effects of small scale space–time variability of rainfall on basin flood response. Journal of Hydrology, 514, 313-327. doi: 10.1016/j.jhydrol.2014.04.014

Pathiraja, S., Westra, S., & Sharma, A. 2012. Why continuous simulation? The role of antecedent moisture in design flood estimation. Water Resources Research, 48(6). doi: 10.1029/2011WR010997

Paquet, E., Garavaglia, F., Garçon, R., & Gailhard, J. 2013. The SCHADEX method: A semi-continuous rainfall–runoff simulation for extreme flood estimation. Journal of Hydrology, 495, 23-37. doi:10.1016/j.jhydrol.2013.04.045

Perdigão, R. A., & Blöschl, G. 2014. Spatiotemporal flood sensitivity to annual precipitation: Evidence for landscape-climate coevolution. Water Resources Research, 50(7), 5492-5509. doi: 10.1002/2014WR015365

Raimondi, A., & Becciu, G. 2015. On pre-filling probability of flood control detention facilities. Urban Water Journal, 12(4), 344-351. doi:10.1080/1573062X.2014.901398

Rogger, M., Kohl, B., Pirkl, H., Viglione, A., Komma, J., Kirnbauer, R., ... & Blöschl, G. 2012. Runoff models and flood frequency statistics for design flood estimation in Austria–Do they tell a consistent story? Journal of Hydrology, 456, 30-43. doi: 10.1016/j.jhydrol.2012.05.068

Rossman, L. A. 2010. Storm water management model user's manual, version 5.0 (p. 276). Cincinnati: National Risk Management Research Laboratory, Office of Research and Development, US Environmental Protection Agency.

Ruiz-Villanueva, V., Borga, M., Zoccatelli, D., Marchi, L., Gaume, E., & Ehret, U. 2012. Extreme flood response to short-duration convective rainfall in South-West Germany. Hydrology and Earth System Sciences, 16(5), 1543-1559. doi: 10.5194/hess-16-1543-2012

Salvadori, G., Michele, C. D., & Durante, F. 2011. On the return period and design in a multivariate framework. Hydrology and Earth System Sciences, 15(11), 3293-3305. doi:10.5194/hess-15-3293-2011

Serinaldi, F. 2014. Dismissing return periods!. Stochastic Environmental Research and Risk Assessment, 29(4), 1179-1189. doi: 10.1007/s00477-014-0916-1

Serinaldi, F. 2015. Erratum to: Dismissing return periods!. Stochastic Environmental Research and Risk Assessment, 29(4), 1191-1192. doi: 10.1007/s00477-015-1044-2

Shaw, S.B. & Walter, M.T. 2009. Formulating storm runoff risk using bivariate frequency analyses of rainfall and antecedent watershed wetness. Water Resources Research, 45, doi: 10.1029/2008WR006900,

Shin, J. Y., Lee, T., & Ouarda, T. B. 2015. Heterogeneous Mixture Distributions for Modeling Multisource Extreme Rainfalls*. Journal of Hydrometeorology, 16(6), 2639-2657. doi: http://dx.doi.org/10.1175/JHM-D-14-0130.1

Smith, J. A., Villarini, G., & Baeck, M. L. 2011. Mixture distributions and the hydroclimatology of extreme rainfall and flooding in the eastern United States. Journal of Hydrometeorology, 12(2), 294-309. doi: http://dx.doi.org/10.1175/2010JHM1242.1

Terranova, O. G., Gariano, S. L., & Greco, R. 2014. Spatial and temporal features of heavy rainstorm events in Calabria, Southern Italy. EGU General Assembly 2015. Vol. 17, EGU2015-2008, 2015.

United States Department of Agriculture (USDA) National Resource Conservation Service (NRCS). 2015. Web Soil Survey. Available Online: http://websoilsurvey.sc.egov.usda.gov/App/HomePage.htm

United States Department of Agriculture (USDA) National Resource Conservation Service (NRCS). 1986. Urban Hydrology for Small Watersheds. Technical Report 55.

United States Geological Survey (USGS). 2015a. USGS 04233300 Six Mile Creek at Bethel Grove. Available Online: http://waterdata.usgs.gov/usa/nwis/uv?site_no=04233300

United States Geological Survey (USGS). 2015b. The National Elevation Dataset. Available Online: http://nationalmap.gov/elevation.html

Vandenberghe, S., Verhoest, N. E. C., Buyse, E., & Baets, B. D. 2010. A stochastic design rainfall generator based on copulas and mass curves. Hydrology and Earth System Sciences, 14(12), 2429-2442. doi:10.5194/hess-14-2429-2010

Vernieuwe, H., Vandenberghe, S., De Baets, B., & Verhoest, N. E. 2015. A continuous rainfall model based on vine copulas. Hydrology and Earth System Sciences Discussions, 12(1), 489-524. doi:10.5194/hessd-12-489-2015

Wang, X., Gebremichael, M., & Yan, J. 2010. Weighted likelihood copula modeling of extreme rainfall events in Connecticut. Journal of Hydrology, 390(1), 108-115. doi:10.1016/j.jhydrol.2010.06.039

Walter, M. T., Mehta, V. K., Marrone, A. M., Boll, J., Gérard-Marchant, P., Steenhuis, T. S., & Walter, M. F. 2003. Simple estimation of prevalence of Hortonian flow in New York City watersheds. Journal of Hydrologic Engineering, 8(4), 214-218. Doi: 10.1061/(ASCE)1084-0699(2003)8:4(214)

Watt, E., & Marsalek, J. 2013. Critical review of the evolution of the design storm event concept. Canadian Journal of Civil Engineering, 40(2), 105-113. Doi: 10.1139/cjce-2011-0594

Willems, P. 2000. Compound intensity/duration/frequency-relationships of extreme precipitation for two seasons and two storm types. Journal of Hydrology, 233(1), 189-205. doi: 10.1016/S0022-1694(00)00233-X

Wu, S. J., Hsu, C. T., Lien, H. C., & Chang, C. H. 2015. Modeling the effect of uncertainties in rainfall characteristics on flash flood warning based on rainfall thresholds. Natural Hazards, 75(2), 1677-1711. doi: 10.1007/s11069-014-1390-2

Yen, B.C., and Chow, V.T. 1983. Local design storm. Vol. II. Report No. FHWA/RD-82-064. Federal Highway Administration, Washington, D.C.

CHAPTER 2

HYDROLOGIC STATE INFLUENCE ON RIVERINE FLOOD DISCHARGE FOR A SMALL TEMPERATE WATERSHED (FALL CREEK, USA): NEGATIVE FEEDBACKS ON THE EFFECTS OF CLIMATE CHANGE

1. Introduction

Precipitation induced watershed flooding is a function of the distribution of precipitation characteristics and the distribution of hydrologic catchment conditions, frequently referred to as hydrologic state variables. Increased global temperatures will raise the moisture holding capacity of the atmosphere and result in more intense precipitation events (Kunkel et al., 2013; Balling and Goodrich, 2012; Wehner, 2012; Hayhoe et al 2007, 2008; Diffenbaugh et al., 2005). Recent interest in climate change induced shifts in precipitation patterns has instilled a commonly held belief that flooding risk is increasing globally (e.g. Trenberth, 2011; Schiermeier, 2011). Trenberth (2011) and Schiermeier (2011) logically approach the problem of global riverine flood hazard from the point of view of precipitation forcing. Riverine flooding is commonly the result of the rainfall-runoff hydrologic response of the landscape and it is therefore reasonable to assume that a shift towards more intense precipitation over a watershed will result in a uniform corresponding shift in the flood hazard regime towards increased flooding risk. Though we expect a net increase in global flooding, the increase in flooding may not be uniform. For example Hirabayashi et al. (2013) demonstrate that there is a spatial heterogeneity of the anticipated change in flood risk, with some areas showing an expected decrease. Significant work has been done to

estimate future meteorological conditions, though much is currently unknown about future changes to distributions of hydrologic state variables, and how these changes in turn will influence riverine flood hydrology.

The runoff response of riverine systems is a constantly changing function of geomorphic (e.g. Wyzga et al, 2015), hydrologic (e.g. Nied et al., 2013), anthropogenic (e.g. Blöschl et al, 2015; Li et al, 2014), ecological (e.g. Butler, 1989), and atmospheric (e.g. Wood et al., 2015) conditions. High frequency (daily to weekly) fluctuations in hydrologic states of a watershed have an influence on the runoff response to precipitation and therefore riverine flood discharge. Despite the potential for a rapidly varying hydrologic state to introduce additional variations in the rainfall-runoff watershed response, the importance of these conditions for making accurate discharge predictions remains the subject of some debate (Wood et al., 2015).

The concept of decadal non-stationary flood risk is receiving more attention as climate induced changes in precipitation intensity and frequency threaten to increase flood hazard globally. Hirsch and Ryberg (2012) performed a statistical analysis to demonstrate that observed trends in riverine flow may not be linked to long term changes in atmospheric $C0_2$. Malakpour and Villarini (2015) presents an alternate conclusion where the frequency of riverine flooding events has increased under the driving assumption that an atmosphere at a higher temperature has resulted in increased precipitation. Bouwer (2010) and Blöschl et al. (2015) suggest that the observed global increase in flooding could be due to increased intense precipitation, though it is likely that land use and population changes have also modified the structure of risk. We propose that some of the disparity in these results is due to the

differing hydrologic states of the watersheds considered. Hydrologic conditions are anticipated to respond to climate change and therefore have some inherent ability to transform the relationship between changing climate patterns and riverine flood hazard (e.g. Bell et al., 2016; Koplin et al., 2014, Blöschl et al., 2007).

Decadal shifts in flood hazard, such as those associated with climate change, are of concern for long term urban planning (Gersonius et al., 2012; Kundzewicz etal., 2014; Jabareen, 2013). Obeysekera and Salas (2014), Tramblay et al., (2014), Salas and Obeysekera (2013), Seidou et al., (2012), Westra et al., (2010), Serinaldi (2015), Gilroy and McCuen, (2012), and Stedinger and Griffis (2011) present methodologies for assessing the potential for climate-induced non-stationary flood risk. Condon et al., (2015) and Tramblay et al., (2013) present case studies for future projected non-stationary flood hazard under climate change. These studies, while informative for planning, do not investigate the possibility that hydrologic state feedbacks on riverine flooding are occurring within the system, which may have the effect of further increasing or decreasing the distribution of flood hazard. Higher frequency changes in flood discharge occur on seasonal as well as daily time scales. Hydrologic state variables (soil moisture, groundwater elevation, snowpack, and potential evapotranspiration) and environmental variables (temperature and downstream hydraulic boundary conditions) may have a significant effect on flood discharge over weekly to monthly time scales (Lo and Famiglieti, 2010; Wood et al., 2015) and may themselves change in response to a changing climate (Blöschl et al., 2007).

The importance of hydrologic state and environmental variables for predicting rainfall-runoff responses has been studied extensively as a component of flood

prediction systems. Wood et al (2015) and Wood and Schaake (2008) suggest that these hydrologic state variables (i.e. initial conditions) may have a significantly lower effect on the skill of flood hazard predictions than the forecasted meteorological conditions. Alternately, Yossef et al. (2013) demonstrate that initial hydrologic conditions may be significant in certain types of watersheds. Hydrologic forecasts for basins influenced by snowmelt cycles were shown to be highly dependent on initial conditions of the snowpack. Yossef et al. (2013) also conclude that in larger basins the groundwater and unsaturated zone moisture content may have a noticeable effect on forecasted streamflow. Mahanama et al. (2012) demonstrate that knowledge of both snowmelt and soil moisture significantly improved model-based streamflow predictions in the northeast US.

1.1 Research Objectives

First, we demonstrate which hydrologic state variables have an influence on the rainfall-runoff flood stage response of the Fall Creek watershed (Tompkins County, NY USA). Fall Creek is a relatively small basin (drainage area 324 km^2) with a flood regime strongly influenced by spring precipitation and snowmelt events (USGS, 2015). We propose that small watersheds with saturation-excess precipitation runoff responses and a significant snowfall and melt cycle, such as those found within Tompkins County NY USA, may be largely influenced by the present day hydrologic state similar to conclusions presented by Yossef et al. (2013) and Mahanama et al. (2012).

We further illustrate the sensitivity of riverine flood stage to hydrologic conditions by examining the temporal persistence of riverine flood stage with respect

to extreme hydrologic initial conditions. Weijs et al. (2013a, b) demonstrate the tendency for hydrologic states (in their case, streamflow) to be highly compressible data sets due to a strong temporal persistence. They show that hydrologic time series can be described with less computer memory based on our knowledge of how present conditions are strongly related to past conditions. Hydrologic conditions often have a high autocorrelation particularly during drought conditions. We propose that hydrologic state variables are not only a consideration for flood initiating conditions at the onset of precipitation, but also introduce a form of memory to the rainfall-runoff response of a landscape.

Finally, we present estimates of the influence of anticipated climate change forcing (temperature and precipitation) on changes to the seasonal distributions of hydrologic state variables, and in turn, the flood regime. While our methodology is applied to a small temperate watershed with a seasonal snowmelt pattern, the approach is generalizable to any watershed type. We agree that more intense precipitation may result in a greater proportion of runoff, but will likely lower soil water, groundwater. Similarly, increased winter temperatures will decrease snowpack recharge. We hypothesize that the flood discharge from a small temperate watershed with a shallow confining layer and seasonal snow accumulation and melt may not necessarily increase with respect to climate change. We present research which considers only hydrologic state variables in isolation to determine the direction of the effect of this system component under hypothetical climate-change forcing. We present detailed hydrologic modeling of a watershed forced with hypothetical climate change precipitation and

temperature datasets to investigate hypothetical changes to the seasonal distributions of hydrologic state variables and subsequent effects on flood discharge.

2. Methodology

2.1 Study Location: Fall Creek Watershed

Fall Creek is a fourth order stream which flows through Ithaca, NY USA (Figure 2.1). Within Ithaca, Fall Creek is contained within a man-made 30 m wide trapezoidal earthen channel. Extreme precipitation events over the Fall Creek watershed have resulted in several flooding events within Ithaca, NY in recent history (Michael Thorn, city engineer, personal communication). Flooding of Fall Creek and the surrounding neighborhoods occurred in 2005 and 1993 (USGS, 2015) as peak flows overwhelmed the capacity of the existing channel within Ithaca and overtopped the earthen levees. The flood elevation for Fall Creek is 3 m above the channel bed and stream gage datum. All hazard estimates presented within this research are representative of the flow depth of Fall Creek at Ithaca, NY.

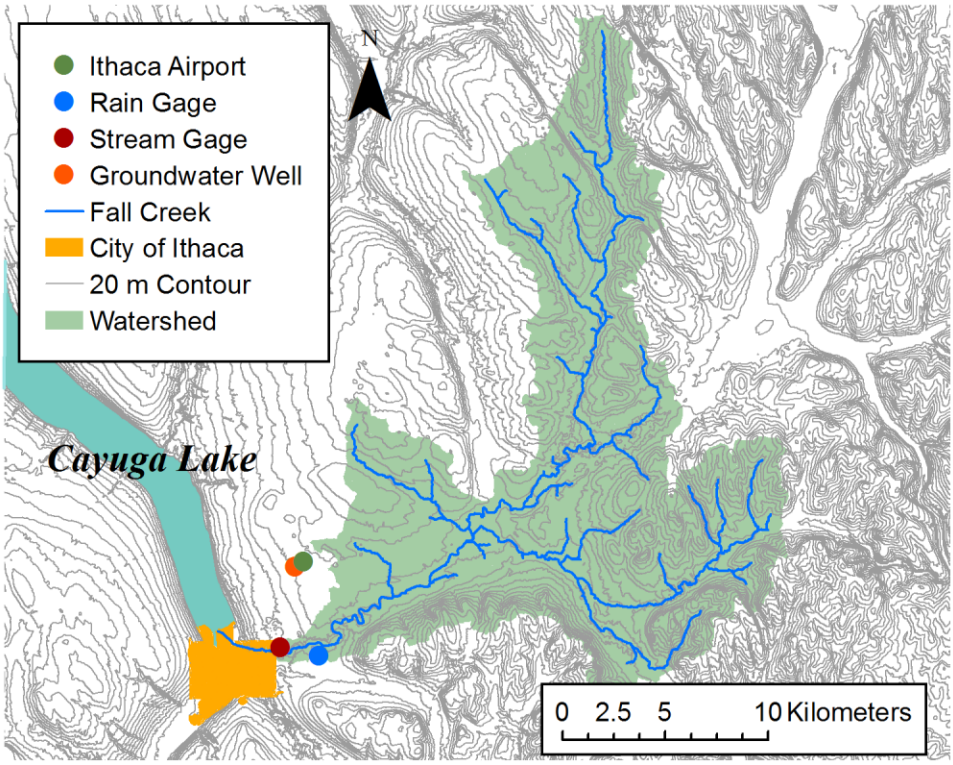

Figure 9 – Fall Creek Watershed, City of Ithaca and locations of air temperature, snowpack depth, groundwater elevation and streamflow monitoring stations

The contributing watershed to Fall Creek is a 324 km^2 mixed forested and agricultural watershed located in Tompkins County, NY (Latitude: 42° 28', Longitude: 76° 27'). The soil profile consists primarily of silt loam and silty clay loam with a shallow confining layer at a depth of approximately 0.5 to 1 m (USDA NRCS, 2015). Easton et al. (2007) and Dahlke et al. (2009) propose that the rainfall-runoff response of NY primarily exists as a saturation-excess hydrologic condition. They propose that precipitation events typically do not generate overland runoff from most of the watershed and only do so when and where soils are highly saturated as a saturation excess process.

Fall Creek drains to Cayuga Lake on the north side of Ithaca, NY. The water surface elevation of Cayuga Lake varies seasonally and serves as a downstream boundary condition on Fall Creek. The elevation of Cayuga Lake is recorded at a daily

time interval from 1956 – present (USGS, 2015). Lake levels are the downstream boundary condition on Fall Creek. High lake levels could feasibly cause flooding during smaller precipitation events due to a higher hydraulic grade line (HGL) required to push flow out to Cayuga Lake against the boundary condition. Daily values are assumed constant over a given day. Hourly air temperature data for the Fall Creek watershed were obtained from the Ithaca Airport (NOAA NCEI, 2015). Hydrologic computations within SWMM interpolate between hourly air temperature values. Precipitation data for Fall Creek were obtained from a 60-year record of hourly precipitation depths recorded at the Game Farm Road weather station in Tompkins County, NY USA (Latitude: 42° 27' N Longitude: 76° 27' W) at an elevation of 292 m NAVD88 (NRCC, 2015).

Fall Creek at Ithaca, NY has a mean 15-minute flow rate of 3.71 m^3/s (10th and 90^{th} percentiles of 1.61 m^3/s and 10.62 m^3/s respectively) (USGS, 2015). The watershed experiences mean annual precipitation of 94.7 cm (10^{th} and 90^{th} percentiles of 84.3 cm and 114.5 cm), with approximately 17% of the mean annual precipitation falling as snow (NRCC, 2015). Air temperatures range from -11.6 to 17.2° C (10^{th} and 90^{th} percentiles of hourly air temperatures) (NRCC, 2015). Cayuga Lake water surface elevations range from 115.67 to 116.74 m NGVD1929 (10^{th} and 90^{th} percentiles of daily average lake elevation) (USGS, 2015).

2.2 Flood Stage and Discharge Modeling with EPA SWMM

We develop a United States Environmental Protection Agency (EPA) Storm Water Management Model (SWMM) (build 5.1.010) of Fall Creek to predict hydrologic responses and flood stage and discharge. SWMM is a combined hydrologic

(rainfall-runoff) and hydraulic (stream routing) model. The hydrologic module of SWMM is capable of predicting infiltration-excess and saturation-excess rainfall-runoff responses, unsaturated zone soil moisture fluctuations, groundwater flow and snow accumulation and melt (Rossman, 2010).

Snowmelt is calculated based on heat budget accounting via a modified degree-day method. Melt from the accumulated snowpack is determined from existing snow pack temperature and moisture content, energy inputs from air and precipitation, and user supplied base temperature and melt coefficients scaled to the day of the year (for additional details on SWMM snowmelt see Rossman [2010]). We note that SWMM does account for mean watershed elevation in computing snowmelt, yet does not account differences in elevations between subcatchments which may have an influence on snowmelt. Grusson et al (2015) demonstrate this effect of elevation on snowmelt within the Soil and Water Assessment Tool (SWAT).

Infiltration is solved with the Green & Ampt infiltration model. The groundwater module imposes saturation-excess conditions when the simulated water Table 2.rises to the ground surface. The unsaturated zone moisture content controls the instantaneous infiltration rate. SWMM is a lumped term hydrologic model. Each subcatchment is defined by one set of representative parameter values (e.g. slope, soil textures). The hydraulic model of SWMM is one-dimensional routing model based on the dynamic-wave solution of the St. Venant equations.

The Fall Creek watershed model is composed of 424 individual subcatchments with a mean contributing area of 0.6 km^2. The hydraulic model is a simplified drainage network composed of 363 conduits. Model topography and bathymetry were

determined from the National Elevation Dataset (USGS, 2016). We force the model with hourly precipitation and air temperature data and daily lake water surface elevations. The time step used for all hydrologic calculations (e.g. infiltration, runoff, snowmelt) is 5 minutes. The hydraulic time step for in-channel routing was 30 seconds to meet the Courant-Friedrichs-Lewey condition of the explicit dynamic-wave solution technique.

2.3 Model Corroboration

Brigode et al. (2014) suggest that the hydrologic model parameterization is a significant component of a probabilistic flood hazard prediction. They suggest that hydrologic calibration is potentially more important than initial hydrologic conditions in flood hazard estimation; however they note that these findings may be erroneous in watersheds with a strong groundwater influence. We propose that the shallow confining layer of Tompkins County will result in hydrologic state variables having a significant influence on flood hazard. The influence of hydrologic parameterization on flood hazard estimates is acknowledged as important.

We calibrated our hydrologic model to observed daily snowpack, daily groundwater elevations and hourly streamflow data from January 1, 2013 – January 1, 2014. By evaluating snowpack, groundwater and streamflow we may ensure that the Fall Creek SWMM model is adequately representing multiple components of the hydrologic cycle. Daily snow pack observations were obtained from the Ithaca Cornell U. station 304174 (NOAA, 2016). Daily groundwater elevations were obtained from USGS groundwater station 422920076275301 (USGS, 2016). We compare average watershed daily snowpack and groundwater depth to point measurements of each

observation. We acknowledge that snowpack and groundwater depth observations were made outside of the Fall Creek watershed; however, we believe these are representative measurements due to the very close proximity (Figure 2.1) and similarity in geology (NRCS, 2016). Hourly streamflow data for the Fall Creek watershed was obtained from USGS gage 04234000 (USGS, 2015).

We perform parameter calibration using the dynamically dimensioned search (DDS) hydrologic parameter calibration algorithm (Tolsen and Shoemaker, 2007) with the Nash Sutcliffe Efficiency (NSE) (Nash & Sutcliffe, 1970) as the model performance objective function. In the case of the snowpack model we use two objective functions, NSE and percentage of days in which the model correctly simulates snow presence versus absence (P/A) to avoid allowing large pack accumulations from dominating the NSE and therefore the snow pack calibration. For each sub-model (snow, groundwater, streamflow) we ran the DDS algorithm for 1,000 simulations with a disturbance factor of 0.2 to identify the region of the optimal parameter set. We then perform a second set of 1,000 simulations with a disturbance factor of 0.05 to refine the model parameters. EPA SWMM parameters feasible ranges supplied to the DDS algorithm values are presented in Table 2.1.

Table 5 – *SWMM Model calibration parameter ranges and final calibrated values*

Model	Parameter	Units	Min	Max	Calibrated
Snowpack	Dividing Temp[1]	degrees C	-3	3	1.024
	ATI weight[2]	Fraction	0	1	0.928
	Negative melt ratio	Fraction	0	1	0.703
	Min. Melt coefficient	$mm*hr^{-1}*deg\ C^{-1}$	0.0001	0.1	0.063
	Max. Melt coefficient	$mm*hr^{-1}*deg\ C^{-1}$	0.0001	0.1	0.063
	Base temperature[3]	degrees C	-3	3	0.310
	Fraction free water	Fraction	0	1	0.358
Groundwater	Aquifer Porosity	Fraction	0.2	0.6	0.358
	Wilting Point	Fraction	0.01	0.2	0.147
	Field Capacity	Fraction	0.2	0.6	0.255
	Aquifer K_{SAT}[4]	$mm*hr^{-1}$	0.01	20	2.150
	Evaporation Ratio[5]	Fraction	0	1	0.598
	A1[6]	dimensionless	5.0E-05	1.0E-03	8.1E-04

Streamflow	Percent Impervious	Fraction	0	50	25.100
	Pervious Dep. Stor.	mm	0	20	5.081
	K_{SAT} Mult.[7]	dimensionless	1	5	1.489
	Channel roughness	Manning's n	0.01	0.2	0.041

[1] dividing temperature between precipitation falling as rain and snow

[2] antecedent temperature index (ATI)

[3] temperature at which melt from the snowpack begins

[4] groundwater K_{SAT} can be specified separately from surface K_{SAT}

[5] proportion of surface ET occurring within the unsaturated zone

[6] baseflow equation coefficient (Rossman, 2009)

[7] multiplier on initial subcatchment K_{SAT} values, all model subcatchments adjusted together

2.4 Flood Stage Response to Hydrologic State Variables

2.4.1 Development of Initial Hydrologic Conditions

We first estimate the riverine flood stage response with respect to naturally varying hydrologic conditions. We utilize artificial combinations of annual forcing time series as opposed to chronologically observed data to simulate more extreme

combinations of temperature, precipitation, and lake elevation than have been observed throughout the existing period of record.

We generate synthetic 10-year time series of daily lake elevation and hourly air temperature data by resampling from the historical observed records of each dataset. This sampling procedure was chosen to preserve the temporal autocorrelation among variables. Variables are resampled independent of each other. Corresponding daily Actual Evapotranspiration (AET) values were simulated from daily minimum and maximum temperatures (Archibald & Walter, 2014; Fuka et al., 2013).

We develop a corresponding ten year synthetic record of hourly precipitation representing present day meteorological conditions through copula modeling of the dependence of precipitation event statistics. Our methodology is similar to those presented in Haberlandt and Radtke, (2014) and Paschalis et al., (2014). Genest and Favre (2007) present a review of the application of the copula concept within hydrology. We first develop probability distributions of the precipitation event statistics of depth, peak intensity, duration, temporal loading and interevent time from the observed 60 year precipitation record. We then fit a t-copula model to the conditional event statistics of depth, intensity, duration and temporal loading. The copula model and marginal distributions for duration and interevent time are then randomly sampled to generate synthetic precipitation event statistics. Further details of precipitation generation methodology are outlined in Knighton & Walter (2016). We use these statistics to construct a synthetic hourly time series of precipitation.

We apply these synthetic-forcing-data time series to the SWMM model to develop daily estimates of subcatchment groundwater elevation, unsaturated zone soil

moisture content, and Snowpack Water Equivalent (SWE) for each subcatchment to be used as initial hydrologic conditions.

2.4.2 Sensitivity of Flood Stage Response to Hydrologic State Variables

Next, we perform a second series of simulations to determine what the runoff response to a fixed amount of precipitation would have been on each day over the 10 year synthetic period. In this way we may determine how changing hydrologic state variables affect the flood stage response independent of the probability of precipitation. Our methodology is similar to the "Long Term Hydrologic Simulation Method" for flood hazard responses described in Lawrence et al. (2013). Lawrence et al. (2013) use this methodology to estimate the distribution of aleatory uncertainty surrounding the rainfall-runoff response for a given design precipitation event. While our methodology is similar, we employ this procedure to evaluate both uncertainty surrounding flood depth and runoff responses to the 1-year precipitation event as well to study relationships between hydrologic state variables and flooding potential.

Hydrologic state variables for each day are initialized using the daily hydrologic conditions determined in Section 2.3.1. Next we replace the actual precipitation with a synthetic 44.6 mm precipitation event occurring over 24 hours distributed based on the SCS Type-2 hyetograph (SCS, 1986). This event is approximately the 1-year storm for Ithaca, NY as estimated by Perica et al., (2015). The somewhat arbitrary precipitation forcing event was chosen to be large enough that infiltration-excess runoff would occur during periods of drought and small enough that saturation-excess conditions would not dominate each simulation independent of the initial hydrologic conditions. Each fixed precipitation simulation was carried out for

three days to capture all flood routing within Fall Creek. Following each simulation, initial hydrologic conditions are reset to those determined in Section 2.3.1 and the design precipitation is advanced forward one day. This procedure is repeated throughout the entire time series.

We divide the dataset into "warm" and "cool." The dividing dates between the datasets are May 1st and October 1st. First- and second-order interactions between hydrologic state variables and flood stage are evaluated. We perform a regression analysis of each initial condition hydrologic state variable against the resulting peak water surface elevation of Fall Creek within Ithaca, NY as a measure of the flood hazard. We use the linear regression coefficient of determination (R^2) and Spearman's Ranked Correlation Coefficient (ρ) as measures of the importance of this particular state variable on flood stage prediction.

2.5 Flood Stage Persistence Due to Hydrologic States

We evaluate how much future hydrologic flood regime is controlled by present day hydrologic conditions. Our hypothesis is that hydrologic extremes will influence the rainfall-runoff response for a significant period of time. Previous research has demonstrated that hydrologic state variables may be used to refine predictions of future discharge (Wood et al. 2015, Yossef et al. 2013, Mahanama et al. 2012, and Lo and Famiglieti 2010). Similarly, Weijs et al., (2013a, b) demonstrate that this prediction capability exists because of the temporal persistence of hydrologic states. We intend to demonstrate this temporal influence by performing random walk forecasts beginning from two hydrologic extremes: "saturated" and "drought."

To demonstrate this effect, we select two days within the synthetic 10-year continuous record to represent present day conditions under high and low runoff potential. We select the high runoff day (herein referred to as the "saturation" case) as a day immediately following a large precipitation recharge event with a significant snowpack during the spring season where the ambient air temperature regularly crosses the dividing temperature between snow and rain. We select the low runoff day (herein referred to as the "drought" case) as a day with seasonally low water Table 2.and unsaturated zone moisture content during the summer months with no snowpack. We present these two case studies to demonstrate not only the immediate effect of hydrologic state variables on flood risk, but the ability for extreme hydrologic conditions of the landscape to control the persistence of flood stage.

For each case, we project future hydrologic and environmental conditions by allowing hydrologic (snowpack, soil moisture, groundwater) and environmental (lake elevation) variables to progress along a random walk (Equation 1). We define the random walk step length as the change in hydrologic state value from the first time step of each day. The distribution defining each random walk step length was derived from the time series of each hydrologic state variable as determined in Section 2.3.1.

$$H_t = H_{t-1} + \varphi_t \quad (1)$$

Where,

H_t – hydrologic or environmental state at time t

Φ_t – random disturbance drawn from distribution of hydrologic state variable daily step lengths

Temperatures were modeled as a random walk with mean reversion to the monthly mean temperature (Equation 2).

$$T_t = \mu + \beta(T_{t-1} - \mu) + \varphi_t \quad (2)$$

Where,

T_t – air temperature at time t

Φ_t – random disturbance drawn from distribution of air temperature daily step lengths

β – auto-regression coefficient

μ – distribution mean (monthly average temperature)

The auto-regression coefficient (β) derived from the historical daily temperatures was 0.9116. Temperature random walks were permitted to vary between (-31, 27) °C based on historically observed extremes. Temperatures that fell outside of these thresholds were resampled. Random walks days with above freezing temperatures have the snowpack depth reduced based on the modified degree day method of SWMM (described in Section 2.2).

For each random walk for each hydrologic state we simulate the 1-year precipitation event at each day to determine the distribution of flood stage responses of Fall Creek. For each case, we compute 100 parallel walks each with a random walk length of 100 days.

2.6 Future Flood Frequency Estimation

2.6.1 Development of Sub-Daily Future Meteorological Forcing Data

We develop hypothetical future climate forcing data for the Fall Creek watershed. We review seven CMIP5 multi-model ensemble projections for the year 2100 (Taylor et al., 2012; Table 2.2) for Representative Concentration Pathway 8.5 (RCP8.5) to bracket the potential ranges considered for probable future annual precipitation and daily minimum and maximum temperatures.

CMIP5 RCP8.5 multi-model ensemble projections show agreement in the median annual maximum and minimum daily temperature increase of approximately 3 to 5 °C by 2100 (Table 2.2). We develop sets of synthetic hourly air temperature forcing data based on the ad hoc assumption that future annual temperatures can be represented by historical temperature time series shifted up by 2, 3 and 4 °C. Though more significant changes in the ambient air temperature in the form of extreme temperature events are likely to occur (Diffenbaugh et al., 2005) we adopt this simplifying assumption as we are primarily interested in examining the effects of increased time spent above 0 °C.

CMIP5 multi-model ensemble projections demonstrate a range of future annual average precipitation for Ithaca NY USA from no substantial change (ACCESS1.3, BCC-CSM1.1, BNU-ESM, CANESM2, CCSM4, CNRM-CM5, and GFDL-ESM2G) to a decrease (INM-CM4) in median annual precipitation totals by 2100 (Table 2.2). CMIP5 projections include daily total precipitation which do not properly inform us on flooding responses within smaller catchments which are possibly controlled by sub-daily duration precipitation events (Knighton and Walter, 2016). To develop sub-daily precipitation time series we manipulate the copula rainfall distribution (described in Section 2.3.1) parameters of peak intensity and event depth. DeGaetano (2009)

provides evidence that the distributions of extreme precipitation events are shifting towards more intense events. DeGaetano (2009) shows that the Generalized Extreme Value (GEV) distribution's describing precipitation event statistics display a change in the distribution location parameter, but consistency in the shape and scale parameter. We propose therefore that the shape of distributions of rainfall event statistics determined for Tompkins County, NY USA can be maintained and the location parameters may be modified to simulate changes to future precipitation patterns based on climate change.

Palecki et al. (2005) present changes in the Northeast US 15-minute precipitation patterns through a cluster analysis of records from 1972 – 2002. They present observed changes to distributions of the precipitation event statistics depth, average intensity, peak intensity and event duration. These published values suggest that peak 15-minute intensity is generally increasing, whereas total depth and duration of precipitation are decreasing. Alternately, Diffenbaugh et al. (2005) present global climate simulations which suggest total precipitation depth is likely to remain constant under climate change; however, we will still see some increase in event intensity. These results are generally in agreement with the range of future annual precipitation presented in the CMIP5 multi-model ensemble projections. As discussed in Diffenbaugh et al. (2005) the interevent frequency of precipitation events in the Northeast US is not likely to change under the effects of a changing climate. We therefore propose no modification to the interevent parameter of the rainfall event statistics.

We develop six ad hoc climatic forcing scenarios (Table 2.3) to capture a wide range of possible shifts in hydrologic forcing. We propose Scenarios A, B, and C, which assume that total precipitation decreases while event average and peak intensity increase following observed trends identified by Palecki et al. (2005), Frumoff et al. (2007) and Hayhoe et al. (2008, 2007) and CMIP5 model INM-CM4. Scenarios D, E, and F consider average and peak precipitation intensity to increase, while total precipitation depth remains constant as in Diffenbaugh et al. (2005) and CMIP5 models ACCESS1.3, BCC-CSM1.1, BNU-ESM, CANESM2, CCSM4, CNRM-CM5, and GFDL-ESM2G. Similarly, Ye et al. (2016) present findings for Eurasia which suggest higher atmospheric temperatures may be associated with an increasing in event intensity, but not a change to event depth.

Table 6 – CMIP5 mulit-ensemble global climate models used to estimate future changes to annual precipitation and daily maximum and minimum temperatures

Model	Institute ID	Δ Precipitation[1]	Δ Temperature[2]
ACCESS1.3	CSIRO-BOM	3.5%	4.3
BCC-CSM1.1	BCC	8.6%	4.2
BNU-ESM	GCESS	-3.1%	4.4
CANESM2	CCCMA	9.0%	4.8
CCSM4	NCAR	5.7%	3.4
CNRM-CM5	CNRM-CERFACS	8.0%	2.5
GFDL-ESM2G	NOAA GFDL	6.3%	4.1
INM-CM4	INM	-14.8%	3.1

[1] estimated difference in median annual precipitation between the periods of 2015 – 2025 and 2080 – 2099

[2] estimated difference in median annual maximum air temperature between the periods of 2015 – 2025 and 2080 – 2099

Table 7 – Hypothetical climate change scenarios used to force the hydrologic model to determine changes in hydrologic state variables and flood hazard

Scenario	Δ T (°C)[1]	Event Depth	Event Duration	Peak Hourly Intensity[2]
A	+ 2	- 10%	- 10%	+ 10%
B	+ 3	- 20%	- 20%	+ 20%
C	+ 4	- 30%	- 30%	+ 30%
D	+ 2	0%	- 10%	+ 10%
E	+ 3	0%	- 20%	+ 20%
F	+ 4	0%	- 30%	+ 30%

[1] Change in instantaneous ambient air temperature from historical observed temperatures

[2] Peak hourly average precipitation intensity

2.6.2 Landscape Flood Discharge Response to Changes in Climatic Forcing

Next we isolate the effects of watershed hydrology on the future flood discharge estimates. We evaluate the effects of changes to temperature and precipitation forcing data on high-frequency changes in hydrologic state variables and in turn the effect this has on riverine flood discharge. We use the hypothetical future climate data (Section 2.4.1) to force the Fall Creek SWMM model to develop time series of hydrologic state variables under climate change. These hydrologic time series

(soil moisture, groundwater elevation and SWE) are then used to initialize simulations as described in Section 2.3.2 to determine the flood discharge response to a fixed precipitation event.

We evaluate the changes in flood discharge response to the present day 1-year 24-hour precipitation event attribuTable 2.to hydrologic state variables as outlined in Sections 2.4.1 and 2.4.2. This analysis methodology specifically does not present the anticipated changes in flood discharge probability distributions, but rather isolates the effects of altered hydrologic state variables on flood discharge. Therefore we do not modify the depth of 1-year precipitation event between cases evaluated. By holding the design precipitation constant we assess how the landscape response to climate change could affect flood discharge, focusing specifically the direction of the influence.

3. Results and Discussion

3.1 Model Corroboration

We corroborated the Fall Creek SWMM model by simulating January 1, 2013 – January 1, 2014 with observed hourly precipitation and temperature data and daily lake water surface elevations. The snowmelt model (NSE: 0.41, P/A: 89%), groundwater (NSE: 0.47) and streamflow (hourly NSE: 0.45, daily: 0.5) (Table 2.1, Figure 2.2) are adequate representations of the hydrology (Moriasi et al 2007). For the snowpack model we note that some observed trace snowpack accumulations were not simulated; however, the major snowmelt events of 2013 are captured. The SWMM model adequately represents both winter and summer groundwater and streamflow dynamics, specifically event peak flow rates (Figure 2.2). We note however, as stated

in Blöschl et al. (2007) that our model is imperfect and this imperfect representation of hydrology likely has some effect on our results.

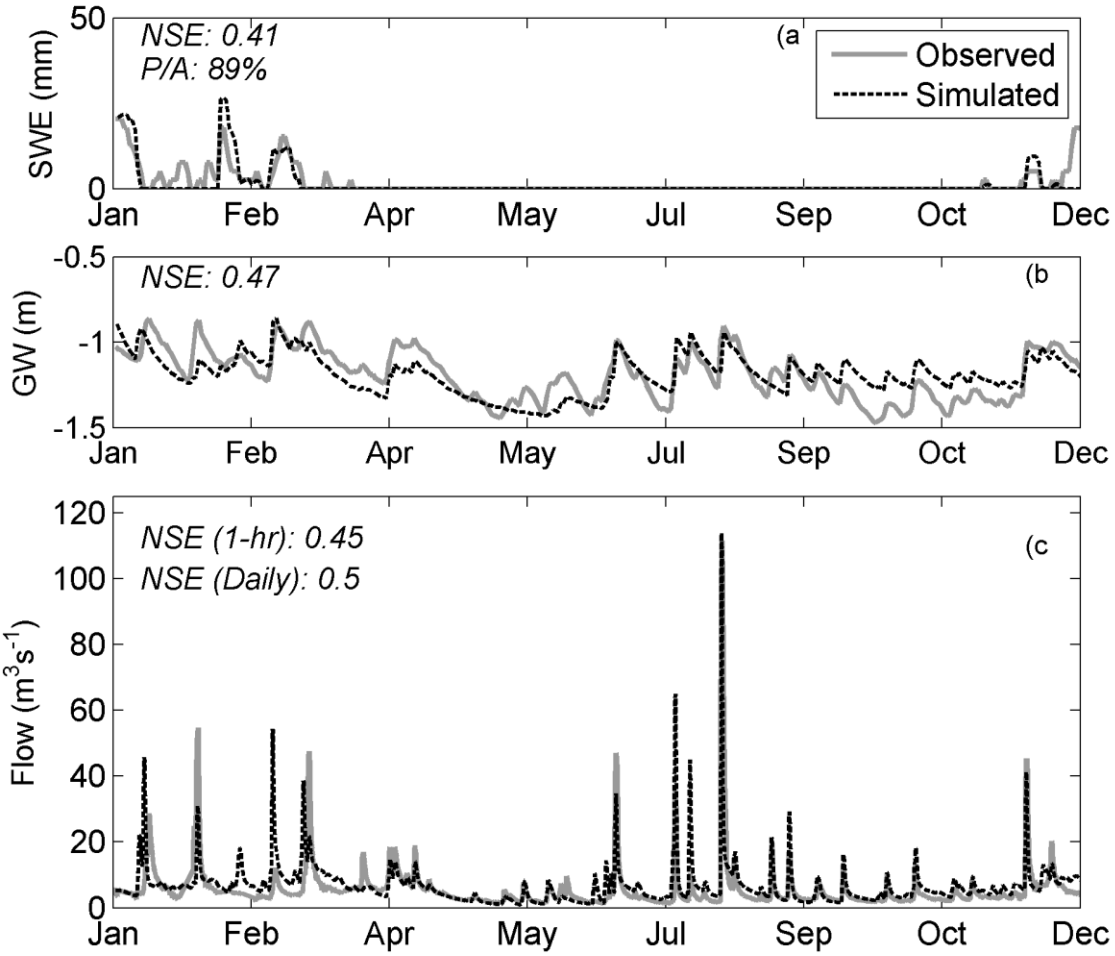

Figure 10 – Model corroboration for Fall Creek a) snowpack depth, b) groundwater elevation, and c) streamflow for 2013

3.2 Flood Stage Response to Hydrologic State Variables

The continuous synthetic record of hydrologic state variables was generated and simulated with the Fall Creek EPA SWMM model. Figure 2.3 the 10 simulated years. The rainfall-runoff flood stage response to the 1-year precipitation event over a two year period varies considerably from 0.1 m to 4 m (Figure 2.3). Simulated runoff

responses during summer months show a consistent flood stage of approximately 1 to 1.5 m within Fall Creek. During winter months the flood stage was less predicTable 2.with alternating days of low and high stage. This result suggests a more complicated runoff response to hydrologic conditions during the cool season.

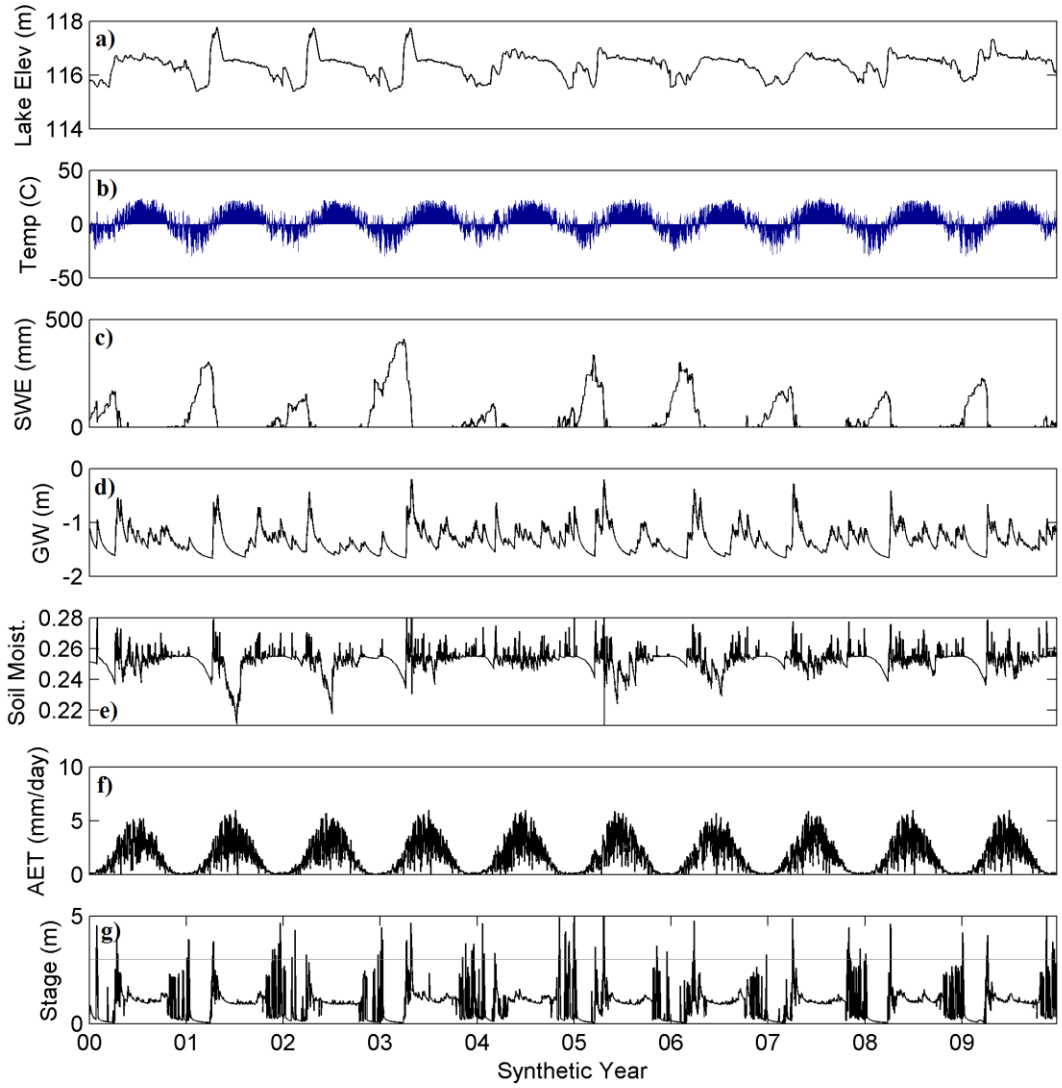

Figure 11 – Synthetic years of a) lake elevation, b) air temperature, c) snow water equivalent, d) groundwater elevation, e) unsaturated zone soil moisture, f) PET, and g) the stream depth response to 1-year 24 hour precipitation event for each day, and the flood stage elevation (gray horizontal line)

The periods of the year showing the highest influence of hydrologic state variables on flood stage are the spring and fall seasons. During these periods of time an elevated water table, soil moisture, potential presence of a snowpack and temperatures crossing the precipitation/snow dividing boundary create a potential for large combined runoff and snowmelt events.

Table 8 – Correlation of hydrologic state variables and flood hazard as measured by coefficient of determination for a linear relationship (R^2) and Spearman's Ranked Correlation Coefficient (ρ)

	Warm-Season		**Cool-Season**	
Variable	**ρ**	**R^2**	**ρ**	**R^2**
Lake	0.069	0.043	-0.020	0.000
Air Temp	0.056	0.003	-0.048	0.002
SWE	-0.153	0.023	0.053	0.003
GW	0.656	0.431	0.102	0.010
Soil Moisture	0.238	0.056	0.042	0.002
PET	-0.017	0.000	-0.053	0.003

The effect of each hydrologic state variable on the watershed flood response was estimated using first order interactions (Table 2.4) and then by considering two-dimensional hydrologic state regressions against the magnitude of the flood stage (Figures 4 and 5). We consider these two-dimensional representations of the results as they allow evaluation of the effects of marginal distributions as well as interactions between variables.

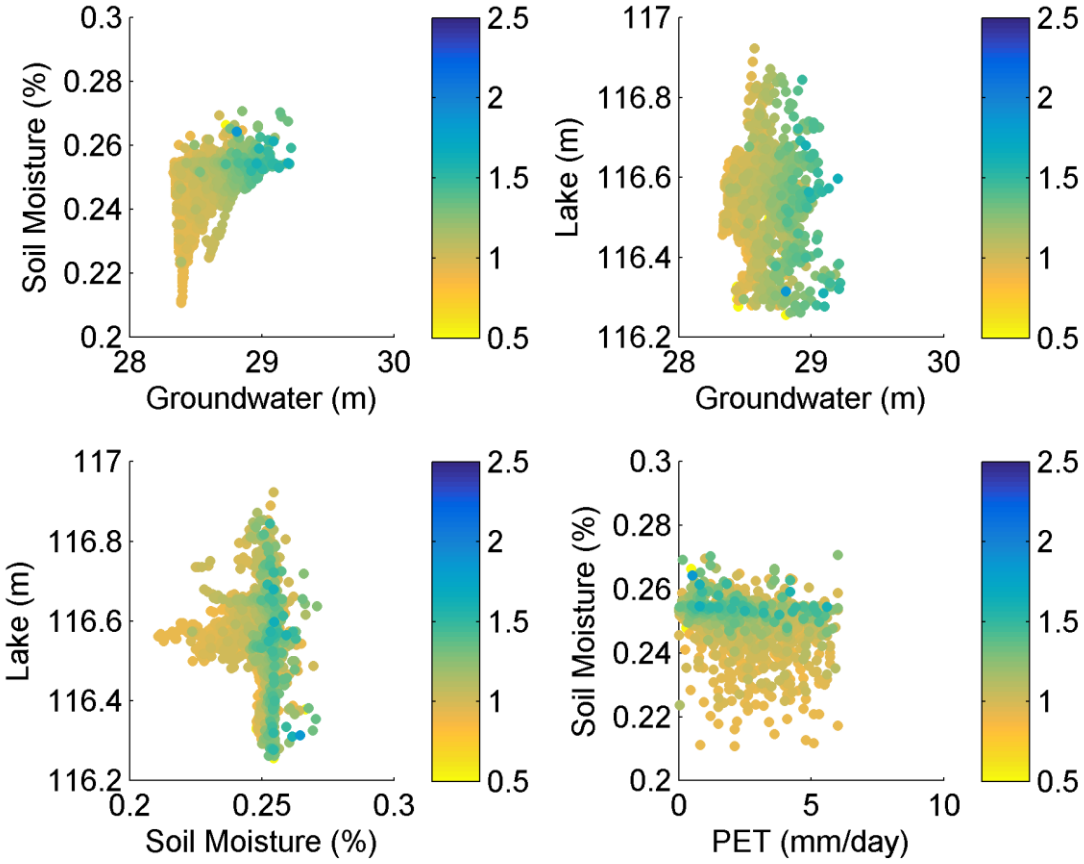

Figure 12 – Two-dimensional distributions of flood stage for warm-season days; color scale indicates flood depth within Fall Creek in meters

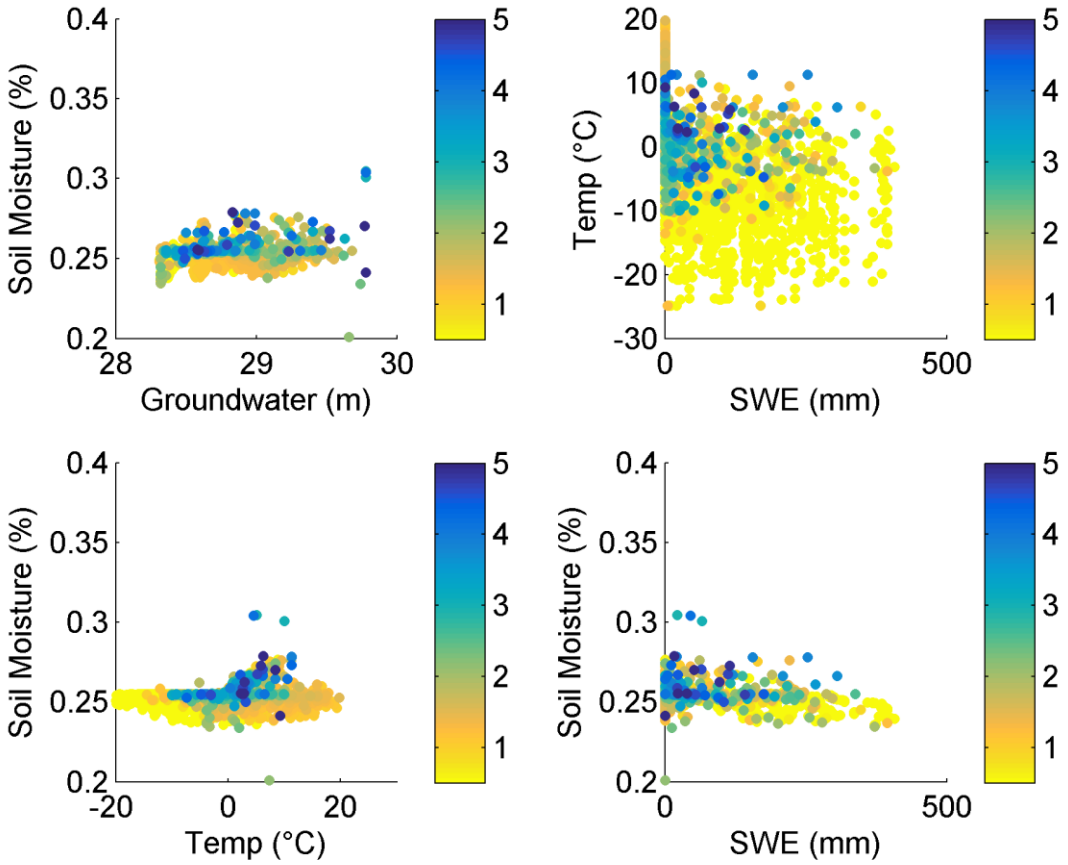

Figure 13 – Two-dimensional distributions of flood stage for cool-season days; color scale indicates flood depth within Fall Creek in meters

During warm-season days the flood stage is primarily a function of the groundwater elevation and soil moisture content (Table 2.4, Figure 2.4a). The Fall Creek watershed does experience a saturation excess response (Walter et al. 2005; Easton et al., 2007); however, it should be noted that the results suggest that infiltration-excess conditions throughout the watershed are also a consideration for predicting flood stage responses from larger precipitation events, particularly during the summer months. The highest flooding events occur during periods of high groundwater elevation and high soil moisture content.

Within natural watersheds the soil moisture content at the start of precipitation has been shown to be a significant consideration for estimating the runoff response of a watershed (Massari et al., 2014a, b; 2015; Nied et al., 2013; Mahanama et al., 2012; Norbiatio et al., 2008; Ravazzani et al., 2007; Smith et al., 2015; Elbialy et al., 2014). The (Simulation Climato-Hydrologique pour l'Appréciation des Débits EXtrêmes) SCHADEX program is an example of a flood prediction system that provides estimates of future flood hazard based in part on historical hydrologic states including soil moisture content (Paquet et al., 2013). Soil profiles with a shallow confining layer exhibit a precipitation runoff response that is dependent on the depth to water Table 2.(Lo and Famiglieti, 2010). Under infiltration-excess conditions, soil moisture controls the infiltration capacity and storage within the unsaturated zone. Within Tompkins County, NY a large proportion of runoff is related to saturation-excess conditions, which persist when the water Table 2.rises close to the land surface (Easton et al., 2007; Dahlke et al., 2009). An elevated water Table 2.reduces the total storage volume in the soil unsaturated zone, which would otherwise buffer additional rainfall or snowmelt depths. When the water Table 2.intersects the ground elevation (or nearly so) an impermeable surface is created which converts all rain to surface runoff. We therefore expect that the elevation of the water Table 2.should be a significant consideration for flood hazard in regions with shallow confining layers. Our results are therefore consistent with previous research.

Cayuga Lake serves as the downstream hydraulic boundary condition on Fall Creek, and therefore may have some effect on the water surface elevation within the regionally relatively heavily populated areas of Ithaca, NY (Figure 2.4). The results of

the flood stage regression suggest that the lake water surface elevation has a minimal impact on the peak flood elevation within Fall Creek as the channelized portion within Ithaca, NY is the hydraulically limiting element. The highest magnitude floods do occur at the high lake elevations; however, we also see high magnitude floods at lower lake elevations (Figures 4b). We therefore consider lake elevation to be a relatively non-sensitive state variable.

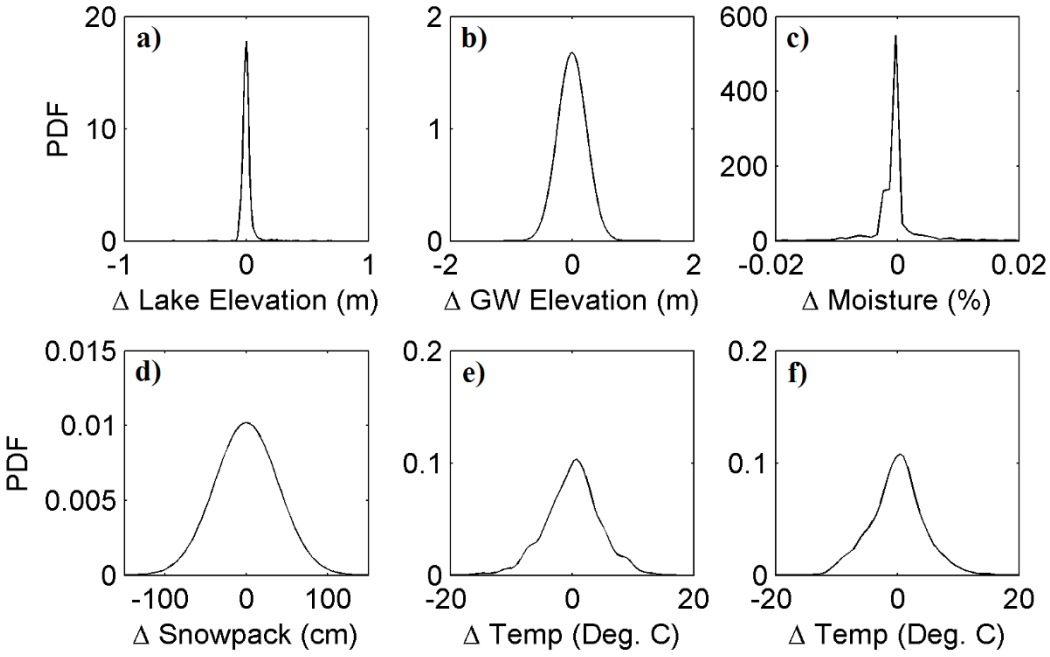

Figure 14 - Empirical probability density functions for daily changes to a) Cayuga Lake elevation, b) groundwater elevation, c) unsaturated zone soil moisture, d) snowpack, e) air temperature during warming period, and d) air temperature during cooling period

The instantaneous evapotranspiration of the landscape had no discernible influence on the precipitation-runoff response or the flood stage (Table 2.4, Figure 2.4d). The precipitation rate was significantly larger than the rate of AET and overwhelmed the effects of varying Potential Evapotranspiration (PET) losses during

runoff. We note however, that as AET has an influence on the unsaturated zone soil moisture, it is likely important over longer time scales.

Watersheds that experience freezing temperatures are subject to precipitation falling as snow and the accumulation of snowpacks. Days with warmer temperatures and increased solar radiation can induce greater runoff through snowmelt events. The extent and depth of the accumulated snowpack coupled with energy inputs has an influence on streamflow (Harrison and Bales, 2015; Perju et al., 2013; Ceppi et al., 2013; Freudiger et al., 2013; Lawrence et al., 2013; Mahanama et al., 2012, Jorg-Hess et al., 2015). Ceppi et al. (2013) present a compelling case for evaluating the uncertainty in ambient air temperatures as well as precipitation when forecasting flood hazard to identify the proportion of precipitation partitioned as snow. Lawrence et al. (2013) expand on the work of Paquet et al. (2013) to introduce the effects of snow accumulation and melt coupled with extreme precipitation to improve prediction skill. During the cool-season, flood stage is primarily correlated with air temperature (Figure 2.5c). The days producing the greatest runoff are days near 0 °C. Air temperatures near 0 °C ensures an accumulated snowpack close to melting. High discharge occurs across a wide range of groundwater and snowpack depths. This result suggests that while peak river stage is much more variable during the cool season it remains a function primarily of air temperature.

During periods with an accumulated snowpack, the influence of hydrologic state variables becomes less clearly defined overall (Table 2.4, Figure 2.5). The groundwater elevation and soil moisture have some influence on the flood stage. The ambient temperature has some influence as shown by the reduced flood stage

responses for temperatures below 0 °C. There is no discernable influence of the size of the accumulated snowpack on the flood stage (Table 2.4, Figure 2.5). This result suggests that while snowpack melt does occur and has some influence on flood stage, the proportion of the snowpack that is melted on a given day is likely less than the total accumulated snowpack. We conclude that the only consideration with respect to snowpack is presence versus absence.

3.3 Flood Stage Persistence Due to Hydrologic States

Next we demonstrate the temporal influence of extreme hydrologic state conditions with respect to flood stage. We develop probability distributions of changes in hydrologic state and environmental variables (Figure 2.6) based on the ten year continuous simulation described in Section 2.3.1. These distributions demonstrate that changes to most hydrologic variables over a 24 hour period are fairly constrained. The lake water surface elevation changes gradually due to the large buffering capacity of the lake relative to the volume of runoff and precipitation inputs. Groundwater elevation and soil moisture content similarly have a high temporal persistence. The temporal persistence of these hydrologic state variables provides us with some ability to then predict, with some confidence, the probability of future hydrologic states, and therefore future runoff potential.

Temperature and snowpack demonstrate less temporal persistence. Large changes in the mean daily temperature result in significant melt events. Similarly, temperatures dropping below 0 °C result in snowpack accumulation events as all precipitation contributes to the snowpack. We considered the distribution of daily

mean temperature changes based on separate warming (February 1 – August 1) and a cooling seasons (August 1 – February 1).

The random walks of each hydrologic state were considered to be independent, with the exception of the effect of temperature on snowpack accumulation as discussed in Section 3.2. We perform hypothetical flood stage projections for a "saturated" and "unsaturated" case (Section 2.4).

Figure 2.7, representing the saturated case, illustrates how the upper bound of the 90% confidence interval for flood stage remains elevated for a period of approximately 20 days following a large snowmelt and groundwater recharge event. Beyond 20 days the flood stage distribution returns to the long term average. The high variability immediately following the event is the result of temperatures above zero jointly occurring with a snowpack. Random walks that develop positive temperatures eventually deplete the snowpack. Random walks with below 0° C temperature build up the snowpack, but contribute less runoff. As the random walks diverge from the dividing temperature for precipitation type, the probability of such an extreme runoff-snowmelt event decreases. The upper envelop of flood stage estimates shows potentially large floods of up to 5 m which significantly decrease in likelihood beyond 20 days. This result further demonstrates temperatures near 0° C as being correlated with large flood potential as in Section 3.2.

The "drought conditions" scenario (Figure 2.8) shows a similar temporal persistence of the flood stage. The absence of an initial snowpack simplifies the

predictions and reduces the large variance in flood stage seen in the "saturated condition" simulations.

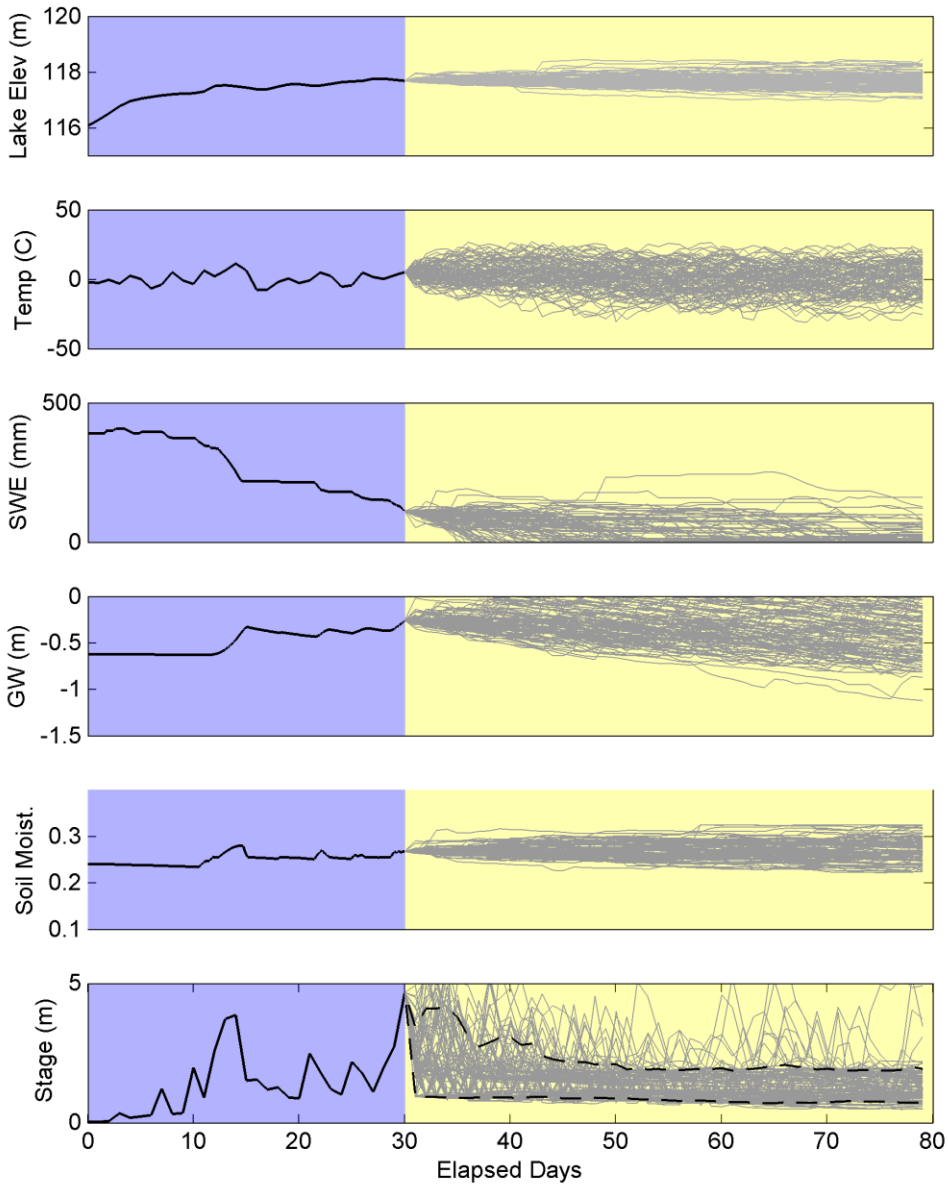

Figure 15 - Flood hazard predictions as a function of hydrologic state during saturated conditions for past known conditions (blue), and future projected conditions (yellow). The dashed line indicates the upper bound of the 90% confidence interval.

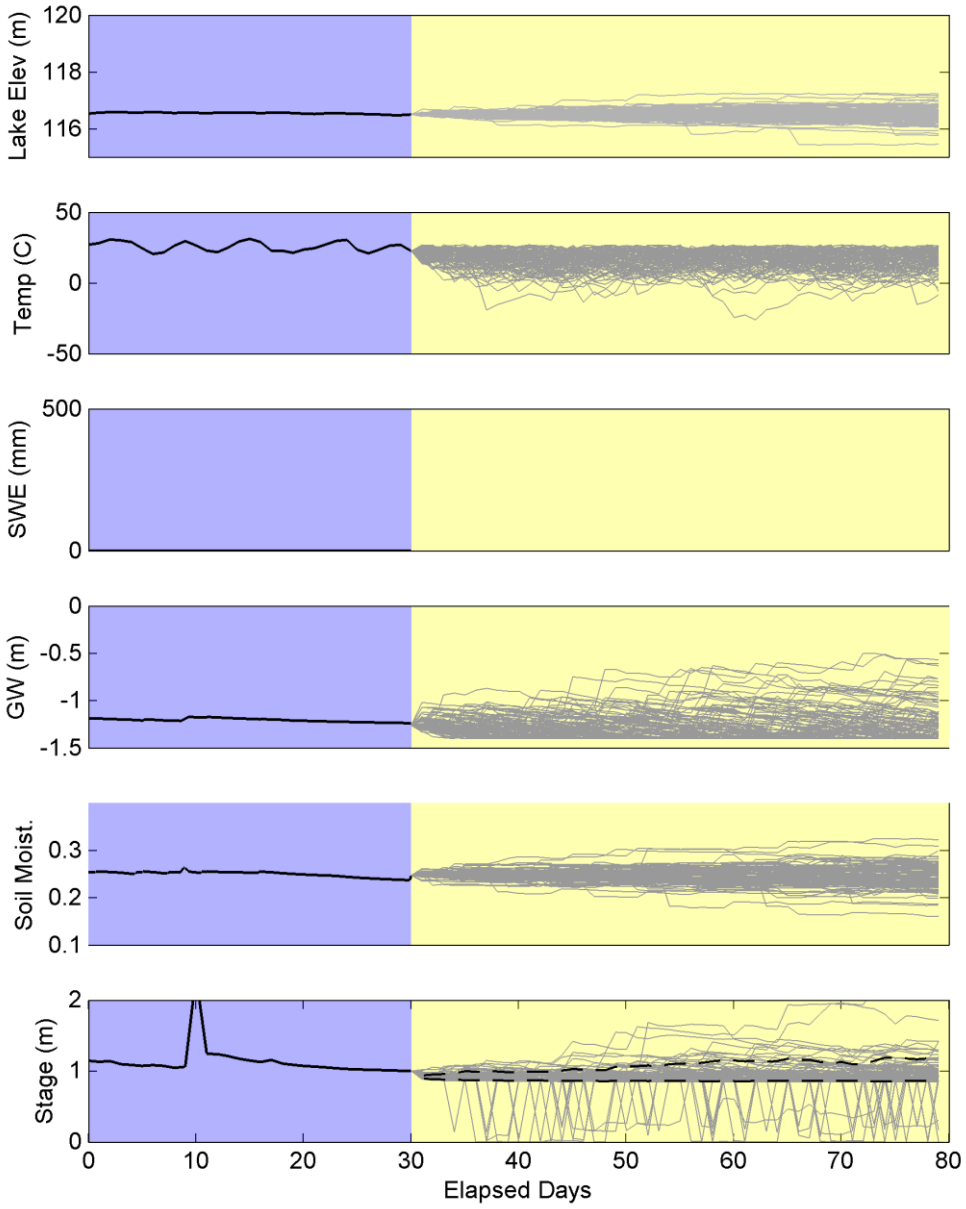

Figure 16 - Flood hazard predictions as a function of hydrologic state during drought conditions for past known conditions (blue), and future projected conditions (yellow). The dashed line indicates the upper bound of the 90% confidence interval.

Understanding the present day hydrologic state of a saturation excess landscape with a snow season, like Fall Creek, provides considerable refinement of expected flood stage for an extended period of time (Figures 7 and 8). We demonstrate that hydrologic state variables act as a source of memory for systematic predictions of flood stage responses. With respect to a monthly flood stage prediction, these higher-frequency changes in the landscape result in a somewhat variable flood stage response. Hydrologic initial conditions beyond 20 days are generally unpredicTable 2.and therefore result in large uncertainty in a flood stage forecast. When viewed at a daily to weekly time scale, however, these gradually changing hydrologic conditions can have a lasting influence on the rainfall-runoff response of a watershed. We demonstrate how extreme hydrologic conditions affect not only the runoff response of the next precipitation event (as demonstrated in Nied et al. [2013]), but may constrain the possible range of the rainfall-runoff response for several weeks throughout multiple precipitation events.

3.4 Landscape Flood Discharge Response to Changes in Climatic Forcing

The hypothetical climate datasets (described in Section 2.3.1) were used to force the Fall Creek watershed model to estimate responses in hydrologic state variables. We then introduce a design precipitation event on each day initialized by the long term hydrologic state (as described in Sections 2.3.1, 2.3.2 and 2.5) to determine what effect climate change may have on the hydrologic state variables and how in turn this affects the aleatory uncertainty of the 1-year precipitation event runoff response of Fall Creek

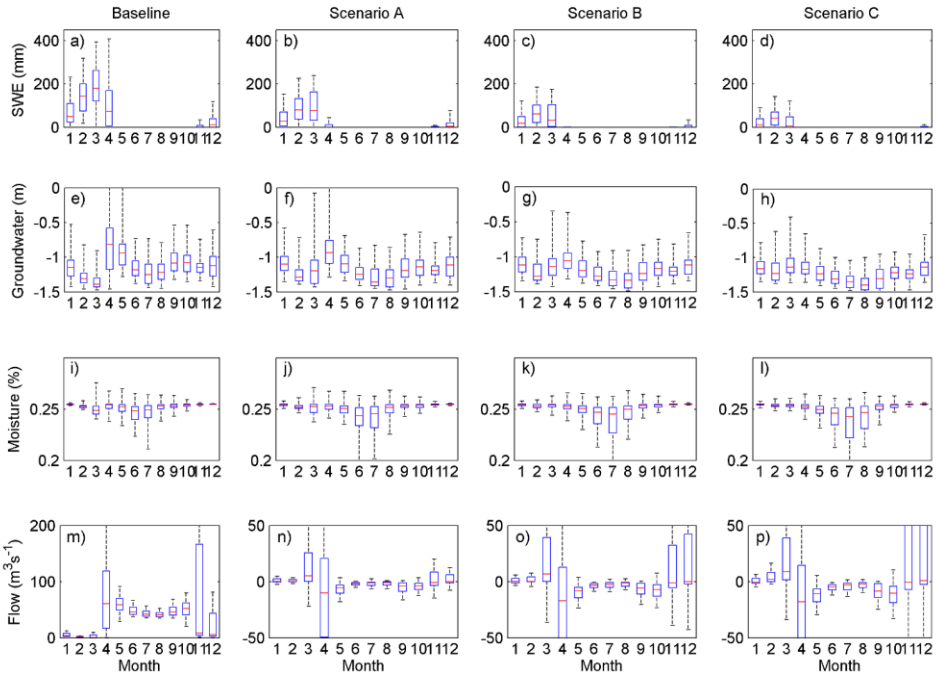

Figure 17 – Monthly distributions of hydrologic state variables and peak runoff for a fixed precipitation event under current (baseline) and projected climate change conditions (Scenarios A, B, and C). Subfigures n, o and p show distributions of difference in flow from baseline case (m) (hypothetical scenario minus baseline).

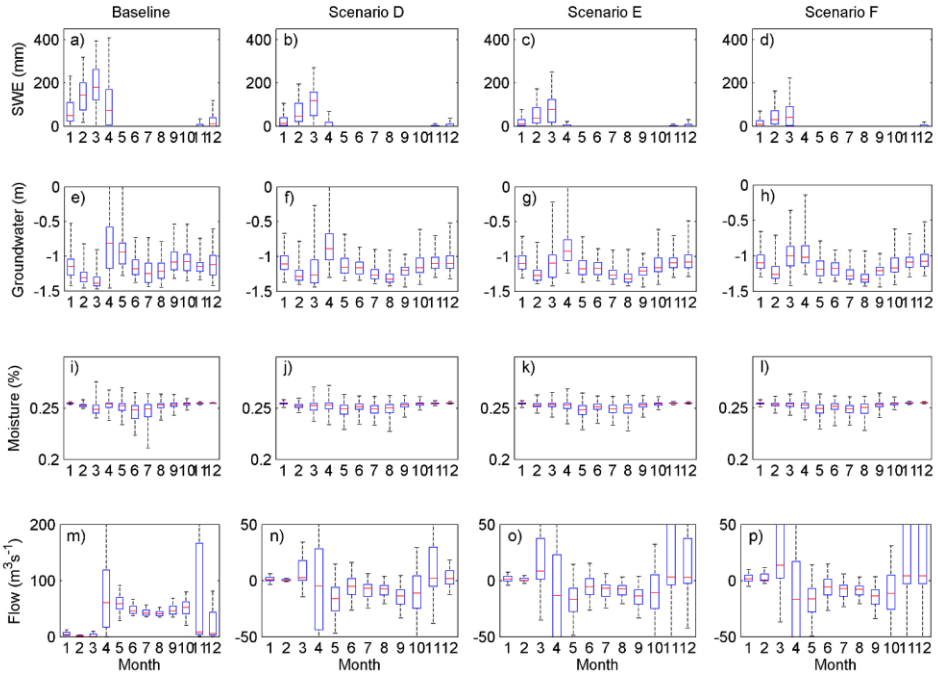

Figure 18 - Monthly distributions of hydrologic state variables and peak runoff for a fixed precipitation event under current (baseline) and projected climate change conditions (Scenarios D, E, and F). Subfigures n, o and p show distributions of difference in flow from baseline case (m) (hypothetical scenario minus baseline).

Scenarios A, B, and C assume air temperatures increase, total precipitation depth decreases, and average and peak intensity increase as in Palecki et al. (2005), Frumoff et al. (2007), and Hayhoe et al. (2008, 2007). Increasing temperature significantly decreases the accumulated snowpack during winter months (Figure 2.9a-d). The anticipated reduced snowpack accumulation over the winter results in less spring melt runoff and groundwater recharge. Groundwater elevation and soil moisture similarly trend towards drier average conditions with the exception of March where earlier snowmelt due to higher temperatures results in increased ground saturation. We observe lower or unchanged median peak discharge for all months except March

(Figure 2.9n-p, Table 2.5). The hydrology of the peak flood controlling month, April, is strongly influenced by spring precipitation and snowmelt events. The reduced April snowmelt results in a general decrease in annual peak floods. Similarly, in summer the effects of climate change on hydrologic state variables indicates that an overall negative feedback on flood discharge is likely to be created similar to conclusions presented by Surfleet and Tullos (2013). The watershed soils become drier for greater periods of the year due to higher winter temperatures, lower total precipitation and increased average and peak intensities and therefore have a greater infiltration potential.

Table 9 – Median difference in 1-year precipitation peak discharge (m^3s^{-1}) between hypothetical climate change scenarios and baseline conditions. The values represent the hypothetical scenario minus the baseline, where a negative indicates a decrease in future flow which is attribuTable 2.to the hydrologic state changes

	Scenario A	**Scenario B**	**Scenario C**	**Scenario D**	**Scenario E**	**Scenario F**
January	0.4	0.1	-0.4	0.8	1.1	1.5
February	0.1	0.1	2.0	0.2	0.3	0.6
March	5.3	6.9	8.8	2.6	8.4	13.8
April	-10.2	-17.1	-18.2	-4.9	-13.3	-16.9
May	-5.4	-8.2	-10.6	-16.1	-16.8	-16.4
June	-1.9	-3.3	-4.8	-5.1	-5.4	-5.9
July	-1.3	-2.4	-3.3	-6.7	-6.8	-7.0
August	-0.8	-1.5	-2.2	-7.4	-7.5	-7.8
September	-3.9	-5.9	-8.5	-13.6	-13.6	-13.7

October	-3.9	-7.0	-10.4	-11.0	-10.7	-11.3
November	-0.8	-1.1	-0.5	2.1	3.1	4.3
December	-0.1	0.0	0.9	1.8	2.7	4.0

Scenarios D, E, and F assume that air temperatures increase, average and peak intensity increases, while total depth remains constant as in Diffenbaugh et al. (2005) and Ye et al. (2016). As in scenarios A – C, we see a reduced snowpack (Figure 2.10a-d), wetter March and drier April through September (Figure 2.10e-l); however, the overall change in each hydrologic state variable from the baseline condition is significantly less (Figures 9 and 10). The runoff response of the watershed for scenarios D, E, and F similarly shows a similar decrease (Figure 2.10m-p, Table 2.5); however the peak flow month, April, does not decrease as significantly as in Scenarios A, B, and C. This result suggests that the air temperature, and precipitation characteristic of total rainfall event depth may be more influential than peak hourly intensity in defining future hydrologic changes. We observe that the seasonality of the groundwater elevation is somewhat exaggerated in scenarios D, E, and F. Summer months become drier; however, spring and fall remain similar to baseline conditions.

We demonstrate in Section 3.2 that initial hydrologic state conditions have a significant effect on flood response of the Fall Creek watershed to a design precipitation event. We then demonstrate in Section 3.3 that hydrologic conditions introduce a form of memory in flood stage estimation that may persist up to 20 days beyond extreme conditions. This memory further explains why climate change induced alterations of the hydrologic cycle within the Northeast US may have an

important negative feedback effect on flood hazard. Periods of reduced groundwater recharge (i.e. drought) influence not only the runoff response for the next precipitation event, but lasts until a significant precipitation depth has fallen to replenish the depleted reservoirs within the soil layers.

We present evidence that climate change may not necessarily increase flood discharge within Fall Creek despite an expected increase in intense precipitation which is similar to regional conclusions presented by Hirabayashi et al. (2013). Changes to the hydrologic states show the response of the landscape is potentially trending towards a decreased rainfall-runoff response under climate change meteorological forcing. We agree that increased air temperatures and increased hourly precipitation intensity should, in general, result in increased flooding as is proposed globally in Trenberth (2011) and Schiermeier (2011); however, we present evidence which allows us to refine this conclusion for small snowmelt influence watersheds with shallow confining layers.

Blöschl et al. (2007) hypothesize that feedbacks on hydrologic systems will form at the catchment scale as a result of modifying climate forcing. We observe this concept for Fall Creek in the form of reduced snowpack accumulation and soil saturation. Probability distributions for groundwater elevation and soil moisture content respond differently under the climate change forcing (Figure 2.9). While both variables trend towards drier conditions, we see a reduced variance in groundwater elevation and an increased variance in soil moisture content across all months for Scenarios A, B, and C (Figure 2.9). Similarly, the shape and location of the probability distributions of watershed runoff from the 1-year rainfall changes for each month

through all cases evaluated. We observe not only reduced median peak runoff, but a reduced variance in the monthly distributions of the design precipitation runoff response. Our results suggest that feedbacks from hydrologic state variables may change both the location and shape of flood discharge probability distributions, despite consistency in the shape of precipitation event statistic distributions (DeGaetano, 2009).

4. Conclusions

1. We demonstrate that the hydrologic state variables of temperature, SWE, unsaturated zone soil moisture content and groundwater elevation have an effect on flood stage using a long-term flood hazard methodology similar to that described in Lawrence et al. (2013). Flood stage in systems like Fall Creek is largely dominated by unsaturated zone soil moisture and groundwater elevation. Despite a more complex flooding response during the cool season months we do not observe strong second-order interactions among hydrologic state variables and flood stage.

2. We demonstrate the effects of extreme hydrologic state conditions on the temporal persistence of flood stage. From a fixed point in time we estimate future probable hydrologic states through random walk modeling. Each random walk chain is simulated to estimate the probability distribution of flood stage runoff response for a fixed precipitation depth. Flood stage predictions for “saturated” and “drought” conditions evaluated each show a similar flood stage persistence of about 20 days before flood stage returns to a long term average. The strong temporal persistence of hydrologic state variables causes a medium-range (20 day) constraint of possible flood

stage. These findings further demonstrate the importance of hydrologic state variables for defining the rainfall-runoff response of a watershed.

3. Watershed flooding is a function of both precipitation and hydrologic catchment conditions. Climate change is anticipated to result in increased air temperatures and altered precipitation patterns. While significant work has been done to estimate future meteorological conditions, much is currently unknown about future changes to distributions of hydrologic state variables and how they will affect the future flood regime. We demonstrate that watershed hydrology can limit or decrease flood discharge through hypothetical climate change scenarios. Higher summer air temperatures, higher precipitation intensity, and less total precipitation results in higher evaporative demand, and less soil and groundwater recharge. Similarly, higher winter air temperatures result in a reduced snowpack accumulation and earlier melt. Decreased soil saturation and snowpack accumulation results in a lower runoff potential and therefore imposes a negative influence on flood discharge. While changes in precipitation patterns may be pushing towards increasing flood hazard, watershed hydrology likely has some ability to buffer this change.

4. Hypothetical climate change scenarios in which we assume that total depth decreases and peak hourly intensity increases show a significantly larger reduction in the flood discharge than scenarios in which we assume only peak hourly intensity increases. These results suggest negative feedbacks on flood discharge may be more attribuTable 2.to changes in air temperature and total precipitation event depth as opposed to only increased precipitation intensity.

5. Blöschl et al. (2007) hypothesize that feedbacks on hydrologic systems will form at the catchment scale as a result of modifying climate forcing which we observe for Fall Creek in the form of reduced snowpack accumulation and soil saturation. Our hypothetical climate change scenarios demonstrate that hydrologic state responses to climate change occur in both the location and shape of monthly distributions of soil moisture content and groundwater elevation. These results suggest that feedbacks from hydrologic state variables may change both the location and shape of flood discharge probability distributions, despite evidence for consistency in the shape of precipitation event statistic distributions (DeGaetano, 2009).

REFERENCES

Archibald, J. A., & Walter, M. T., 2014: Do Energy-Based PET Models Require More Input Data than Temperature-Based Models?—An Evaluation at Four Humid FluxNet Sites. *Journal of the American Water Resources Association*, **50**, 497-508, doi: 10.1111/jawr.12137

Balling Jr, R. C., & Goodrich, G. B., 2011: Spatial analysis of variations in precipitation intensity in the USA. *Theoretical and Applied Climatology*, **104**, 415-421, doi: 10.1007/s00704-010-0353-0

Bell, V., Kay, A., Davies, H., Jones, R., 2016: An assessment of the possible impacts of climate change on snow and peak river flows across Britain. *Climatic Change*, 136, 539 – 553, doi: 10.1007/s10584-016-1637-x

Blöschl, G., Gaál, L., Hall, J., Kiss, A., Komma, J., Nester, T., Parajka, J., Perdigao, R., Plavcova, L., Rogger, M., Salinas, J., & Viglione, A. 2015: Increasing river

floods: fiction or reality? *Wiley Interdisciplinary Reviews: Water*. doi: 10.1002/wat2.1079

Blöschl, G., Ardoin-Bardin, S., Bonell, M., Dorninger, M., Goodrich, D., Gutknecht, D., Matamoros, D., Merz, B., Shand, P., & Szolgay, J. 2007: At what scales do climate variability and land cover change impact on flooding and low flows? *Hydrological Processes*, **21**, 1241-1247, doi: 10.1002/hyp.6669

Bouwer, L. M. 2011: Have disaster losses increased due to anthropogenic climate change? *Bull. Amer. Meteor. Soc.*, **92**, 39-46, doi: 10.1175/2010BAMS3092.1

Brigode, P., Bernardara, P., Paquet, E., Gailhard, J., Garavaglia, F., Merz, R., Micovic, Z., Lawrence, D., & Ribstein, P. 2014: Sensitivity analysis of SCHADEX extreme flood estimations to observed hydrometeorological variability. *Water Resources Research*, **50**, 353-370, doi: 10.1002/2013WR013687

Butler, D. R. 1989: The failure of beaver dams and resulting outburst flooding: a geomorphic hazard of the southeastern Piedmont. *The Geographical Bulletin*, **31**, 29-38.

Carsell, K. M., Pingel, N. D., & Ford, D. T. 2004: Quantifying the benefit of a flood warning system. *Natural Hazards Review*, **5**, 131-140, doi: 10.1061/(ASCE)1527-6988(2004)5:3(131)

Ceppi, A., Ravazzani, G., Salandin, A., Rabuffetti, D., Montani, A., Borgonovo, E., & Mancini, M. 2013: Effects of temperature on flood forecasting: analysis of an operative case study in Alpine basins. *Natural Hazards and Earth System Science*, **13**, 1051-1062, doi: 10.5194/nhess-13-1051-2013

Condon, L. E., Gangopadhyay, S., & Pruitt, T. 2015: Climate change and non-stationary flood risk for the upper Truckee River basin. *Hydrology and Earth System Sciences*, **19**, 159-175. doi: 10.5194/hess-19-159-2015

Dahlke, H. E., Easton, Z. M., Fuka, D. R., Lyon, S. W., & Steenhuis, T. S. 2009: Modelling variable source area dynamics in a CEAP watershed. *Ecohydrology*, **2**, 337-349. doi: 10.1002/eco.58

DeGaetano, A. T. 2009: Time-dependent changes in extreme-precipitation return-period amounts in the continental United States. *J. Appl. Meteor. Climatol.*, **48**, 2086-2099. doi: 10.1175/2009JAMC2179.1

Diffenbaugh, N. S., Pal, J. S., Trapp, R. J., & Giorgi, F. 2005: Fine-scale processes regulate the response of extreme events to global climate change. *Proceedings of the National Academy of Sciences of the United States of America*, **102**, 15774-15778. doi: 10.1073/pnas.0506042102

Easton, Z.M., Gérard-Marchant, P., Walter, M.T., Petrovic, A.M., & Steenhuis T.S. 2007: Hydrologic assessment of an urban variable source watershed in the Northeast United States. *Water Resources Research*, **43**, doi: 10.1029/2006WR005076

Elbialy, S., Mahmoud, A., Pradhan, B., & Buchroithner, M. 2014: Application of spaceborne synthetic aperture radar data for extraction of soil moisture and its use in hydrological modelling at Gottleuba Catchment, Saxony, Germany. *Journal of Flood Risk Management*, **7**, 159-175. doi: 10.1111/jfr3.12037

Freudiger, D., Kohn, I., Stahl, K., & Weiler, M. 2013: Large scale analysis of changing frequencies of rain-on-snow events and their impact on floods.

Hydrology and Earth System Sciences Discussions, **10**, 13231-13263. doi: 10.5194/hessd-10-13231-2013.

Frumhoff, P. C., McCarthy, J. J., Melillo, J. M., Moser, S. C., & Wuebbles, D. J. 2007: Confronting climate change in the US Northeast. A report of the northeast climate impacts assessment. Union of Concerned Scientists, Cambridge, Massachusetts.

Fuka, D. R., Walter, M. T., Archibald, J. A., Steenhuis, T. S., & Easton, Z. M., 2013: EcoHydRology: a community modeling foundation for eco-hydrology. R package version, 49.

Genest, C., & Favre, A. C. 2007: Everything you always wanted to know about copula modeling but were afraid to ask. *Journal of Hydrologic Engineering*, **12**, 347-368. doi: 10.1061/(ASCE)1084-0699(2007)12:4(347)

Gersonius, B., Ashley, R., Pathirana, A., & Zevenbergen, C. 2013: Climate change uncertainty: building flexibility into water and flood risk infrastructure. *Climatic Change*, **116**, 411-423. doi: 10.1007/s10584-012-0494-5

Gilroy, K. L., & McCuen, R. H. 2012: A nonstationary flood frequency analysis method to adjust for future climate change and urbanization. *Journal of Hydrology*, **414**, 40-48. doi:10.1016/j.jhydrol.2011.10.009

Grusson, Y., Sun, X., Gascoin, S., Sauvage, S., Raghavan, S., Anctil, F., & Sáchez-Pérez, J. M. (2015). Assessing the capability of the SWAT model to simulate snow, snow melt and streamflow dynamics over an alpine watershed. *Journal of Hydrology*, **531**, 574-588. doi: 10.1016/j.jhydrol.2015.10.070

Haberlandt, U., & Radtke, I. 2014: Hydrological model calibration for derived flood frequency analysis using stochastic rainfall and probability distributions of peak flows. *Hydrology and Earth System Sciences*, **18**, 353-365. doi: 10.5194/hess-18-353-2014

Harrison, B., & Bales, R. 2015: Skill Assessment of Water Supply Outlooks in the Colorado River Basin. *Hydrology*, **2**, 112-131. doi: 10.3390/hydrology2030112

Hayhoe, K., Wake, C., Anderson, B., Liang, X. Z., Maurer, E., Zhu, J., Bradbury, J., DeGaetano, A., Stoner, A., & Wuebbles, D. 2008: Regional climate change projections for the Northeast USA. *Mitigation and Adaptation Strategies for Global Change*, **13**, 425-436. doi: 10.1007/s11027-007-9133-2

Hayhoe, K., Wake, C. P., Huntington, T. G., Luo, L., Schwartz, M. D., Sheffield, J., ... & Troy, T. J. 2007: Past and future changes in climate and hydrological indicators in the US Northeast. *Climate Dynamics*, **28**, 381-407, doi: 10.1007/s00382-006-0187-8

Hirabayashi, Y., Mahendran, R., Koirala, S., Konoshima, L., Yamazaki, D., Watanabe, S., ... & Kanae, S. 2013: Global flood risk under climate change. *Nature Climate Change*, *3*(9), 816-821, doi: 10.1038/nclimate1911

Hirsch, R. M., & Ryberg, K. R. 2012: Has the magnitude of floods across the USA changed with global CO2 levels? *Hydrological Sciences Journal*, **57**, 1-9. doi: 10.1080/02626667.2011.621895

Jabareen, Y. 2013: Planning the resilient city: Concepts and strategies for coping with climate change and environmental risk. *Cities*, **31**, 220-229, doi: 10.1016/j.cities.2012.05.004

Jörg-Hess, S., Griessinger, N., & Zappa, M. 2015: Probabilistic Forecasts of Snow Water Equivalent and Runoff in Mountainous Areas. *J. Hydrometeor.*, **16**, 2169-2186. doi: 10.1175/JHM-D-14-0193.1

Jung, M., Reichstein, M., Ciais, P., Seneviratne, S. I., Sheffield, J., Goulden, M. L., ... & Dolman, A. J. 2010: Recent decline in the global land evapotranspiration trend due to limited moisture supply. *Nature*, **467**, 951-954. doi: 10.1038/nature09396

Knighton, J. & Walter, M., In Press: Critical Rainfall Statistics for Predicting Watershed Flood Responses: Rethinking the Design Storm Concept. *Hydrological Processes*, doi: 10.1002/hyp.10888

Koplin, N., Schadler, B., Viviroli, D., Weingartner, R., 2014: Seasonality and magnitude of floods in Switzerland under future climate change. *Hydrological Processes*, 28, 2567 – 2578, doi: 10.1002/hyp.9757

Kundzewicz, Z. W., Kanae, S., Seneviratne, S. I., Handmer, J., Nicholls, N., Peduzzi, P., ... & Sherstyukov, B. 2014: Flood risk and climate change: global and regional perspectives. *Hydrological Sciences Journal*, **59**, 1-28, doi: 10.1080/02626667.2013.857411

Kunkel, K. E., Karl, T. R., Brooks, H., Kossin, J., Lawrimore, J. H., Arndt, D., ... & Emanuel, K. 2013: Monitoring and understanding trends in extreme storms: State of knowledge. *Bull. Amer. Meteor. Soc.*, **94**, 499-514, doi: 10.1175/BAMS-D-11-00262.1

Lawrence, D., Paquet, E., Gailhard, J., & Fleig, A. K. 2013: Stochastic semi-continuous simulation for extreme flood estimation in catchments with

combined rainfall-snowmelt flood regimes. *Natural Hazards and Earth System Sciences Discussions*, **1**, 6785-6828, doi: 10.5194/nhess-14-1283-2014

Li, J., Feng, P., & Chen, F. 2014: Effects of land use change on flood characteristics in mountainous area of Daqinghe watershed, China. *Natural hazards*, **70**, 593-607. doi: 10.1007/s11069-013-0830-8

Lo, M. H., & Famiglietti, J. S. 2010: Effect of water table dynamics on land surface hydrologic memory. *Journal of Geophysical Research: Atmospheres (1984–2012)*, **115**, doi: 10.1029/2010JD014191

Mahanama, S., Livneh, B., Koster, R., Lettenmaier, D., & Reichle, R. 2012: Soil moisture, snow, and seasonal streamflow forecasts in the United States. *J. Hydrometeor.*, ***13***, 189-203, doi: 10.1175/JHM-D-11-046.1

Mallakpour, I., & Villarini, G. 2015: The changing nature of flooding across the central United States. *Nature Climate Change*, **5**, 250-254, doi: 10.1038/nclimate2516

Massari, C., Brocca, L., Moramarco, T., Tramblay, Y., & Lescot, J. F. D. 2014: Potential of soil moisture observations in flood modelling: Estimating initial conditions and correcting rainfall. *Advances in Water Resources*, **74**, 44-53, doi: 10.1016/j.advwatres.2014.08.004

Massari, C., Brocca, L., Barbetta, S., Papathanasiou, C., Mimikou, M., & Moramarco, T. 2014: Using globally available soil moisture indicators for flood modelling in Mediterranean catchments. *Hydrology and Earth System Sciences*, **18**, 839-853, doi: 10.5194/hess-18-839-2014

Massari, C., Tarpanelli, A., Brocca, L., & Moramarco, T. 2014: Assimilating satellite soil moisture into rainfall-runoff modelling: towards a systematic study. *Geophysical Research Abstracts*, **17**.

Moriasi, D. N., Arnold, J. G., Van Liew, M. W., Bingner, R. L., Harmel, R. D., & Veith, T. L. (2007). Model evaluation guidelines for systematic quantification of accuracy in watershed simulations. Transactions of the ASABE, **50**, 885-900. doi: 10.13031/2013.23153

Nash, J. E., & Sutcliffe, J. V., 1970: River flow forecasting through conceptual models part I—A discussion of principles. *Journal of Hydrology*, **10**, 282-290. doi: 10.1016/0022-1694(70)90255-6

National Oceanic and Atmospheric Administration (NOAA) National Centers for Environmental Information (NCEI), 2015: Quality Controlled Local Climatological Data. Available Online: http://www.ncdc.noaa.gov/data-access/land-based-station-data/land-based-datasets

Nied, M., Hundecha, Y., & Merz, B. 2013: Flood-initiating catchment conditions: a spatio-temporal analysis of large-scale soil moisture patterns in the Elbe River basin. *Hydrology and Earth System Sciences*, **17**, 1401-1414, doi: 10.5194/hess-17-1401-2013

Norbiato, D., Borga, M., Degli Esposti, S., Gaume, E., & Anquetin, S. 2008: Flash flood warning based on rainfall thresholds and soil moisture conditions: An assessment for gauged and ungauged basins. *Journal of Hydrology*, **362**, 274-290, doi: 10.1016/j.jhydrol.2008.08.023

Northeast Regional Climate Center (NRCC) 2015: NRCC Hourly Precipitation Database. Available Online: http://www.nrcc.cornell.edu/page_databases.html

Obeysekera, J., & Salas, J. D. 2013: Quantifying the uncertainty of design floods under nonstationary conditions. *Journal of Hydrologic Engineering*, **19**, 1438 – 1446, doi: 10.1061/(ASCE)HE.1943-5584.0000931

Palecki, M. A., Angel, J. R., & Hollinger, S. E., 2005: Storm precipitation in the United States. Part I: meteorological characteristics. *J. Appl. Meteor.*, **44**, 933-946, doi: 10.1175/JAM2243.1

Paquet, E., Garavaglia, F., Garçon, R., & Gailhard, J. 2013: The SCHADEX method: A semi-continuous rainfall–runoff simulation for extreme flood estimation. *Journal of Hydrology*, **495**, 23-37, doi: 10.1016/j.jhydrol.2013.04.045

Paschalis, A., Fatichi, S., Molnar, P., Rimkus, S., & Burlando, P. 2014: On the effects of small scale space–time variability of rainfall on basin flood response. *Journal of Hydrology*, **514**, 313-327, doi: 10.1016/j.jhydrol.2014.04.014

Perica, S., Pavlovic, S., Laurent, M., Trypaluk, C., Unruh, D., Martin, D., Wilhite, O. 2015. NOAA Atlas 14 Precipitation-Frequency Atlas of the United States. Volume 10. Version 2.0 Northeastern States (Connecticut, Maine, Massachusetts, New Hampshire, New York, Rhode Island, Vermont).

Perju, E. R., Balin, D., Lane, S., & Zaharia, L., 2013: Changing flood magnitude and frequency in snow-melt dominated catchments: the case of the Bucegi Mountains, in the Romanian Carpathian region. In *EGU General Assembly Conference Abstracts* (Vol. 15, p. 10110).

Ravazzani, G., Mancini, M., Giudici, I., & Amadio, P., 2007: Effects of soil moisture parameterization on a real-time flood forecasting system based on rainfall thresholds. *IAHS Publication*, **313**.

Rossman, L. A. 2010: Storm water management model user's manual, version 5.0 (p. 276). Cincinnati: National Risk Management Research Laboratory, Office of Research and Development, US Environmental Protection Agency.

Salas, J. and Obeysekera, J. 2014: Revisiting the Concepts of Return Period and Risk for Nonstationary Hydrologic Extreme Events. *J. Hydrol. Eng.*, **19**, 554 – 568, doi: 10.1061/(ASCE)HE.1943-5584.0000820, 554-568.

Schiermeier, Q. 2011: Increased flood risk linked to global warming. *Nature*, **470**, 316-316.

Seidou, O., Ramsay, A., & Nistor, I. 2012: Climate change impacts on extreme floods I: combining imperfect deterministic simulations and non-stationary frequency analysis. *Natural hazards*, **61**, 647-659, doi: 10.1007/s11069-011-0052-x

Serinaldi, F., 2014: Dismissing return periods! *Stochastic Environmental Research and Risk Assessment*, **29**, 1179-1189, doi: 10.1007/s00477-014-0916-1

Smith, B. K., Smith, J. A., Baeck, M. L., & Miller, A. J. 2015: Exploring storage and runoff generation processes for urban flooding through a physically based watershed model. *Water Resources Research*, **51**, 1552-1569, doi: 10.1002/2014WR016085

Soil Conservation Service (SCS). 1986. Urban hydrology for small watersheds. Technical Release 55, Soil Conservation Service, US Department of Agriculture, Washington, DC.

Stedinger, J. R., & Griffis, V. W. 2011: Getting From Here to Where? Flood Frequency Analysis and Climate. *Journal of the American Water Resources Association*, **47**, 506-513, DOI: 10.1111/j.1752-1688.2011.00545.x

Surfleet, C., & Tullos, D., 2013: Variability in effect of climate change on rain-on-snow peak flow events in a temperate climate. *Journal of Hydrology*, 479, 24 – 34, doi: 10.1016/j.jhydrol.2012.11.021

Tolson, B. A., & Shoemaker, C. A., 2007: Dynamically dimensioned search algorithm for computationally efficient watershed model calibration. *Water Resources Research*, **43**, doi: 10.1029/2005WR004723

Tramblay, Y., Neppel, L., Carreau, J., & Najib, K. 2013: Non-stationary frequency analysis of heavy rainfall events in southern France. *Hydrological Sciences Journal*, **58**, 280-294, doi: 10.1080/02626667.2012.754988

Tramblay, Y., Amoussou, E., Dorigo, W., & Mahé, G. 2014: Flood risk under future climate in data sparse regions: Linking extreme value models and flood generating processes. *Journal of Hydrology*, **519**, 549-558, doi: 10.1016/j.jhydrol.2014.07.052

Trenberth, K. E. 2011: Changes in precipitation with climate change. *Climate Research*, **47**, 123 – 138, doi: 10.3354/cr00953

United States Department of Agriculture (USDA) National Resource Conservation Service (NRCS) 2015: Web Soil Survey. Available Online: http://websoilsurvey.sc.egov.usda.gov/App/HomePage.htm

United States Geological Survey (USGS) 2015: USGS 04234000 Fall Creek Near Ithaca, NY. Available Online: http://waterdata.usgs.gov/nwis/uv?04234000

United States Geological Survey (USGS). 2016. National Elevation Dataset. Available Online: http://nationalmap.gov/elevation.html

Walter, M., Gérard-Marchant, P., Steenhuis, T., and Walter, M. 2005: Closure to "Simple Estimation of Prevalence of Hortonian Flow in New York City Watersheds by M. Todd Walter, Vishal K. Mehta, Alexis M. Marrone, Jan Boll, Pierre Gérard-Marchant, Tammo S. Steenhuis, and Michael F. Walter." *J. Hydrol. Eng*., doi: 10.1061/(ASCE)1084-0699(2005)10:2(169), 169-170.

Wehner, M. F. 2013: Very extreme seasonal precipitation in the NARCCAP ensemble: model performance and projections. *Climate Dynamics*, **40**, 59-80, doi: 10.1007/s00382-012-1393-1

Weijs, S. V., Van De Giesen, N., & Parlange, M. B. 2013: Data compression to define information content of hydrological time series. *Hydrology and Earth System Sciences*, **17**, 3171-3187. doi: 10.5194/hess-17-3171-2013

Weijs, S. V., van de Giesen, N., & Parlange, M. B. 2013: HydroZIP: how hydrological knowledge can be used to improve compression of hydrological data. *Entropy*, **154**, 1289-1310, doi:10.5194/hessd-10-8581-2013.

Westra, S., Varley, I., Jordan, P., Nathan, R., Ladson, A., Sharma, A., & Hill, P. 2010: Addressing climatic non-stationarity in the assessment of flood risk. *Aust J Water Resour*, **14**, 1-16, doi: 10.1080/13241583.2010.11465370

Wood, A. W., & Schaake, J. C. 2008: Correcting errors in streamflow forecast ensemble mean and spread. *J. Hydrometeor.*, **9**, 132-148, doi: 10.1175/2007JHM862.1

Wood, A. W., Hopson, T., Newman, A., Brekke, L., Arnold, J., & Clark, M. 2016: Quantifying Streamflow Forecast Skill Elasticity to Initial Condition and Climate Prediction Skill. *J. Hydrometeor.*, **17**, 651 – 668, doi: 10.1175/JHM-D-14-0213.1

Wyżga, B., Zawiejska, J., & Radecki-Pawlik, A. In Press: Impact of channel incision on the hydraulics of flood flows: examples from Polish Carpathian rivers. *Geomorphology*, doi:10.1016/j.geomorph.2015.05.017

Ye, H., Fetzer, E. J., Behrangi, A., Wong, S., Lambrigtsen, B. H., Wang, C. Y., ... & Gamelin, B. L. 2016: Increasing daily precipitation intensity associated with warmer air temperatures over Northern Eurasia. *Journal of Climate*, **29**, 623-636, doi: 10.1175/JCLI-D-14-00771.1

Yossef, N. C., Winsemius, H., Weerts, A., Beek, R., & Bierkens, M. F. 2013: Skill of a global seasonal streamflow forecasting system, relative roles of initial conditions and meteorological forcing. *Water Resources Research*, **49**, 4687-4699, doi: 10.1002/wrcr.20350

CHAPTER 3

A VULNERABILITY-BASED, BOTTOM-UP ASSESSMENT OF FUTURE RIVERINE FLOOD RISK USING A MODIFIED PEAKS-OVER-THRESHOLD APPROACH AND A PHYSICALLY BASED HYDROLOGIC MODEL

1. Introduction

In the 80 years since the passage of the 1936 Omnibus Flood Control Act (49 Stat 1540, 1936), flood damages have continued to escalate. Under this act the US has systematically increased funding to control floods, only to have flood damage claims increase, a phenomenon sometimes referred to as the "flood control paradox" [Benavides & Winter, 2013]. Fortunately, in recent years engineers and planners have started to explore new potential solutions beyond trying to contain the flood in a stream channel, e.g., green infrastructure. While we explore new solutions to flooding, new tools are needed to improve flood risk assessment and, equally as important, meaningful ways to engage and educate public stakeholders [e.g., Black, 2011].

Flood risk is often defined in terms of flood hazards and their consequences. Flood *hazards* are components of flooding that can cause harm, such as the depth or velocity of floodwater at a given location. The *consequences* of these hazards can then be measured based on the exposure and level of vulnerability of society to these hazards, e.g., the value of assets in harm's way and the sensitivity of those assets to flooding. *Flood risk* is then defined as the product of the probability of the hazard and a measure of the associated consequence, often summed across all potential levels of the hazard [Kron, 2005].

When conveying flood risk information to the public, engineers and hydrologists often focus on a small subset of predetermined hazard assessments - flood plain elevations [e.g. Winsemius et al., 2013], depth-inundation maps [e.g., Aerts et al., 2013; Neal et al., 2013; Alfonso et al. 2016], and flood frequency analysis (FFA) [e.g. Rogger et al., 2013; Viglione, et al., 2013] – that are often presented in terms of exceedance levels and, when applied to riverine flooding, focus almost exclusively on peak flow rates and stage. These conventional hazard assessments, which were recently reemphasized in US Executive Order 13690 (Federal Flood Risk Management Standard) [Obama, 2015], are rooted in design criteria for flood control infrastructure and the need to index flood insurance products based on inundation mapping, neither of which may be directly relevant to the actual *vulnerabilities* to flooding and thus flood *risks* faced by communities today. For instance, these approaches rarely consider issues of water velocity, inundation duration, or more complex combinations of hazards that may be directly relevant to consequences of concern to a community (e.g., road closures linked to exceedance of a critical depth for a specific duration). In addition, the quantification of consequences associated with more conventional hazard estimates (e.g., 100-year floodplain) are often left for subsequent analyses, because translating flood hazard into a risk profile for a specific community can be a complicated process involving structure fragility curves, population density maps, or future development plans and often requires an in-depth local knowledge of community vulnerabilities to flooding that consulting engineers and hydrologists may lack [e.g., Merz et al., 2010; Stephenson & D'Ayala 2014; De Bruijn et al., 2014; Schröter et al., 2014; Botto et al., 2014; Remo et al., 2016].

While a one-size-fits-all approach is often informative, the probability of peak flow rate or stage within the next calendar year may not be the most useful metric to the decision processes of local planners. It is therefore not surprising that public

understanding of risks and the success of risk reduction measures are often linked to stakeholder involvement in the planning process [e.g. McDaniels et al 1999; White et al 2010], trust in expert opinion [Wachinger et al., 2012; Kellens et al., 2013), and the ease of understanding expert flood risk estimates [Morss et al., 2005; Bradford et al., 2012; Pappenberger et al., 2013]. This suggests that hazard-risk relationships should be defined in cooperation with stakeholders to leverage local knowledge of relevant flood hazards and critical hazard thresholds above which the community experiences adverse effects, i.e., thresholds of vulnerability.

A second problem stems from the difficultly of incorporating emerging hydroclimate information into conventional risk analysis for long-term planning. It is well established that simple extrapolations of flood frequency curves beyond gage records can underestimate flood hazard if instrumental records are too short and exclude past extreme events [Greenbaum et al., 2014; Shin et al., 2015; Yan and Moradkhani, 2015, 2016; Halbert et al., 2016]. There is a well-developed literature on methods to reduce estimation uncertainty by pooling gages of variable record length [Stedinger et al., 1985; Renard, 2011; Haddad et al., 2012] and leveraging paleoflood evidence or historical written records of past floods [Stedinger et al., 1986; Kjeldsen et al., 2014; Mei et al., 2016]. However, the threat of anthropogenic climate change has sparked a demand for future projections of flood risk, which may differ from that of the past due to structural changes in the climate system. Yet generating future projections of flood risk is severely complicated by well-acknowledged deficiencies in climate model based representations of precipitation dynamics and the atmospheric water cycle, particularly for extreme events [e.g. Prudhomme et al., 2002; Dai, 2006; Stephens et al., 2010; Haynes et al., 2010; Pritchard et al., 2011; Kendon et al., 2012; Kysely et al., 2015].

In response to this uncertainty, a variety of bottom-up approaches have emerged to help develop climate change adaptations that work reasonably well over a wide range of plausible future scenarios. Prominent approaches include Scenario-Neutral Planning [Prudhomme et al., 2010], Robust Decision Making [Lempert, 2003; Lempert et al., 2004], Many-Objective Robust Decision Making [Kasprzyk et al., 2009; Singh et al., 2015; Hadka et al., 2015], Info-gap Analysis [Ben-Haim, 2006], and Decision Scaling [Brown et al., 2011; 2012]. All of these approaches provide conceptual frameworks to assess the sensitivity of planning decisions to uncertain future conditions [Herman et al., 2015]. One major advantage of these bottom-up approaches is that they enable planners to test how different assumptions of future climate or other conditions would impact the decision process. For instance, the Decision-Scaling and Scenario-Neutral Planning approaches (utilized in this study) first develop system response surfaces that map planning-relevant metrics and decision thresholds for those metrics across a wide range of plausible future climates, and then afterwards superimposes different climate information sources of varying credibility (paleo-reconstructions, climate model output, historical trends) on those response surfaces. If a decision-maker has more confidence in certain data sources (e.g., historical trends) over others (e.g., climate model based output), they can use the approach to quickly see whether the differences between those data sources would translate into different decisions. This can help facilitate discussion between planners and help them reach a consensus on a decision without becoming entangled in a debate on the data sources used in the analysis.

There have been myriad developments in the application of these bottom-up based approaches to climate change adaptation [Steinschneider et al., 2015a,b; Hassanzadeh et al., 2016; Hassanzadeh et al., 2017], but there has not yet been an attempt to distinguish how decision-relevant outcomes vary with different process-

level climate phenomena that are projected to change with varying degrees of confidence. That is, these approaches have not been used to determine how system sensitivity to climate changes if we consider separately the possible shifts in different climate mechanisms, e.g., convection, extra-tropical storms, hurricanes, and changing snowpack and rain-on-snow dynamics. Rather, bottom-up studies have used tools like stochastic weather or streamflow generators [Herman et al., 2016; Steinschneider and Brown 2013] to explore water system sensitivity to changes in summary statistics of hydroclimate variability (e.g., the mean, variance, or autocorrelation of annual or monthly precipitation, temperature, streamflow), without an explicit link to causal changes in the climate system. In the context of flooding, there is an emerging consensus that flood risk assessments could benefit by moving towards an understanding of climate-flood linkages [Merz et al., 2014; Blöschl et al., 2015], with calls for engineers and hydrologists to acknowledge "*causal mechanisms and dominant processes*" of the atmosphere, which may be related to catchment flooding. In many cases these climate-flood linkages have been identified for a particular region [e.g. Steinschneider and Lall, 2015; Berghuis et al., 2016], and the physical differences in their formation, propagation, and lysis may be represented to different degrees of credibility in climate change projections. For instance, while changes to the thermodynamic aspects of extreme rainfall linked to the Clausius-Clapeyron relation may be relatively well understood [Fischer and Knutti, 2016], potential changes in dynamics are not [Shepherd, 2014]. This could result in substantial uncertainty in changes to the frequency of heavy precipitation linked to synoptic-scale storms, but more confidence in temperature driven changes to the intensity of extreme events or the likelihood of heavy winter precipitation falling as rain on antecedent snowpack.

In this study, we propose a flood risk methodology designed to help communicate flood risk using the following elements: 1) a flexible definition of

stakeholder-relevant hazards and hazard thresholds tailored to specific vulnerabilities of concern; and 2) the ability to test how future changes in the frequency and magnitude of specific flood-inducing climate mechanisms will impact decision-relevant measures of flood risk. The approach builds on existing bottom-up methodologies to climate change adaptation and utilizes a novel, model-based adaptation of the commonly employed peaks-over-threshold (POT) technique for flood risk estimation. The method is applicable where the occurrence of hazard exceedances over a decision-relevant threshold is sufficient to characterize vulnerability. Our approach relates causal meteorological processes to local catchment flooding [e.g. Merz et al., 2014], is based on public interest in flood risk [Botzen et al., 2013], is applicable where any risk exceedance is deemed not acceptable [e.g. Srinivasan & Rethinaraj, 2013], is simplistic in its presentation of risk as recommended by Pappenberger et al. [2013], and is in line with the recommendations of Beven et al. [2015, 2016] to acknowledge assumptions and uncertainties.

2. A Model-Based POT Method for Flood Risk Analysis

We present a hydrologic model-based methodology for flood risk assessment adapted from the conventional POT statistical approach for flood hazard assessment [Davidson and Smith, 1990]. In the classic POT methodology, a series of hydrologic values Q above some predefined threshold are collected. The probability density function (pdf) of an extreme value distribution (e.g., Generalized Pareto) is fit to the magnitude of the exceedances, while a separate probability mass function (pmf) (e.g., Poisson) is used to describe the number of such extreme events in a particular year, denoted by N_Q. We focus here on the random variable N_Q. A statistic of particular interest for flood risk planning is the probability of experiencing at least one extreme flood, i.e., $N_Q > 0$, over the next n years [Botzen et al., 2013]. Assuming the number of

floods from one year to the next is independent and identically distributed, this probability can be expressed as:

$$1 - \Pr(N_Q = 0)^n = 1 - \left((\lambda_q{}^0) \frac{\exp(-\lambda_q)}{0!} \right)^n = 1 - e^{-n\lambda_q} \quad (1)$$

where λ_q is the rate parameter of the Poisson distribution describing the expected number of hydrologic exceedances in a year.

In the approach presented here, the POT methodology is adapted to target stakeholder-relevant hazards with a direct link to consequences of interest. This is achieved in part through the use of a rainfall-runoff model that can simulate a wide array of characteristics (e.g. flow, water elevation, velocity, nutrient runoff, sediment load, etc.) that may otherwise be unavailable with existing datasets. The approach also requires stakeholder input to define a consequence they wish to avoid so that the analysis is tailored towards stakeholder vulnerabilities to the flood hazard. The analysis then proceeds by defining a critical value, q_c, of the hydrologic characteristic that leads to the consequence of concern. As described by Merz et al. [2010], defining these consequence-relevant thresholds requires its own effort that may be time-consuming, but once completed the analysis can then be tailored to stakeholder vulnerabilities and presented in a way that is immediately relevant to the quantification of local flood risk.

Once the hydrologic characteristic Q and stakeholder-derived threshold q_c is defined, we decompose the probability that $Q > q_c$ will occur k times in a given year, i.e., $\Pr(N_Q=k)$, into an equivalent expression based on 1) the number of times (u) that precipitation, P**,** exceeds some threshold p_c in a given year, denoted by N_P and 2) the conditional probability that $Q > q_c$ will occur k times given that $P > p_c$ occurs u times:

$$\Pr(N_Q = k) = \sum_{u=0}^{\infty} \Pr(N_Q = k \,|N_P = u) Pr\,(N_P = u) \quad (2)$$

Here, p_c is set to some value below which critical floods are not physically possible and is selected based on expert opinion or a previous hydrologic assessment of the

area. Assuming that the random variable N_P follows a Poisson distribution with rate parameter λ_p, it can be shown that the number of critical hydrologic exceedances N_Q in a given year follows a Poisson distribution with rate $\pi\lambda_p$, where π is the probability that $Q > q_c$ given that $P > p_c$ (see Appendix A):

$$N_Q \sim Poisson(\pi\lambda_p) \tag{3}$$

$$\pi = \Pr(Q > q_c \mid P > p_c) \tag{4}$$

The parameter π maps the occurrence of critical precipitation events to critical local watershed flood events. This mapping will depend on the characteristics of the catchment, as well as antecedent watershed conditions, S (e.g. unsaturated zone soil moisture, accumulated snowpack, temperature), at the time of atmospheric forcing. The parameter π can be estimated by integrating the conditional pdf of the occurrence of a critical flood event over the pdfs of P and S (see Appendix B):

$$\pi = \Pr(Q > q_c \mid P > p_c) = \int_{q_c}^{\infty} \int_{p_c}^{\infty} \int_{\Omega_s} f_Q(q \mid P = p, S = s) f_P(p \mid P > p_c) f_S(s) ds dp dq \tag{5}$$

Here, $f_Q(q|P = p, S = s)$ is the conditional pdf of Q given some value for precipitation, P, and antecedent watershed conditions, S. The pdf $f_P(p \mid P > p_c)$ denotes the truncated pdf of all precipitation values greater than p_c, and $f_S(s)$ denotes the multivariate pdf of antecedent watershed conditions. The multivariate space of possible antecedent conditions is denoted Ω_s. Proposed methods of estimating these terms are detailed later in section 3. Once estimated, we can then substitute $\pi\lambda_p$ for λ_q in Eq. 1 to estimate the likelihood of at least one critical flood event over the next n years. There are several benefits to decomposing the rate of critical flooding, λ_q, into the rate of critical meteorological mechanisms λ_p and the probability π that a critical flooding event will result from a critical meteorological event:

1. Records are often longer and measurements more feasible for precipitation than many hydrologic characteristics besides flow that may be of interest

during flood events. The formulation of Eq. 3 enables us to leverage long precipitation records for the rate estimation of critical events and couple it with a physical hydrologic model to translate those events into (potentially poorly observed) flood characteristics of interest.

2. The use of a hydrologic model places physical limitations (e.g. conservation of mass) on estimates of extreme hydrologic events that purely statistical approaches may neglect.
3. The approach only simulates critical precipitation events that could result in a flood, rather than continuous simulation procedures (e.g., stochastic weather generators driving hydrologic models [Steinschneider et al., 2015a]) that include many periods of low precipitation. This enables a hydrologic-model based approach with substantially less computational expense compared to continuous simulation methods. This is particularly advantageous when trying to incorporate hydrologic model uncertainty into the analysis, as will be demonstrated later.
4. New information (e.g., climate projections) regarding the frequency or magnitude of precipitation can be readily adopted into the model framework. This is difficult in a completely statistical approach that does not utilize a physical hydrologic model.
5. The formulation in Eq. 1-5 can be partitioned for mutually exclusive climate mechanisms linked to flooding. For instance, if two mechanisms are responsible for the flooding in a given region (e.g., wintertime synoptic-scale events and tropical cyclones), and are independent of one another, then separate estimates $\left(\pi^1, {\lambda_p}^1\right)$ and $\left(\pi^2, {\lambda_p}^2\right)$ can be developed for the precipitation and antecedent condition data associated with these different

types of storms, and a final estimate of λ_q is given by $\pi^1{\lambda_p}^1 + \pi^2{\lambda_p}^2$ via the additive property of the Poisson distribution.

6. Other data sources, such as climate model projections, that have different levels of credibility for different climate mechanisms, can then be incorporated into the analysis by adjusting the appropriate parameters for each mechanism separately. For instance, projections of increased future extreme precipitation intensities, $f_P(p \mid P > p_c)$, may be considered relatively credible due an expected increase in air temperatures and the Clausius-Clapeyron relation [Fischer & Knutti, 2016], while projected changes in the frequency of synoptic-scale storms (λ_p) may be considered relatively uncertain due to dynamical influences poorly represented in the climate models [e.g., Shepherd, 2014].

With reference to this last benefit, the approach presented above can be used to support a bottom-up approach to future flood risk assessments. Different combinations of potential climate changes (shifts in λ_p, π, or the components of π, i.e., the pdfs of *P* and *S*) can be considered for specific climate mechanisms to see how these different assumptions map to the metric of flood risk. This allows planners to see what each of these changes and their combinations would imply from a decision-making perspective. Planners can then couple this information with an assessment of the credibility of these changes to more readily determine the extent to which they will incorporate different types of climate change into their planning process.

3. Application

We apply the proposed methodology to Fall Creek in Ithaca NY, a small urban watershed that has recently struggled with flooding in certain low-lying areas of the community. The following sections describe the individual steps we have taken to carry out the methodology and estimate the probabilistic terms in Eqs. 1-5 above (see

Figure 3.1). We note that the methods in Section 2 are generalizable and there are multiple ways to estimate specific terms in Eqs. 1-5. We discuss alternate approaches in the subsequent discussion (Section 5) to highlight how the proposed methodology could be extended to other regions and different modeling choices.

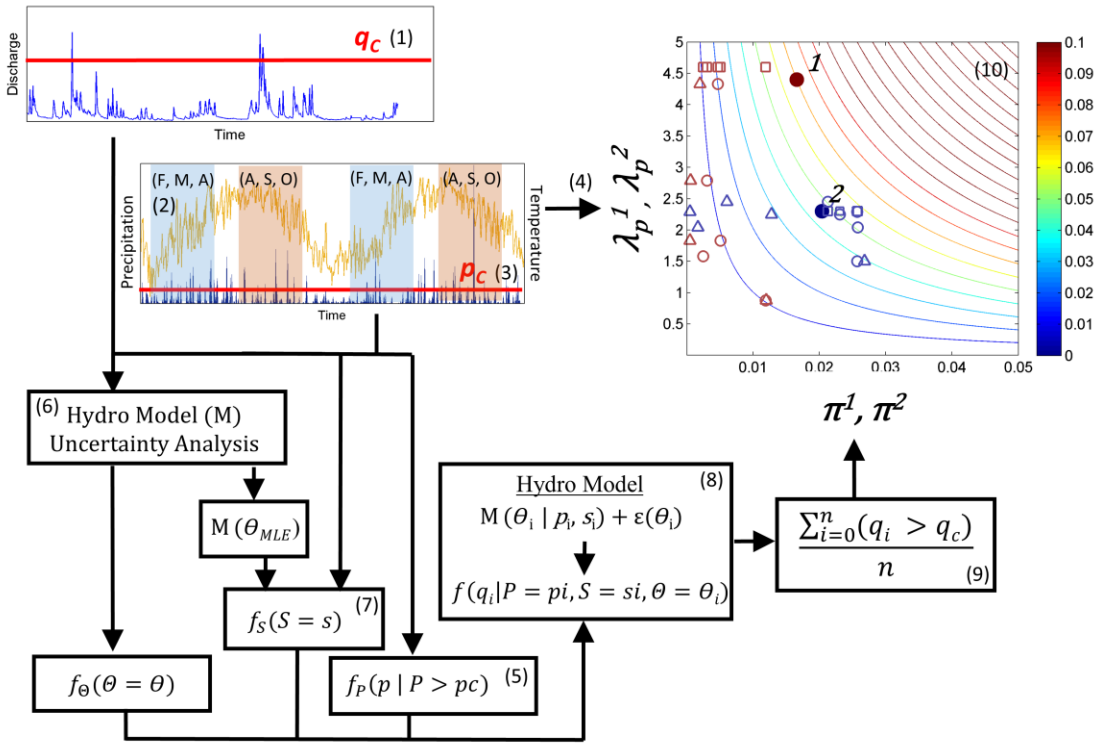

Figure 19 - Flowchart depicting steps taken to generate the response surface and point estimates of flood risk posed by atmospheric mechanisms for Fall Creek

3.1 Study Location: Fall Creek, Ithaca NY USA

Ithaca, NY USA has experienced several riverine floods within the past 30 years from Fall Creek [Michael Thorne, city engineer, personal communication]. Fall Creek's watershed is roughly 325 km2 (time of concentration ~ 5 hours). The fourth order main stem of Fall Creek passes through Ithaca within a mildly sloped (0.07%) trapezoidal channel. Constructed earthen flood protection levees provide a minimum of 2 m of freeboard within Ithaca. Several densely populated Ithaca neighborhoods lie within a relatively flat, low-lying area adjacent to both Fall Creek and Cayuga Lake

(Figure 3.2). Due to the local topography, overtopping of the Fall Creek bank has the potential to flood many properties simultaneously.

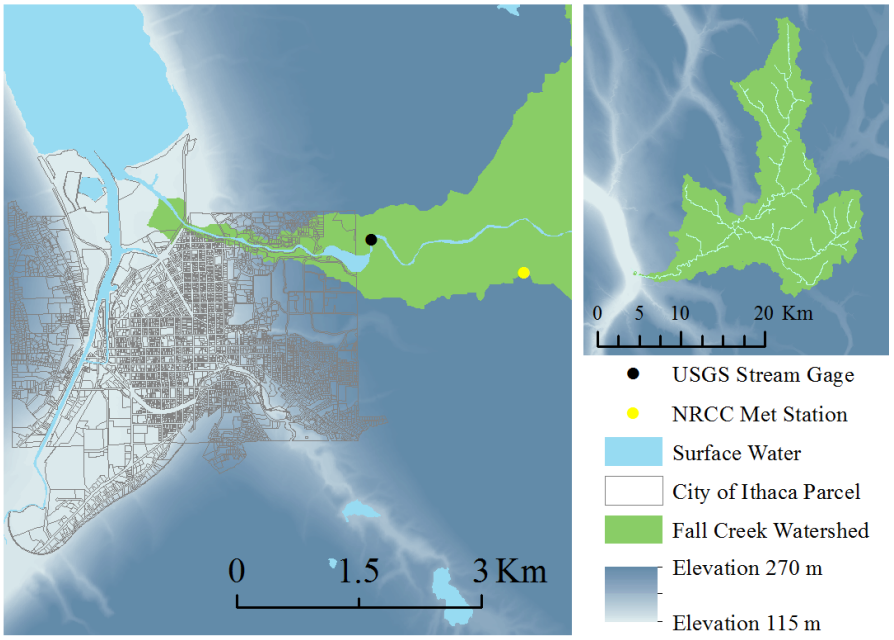

Figure 20 - Fall Creek within Ithaca NY, USA showing ground surface elevation and City of Ithaca property parcels

3.2 Define flood risk criteria

In this work we elaborate on a methodology that defines hazard-risk relationships with an interdisciplinary group to leverage both the local knowledge of flooding vulnerability and expert opinion of hazards. This group first identifies the relevant flood hazards and then critical hazard thresholds below which the community experiences no adverse effects. In this way, the approach implicitly considers the vulnerability of the community to the hazard when defining flood risk. We define a hazard threshold, qc, that is directly relevant to flood vulnerabilities of the community (Figure 3.1; step 1). The authors participated in a series of three meetings in 2016 with the City of Ithaca Superintendent of Public Works, Tompkins County Planning Department, and United States Geological Survey to determine the flooding threshold, qc, for Ithaca. In addition to the authors, these stakeholders contributed knowledge of local vulnerability to flooding, policy, potential governmental pathways to mitigate the

effects of flooding experienced by vulnerable populations, and in-channel hydraulics. This working group defined qc using a two parameter fragility function, which determined that substantial flood damage in Ithaca begins to occur if Fall Creek streamflow exceeds the current hydraulic capacity of the Fall Creek channel within Ithaca (estimated to be 120 m3s-1) with a duration of inundation of at least 6 hours.

3.3 Flood-inducing precipitation from different climate mechanisms

A 25-year record (1990 – 2015) of daily rainfall data (Network ID: GHCND:USC00304174; NCDC [2016]) is then used to group precipitation events by climate mechanism (Figure 3.1, step 2). A daily accumulation period was selected based on our past work on precipitation-flood relationships in the basin (Knighton et al., 2017). Events can be classified by examining the atmospheric circulation using reanalysis products, using existing inventories of historical storm types, or in some regions more simply through a clustering by season. We reviewed historical flooding events for Fall Creek and the region [NCDC, 2016; Agel et al., 2015] to identify flood-associated weather characteristics and mechanisms (Table 3.1). The identified historical floods were all associated with rainfall and generally separated into three mechanisms: spring rain on snow, intense late summer tropical moisture driven rainfall, and intense late summer non-tropical rainfall. We used an existing catalog [Roth, 2012] to identify tropical moisture summer precipitation events in the historic record from 1990 – 2010, and added to this record Hurricane Irene (2011) and Tropical Storm Lee (2011). All other summertime events are categorized as non-tropical events, while all springtime floods are categorized as spring rain-on-snow events.

Table 10 - Historical flooding events for Fall Creek (USGS, 2016)

Date	**Mechanism**	**Precipitation (cm)[a]**	**Discharge (m^3s^{-1})[b]**	**Stream Depth (m)**

6/23/1972	Hurricane Agnes	9.0	132	2.7
10/28/1981	Non-tropical summer event	12.9	337	2.5
1/19/1996	Rain on snow	4.7	268	2.3
4/3/2005	Rain on snow	5.7	175	1.9[c]
9/8/2011	Tropical Storm Lee	11.2	122	2.7

[a] Total daily precipitation accumulation

[b] Peak instantaneous discharge

[c] Inclusion of April 3, 2005 event discussed in supplementary material

Next, we define the precipitation threshold, p_c, below which the event $Q > q_c$ is infeasible (Figure 1; step 3). Here, a precipitation threshold of 18 mm is adopted regardless of climate mechanism. This threshold was determined based on a review of historical records and a series of hydrologic model tests using different p_c values. We note that the selection of p_c is non-trivial, and the hydrologic variable of interest, Q, and threshold, q_c, will inform the selection of p_c.

The rate parameter of critical rainfall frequency (λ_p) (Figure 1; step 4) and truncated pdf of intensity [$f_P(p \mid P > p_c)$] (Figure 1; step 5) for each climate mechanism in the Fall Creek catchment are then estimated. Kirby [1969] suggests exponentially distributed inter-arrival times are a rational justification for considering rare hydrologic events to have originated from a Poisson process. For each mechanism we therefore check the fit of inter-arrival times against an exponential pdf using a one-sample Kolmogorov-Smirnov (KS) test. The marginal pdf of daily rainfall depth, $f_P(p \mid P > p_c)$, is assumed to follow a Generalized Pareto distribution, again after testing the goodness of fit with a one-sample KS test.

3. 4 Estimating the likelihood (π) of a critical flood given a critical precipitation event

Individual terms of Eq. 5 are evaluated to estimate π for a specific climate mechanism. This step requires a series of modeling choices to estimate $f_S(s)$ and $f_Q(q \mid P = p, S = s)$ that can vary between studies and still fit in the more general framework presented in Section 2.

In this case study, the semi-physically-based hydrologic model JoFlo (Archibald et al., 2014) is used to simulate daily streamflow and hydrologic state variables from daily weather forcing data. The model includes the snowmelt model of Walter et al. [2005], the PET model of Archibald and Walter [2014], and simple soil water and groundwater budgets [see Archibald et al., 2014 for a full model description]. We chose JoFlo because previous studies have shown it works well in the region [Archibald et al., 2014] and it has relatively few parameters.

Because hydrologic model uncertainty, and particularly underestimated variance of simulated *Q* values, could artificially deflate the number of times the hydrologic model predicts that $Q > q_c$ [Stedinger et al., 2008], we choose to address this uncertainty directly using a Bayesian approach [Schoups and Vrugt, 2010] (Figure 1; step 6). However, this uncertainty modeling is not necessary in the more general framework of Section 2. In brief, the hydrologic response Q_t for some precipitation event P_t and set of antecedent conditions S_t (snowpack, soil moisture, groundwater, and air temperature at the onset of precipitation) is defined by the sum of a hydrologic model prediction $M_t(\Theta_M|P_t, S_t)$ with some parameter set Θ_M and a residual error term ε_t:

$$Q_t = M_t(\Theta_M|P_t, S_t) + \varepsilon_t \quad (6)$$

The error term is considered random, with its own density function $f_\varepsilon(\epsilon|\Theta_\varepsilon)$ and parameter set Θ_ε. The hydrologic and error model parameters are grouped together as $\Theta = \{\Theta_M, \Theta_\varepsilon\}$. Through the uncertainty analysis [Schoups and Vrugt, 2010], all parameters Θ are considered random variables and their joint posterior pdf, $f_\Theta(\Theta)$, is

estimated, along with the "best-fit" parameterization that maximizes the likelihood estimate, Θ_{MLE}.

After quantifying the uncertainty in the model parameters, we can redefine the estimation of π to explicitly consider hydrologic model uncertainty:

$$\pi = \int_{q_0}^{\infty} \int_{p_0}^{\infty} \int_{\Omega_s} \int_{\Omega_\Theta} f(q \mid P = p, S = s, \Theta = \Theta) f_P(p \mid P > p_c) f_S(s) f_\Theta(\Theta) d\Theta ds dp dq \quad (7)$$

The integration in Eq. 7 is evaluated using a Monte Carlo approach. First, to estimate $f_S(s)$ (Figure 1; step 7), we utilized the Θ_{MLE} parameter set and the 25-year record of historical precipitation and air temperature data to simulate a continuous time series of the hydrologic state variables. The pdf $f_S(s)$ is a multi-variate distribution defining antecedent snowpack (as snow water equivalent [SWE]), soil moisture (as volumetric soil water content [VWC]), groundwater (as groundwater reservoir volume), and air temperature at the onset of precipitation (treatment of air temperature in event-based sampling is discussed in the supplementary material). These times series and that for temperature are then truncated into seasons associated with each climate mechanism (F, M, A and A, S, O), and the data in those series is used to define an empirical, multivariate pdf $f_S(s)$ for each mechanism. The pdfs $f_P(p \mid P > p_c)$ and $f_S(s)$ are defined and sampled independently as no relationship was found between extreme precipitation and either temperature or hydrologic state variables within each season.

Simulations of Q are then produced by sampling P, S, and Θ from $f_P(p \mid P > p_c)$, $f_S(s)$, and $f_\Theta(\Theta)$ respectively, and using JoFlo to transform these forcing data and parameter values into hydrologic predictions to which we add sample residuals drawn from $f_\varepsilon(\epsilon|\theta_\varepsilon)$ (Figure 1; step 8). Our event-based simulations are carried out over 8 days. Here, model initialization is based on the samples of S. During the simulation, we allow for two days of no precipitation prior to the event to ensure stable

antecedent conditions, one day with the sampled values of precipitation, followed by five days to allow for routing or delayed effects of snow melt. The maximum value of simulated discharge is taken as Q from each event simulation. The parameter, π, is then estimated as the fraction of evaluations of Q that exceed q_c (Figure 1; step 9). We evaluate the integral in Eq. 7 using $1x10^6$ Monte Carlo evaluations for each climate mechanism. Further details on our choice of hydrologic model, its calibration, model initialization for the event simulations, and the incorporation of air temperatures into the sampling routine are presented in the Supplementary Material.

3.5 Estimation of Flood Risk over a Specified Duration

Using estimated values of $\pi$and λ_p for specific climate mechanisms, we sum estimates of $\pi\lambda_p$ across mechanisms to estimate λ_Q (Figure 1; step 10), which is used to produce a composite risk estimate for the expression: $1 - P\left(N_Q = 0\right)^n$ (Eq. 1). We demonstrate two estimates of flooding risk over a 1-year (n=1) and 10-year (n=10) planning period. In addition, we can produce a composite estimate of ${\lambda_p}^c$ and π^c through the additive property of the Poisson distribution (shown for three mechanisms):

$$ {\lambda_p}^c = {\lambda_p}^1 + {\lambda_p}^2 + {\lambda_p}^3 \quad (8) $$

$$ \pi^c = \frac{\pi^1{\lambda_p}^1 + \pi^2{\lambda_p}^2 + \pi^3{\lambda_p}^3}{{\lambda_p}^c} \quad (9) $$

Here, ${\lambda_P}^c$ and π^c are estimates of the annual frequency of extreme precipitation and the likelihood that extreme precipitation produces a flood, regardless of climate mechanism.

3.6 Mapping potential changes in the climate to flood risk

The bottom-up approach adopted in this study is most similar to the Decision-Scaling and Scenario-Neutral Planning methodologies that have been explained in

detail elsewhere [Prudhomme et al., 2010; Brown et al., 2011; 2012]. We provide a brief review of the approach in the context of our flood risk application. The procedure begins by systematically varying the parameters π and λ_p at fine intervals over a wide range that encompasses all plausible future values of these parameters, and then testing the sensitivity of a decision-relevant flood risk metric, e.g., $1\text{-}P(N_Q = 0)^n$, to these changes. Plausibility in this context is defined as a range of values that encompasses and exceeds all projected values of π and λ_p based on future climate projections (described next) by some large percentage (i.e., 50%). This approach produces a response surface that maps plausible changes in π and λ_p to changes in flood risk.

We then examine climate model projections to determine how each climate mechanism may change and superimpose these different projections onto the response surface. In this study, future meteorological conditions are gathered from the NASA Earth Exchange Global Daily Downscaled Projections (NEX-GDDP) GCM Scenario under Representative Concentration Pathway (RCP) 8.5 for the years 2075 – 2100 [Taylor et al., 2012]. NEX-GDDP projections are downscaled using the Bias-Correction Spatial Disaggregation (BCSD) approach of Wood et al. [2002, 2004] to produce a daily output at an 8 km spatial resolution. We consider NEX-GDDP climate projections from the BCC-CSM1.1, BNU-ESM, CanESM2, CSIRO-Mk3-6-0, and GFDL-ESM2G GCMs.

Downscaled GCM projections of regional precipitation are used to develop a range of projected changes in π separately for different mechanisms. It was outside the scope of this analysis to separate late summer GCM precipitation into tropical and non-tropical systems. Therefore in the analysis of future climate, all late summer events (tropical and non-tropical events) are clustered and their characteristics estimated with single estimates of λ_p and $f_P(p \mid P > p_c)$ for each GCM.

Estimates of the future seasonal pdf of antecedent conditions, $f_S(s)$, are generated as previously described for current conditions, replacing observed daily precipitation and air temperature records with those of downscaled GCM projections. We estimate a unique pdf $f_S(s)$ for each GCM and mechanism.

Finally, we determine the implications of change in these different parameters, reflective of specific climate mechanisms, for our decision-relevant flood metric. In this process, we first determine how different combinations of changes in $f_P(p \mid P > p_c)$ and $f_S(s)$ projected by the climate (and hydrologic) models influence projected changes in π. We then superimpose different combinations of λ_p and π on the response surface generated above, with values of π determined by a specific combination of change in $f_P(p \mid P > p_c)$ and $f_S(s)$. By considering different combinations of change projected for λ_p, as well as for $f_P(p \mid P > p_c)$ and $f_S(s)$ (and thus π), we can separate out how different aspects of projected future hydrologic change - say, changes to storm intensity or the presence of antecedent snowpack in the spring – influence metrics relevant for decision-making. This separation is designed to help isolate the impacts of future climate changes in which there is more confidence from the impacts of future change that are more uncertain.

3.7 Sensitivity to Risk Threshold

Finally, we also explore the sensitivity of future risk projections to changes in the stakeholder defined risk threshold, q_c. We propose a hypothetical case where the flood protection levees are reduced from elevation 2 m to 1.5 m (an effective channel capacity reduction of 120 m^3s^{-1} to 85 m^3s^{-1}). This scenario is used to demonstrate how estimates of flood risk are sensitive to the exposure level of a community, highlighting the need to consider such information when communicating risk to stakeholders.

4. Results and Discussion

4.1 Rainfall Characteristics

We first present an analysis of the present-day precipitation characteristics associated with the three major storm types considered in this analysis. The cdfs of precipitation event depths greater than pc from spring (Figure 3.3a), late summer non-tropical (Figure 3.3b), and late summer tropical systems (Figure 3.3c) are well approximated by the Generalized Pareto distribution, with 50th (99th) percentile precipitation depths of 24.2 (58.2), 25.8 (86.7), and 39.6 (127.4) mm, respectively. We note that summer rainfall events, particularly tropical systems, tend to be more intense than spring events.

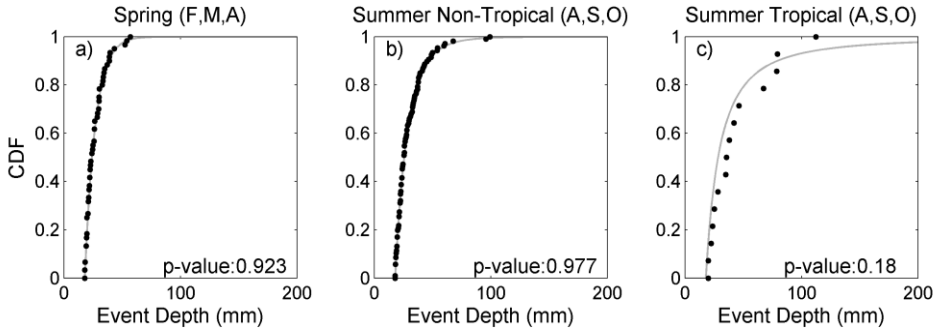

Figure 21 - Observed precipitation event depths (dots) and best fit Generalized Pareto cdfs (gray lines) of precipitation events > 18 mm for a) spring, b) summer non-tropical, and c) summer tropical events. Goodness-of-fit p-values for one-sample KS-tests are also shown.

The inter-event timing of extreme precipitation is approximately exponentially distributed for all storm types (Figure 3.4a-c), suggesting that rain events likely follow a stationary Poisson process [Kirby, 1969]. The estimated Poisson parameter, λp, for winter, summer non-tropical, and summer tropical precipitation events are 2.3, 6.9, and 0.56 events per year respectively. Non-tropical summer events occur more frequently than spring events (Figure 3.4), in addition to being more intense (Figure 3.3), while tropical summer storms are the rarest and most intense event storm type.

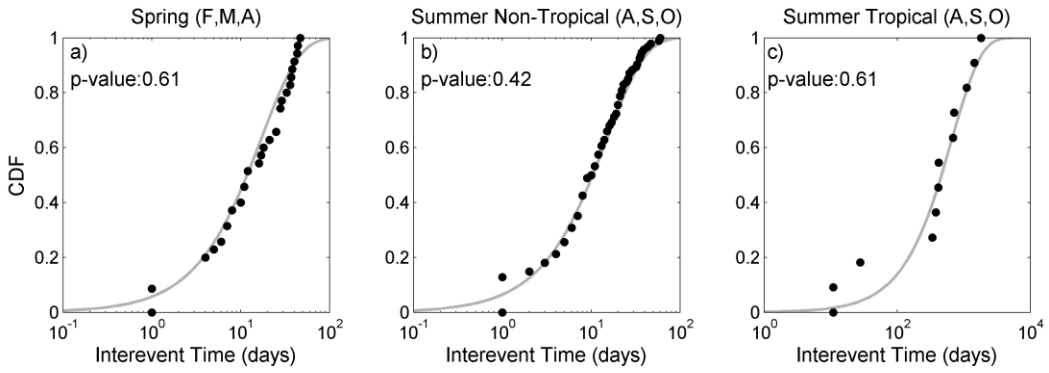

Figure 22 - Observed precipitation inter-event timing (dots) and best fit exponenital cdfs (gray lines) of precipitation events > 18 mm for a) spring, b) summer non-tropical, and c) summer tropical events. Goodness-of-fit p-values for one-sample KS-tests are also shown.

4.2 Flood risk estimation from multiple mechanisms

Using the pdfs for precipitation above, the JoFlo hydrologic model, and the sampling strategies detailed in Section 3.4, the probability π that $Q>q_c$ given $P>p_c$ is estimated to be greatest for tropical storms (π = 0.054), followed by spring precipitation (π = 0.020), and then summer non-tropical precipitation events (π = 0.011). A sensitivity analysis indicates that the inclusion of hydrologic model uncertainty has a non-negligible impact on the estimation of π (see Supplemental Material). Figure 5 shows a mapping of the probability of experiencing at least one adverse flood event within 1-year (n = 1) and 10-year (n=10) planning periods over different values for precipitation event frequency (λ_p) and propensity for flooding (π). Historical point estimates for these parameters for each climate mechanism are also shown. Spring rain on snow events ($\lambda_p\pi$ = 0.047) pose a larger risk than summer tropical events ($\lambda_p\pi$ = 0.030) and summer non-tropical events ($\lambda_p\pi$ = 0.044), despite the fact that summer events are both more intense (Figure 3) and, in the case of non-tropical events, more frequent (Figure 4). This is due to the effect of antecedent conditions in the spring that leads to a moderate value of π, coupled with a high frequency of occurrence (λ_p) of spring events. When the risk associated with spring and late summer events is combined to estimate ${\lambda_p}^c$ and π^c (Eqns. 6 and 7), the

probability of experiencing at least one adverse condition within 1-year and 10-year planning periods is estimate to be 11.4% and 70.2% respectively. A tabulation of these results is presented in the Supplementary Material.

For a point of comparison, a classic POT approach on the direct observations of streamflow (Table 1) indicates 5 exceedances of q_c in a 45-year period (1972 – 2017). The estimate of λ_q based directly on the flow data $\left(\frac{5\ events}{45\ years} = 0.11\right)$ is very similar to the estimate of $\lambda_q = 0.047 + 0.030 + 0.044 = 0.121$ (5.4 exceedances in 45 years) based on the proposed approach, providing an indirect validation of the method.

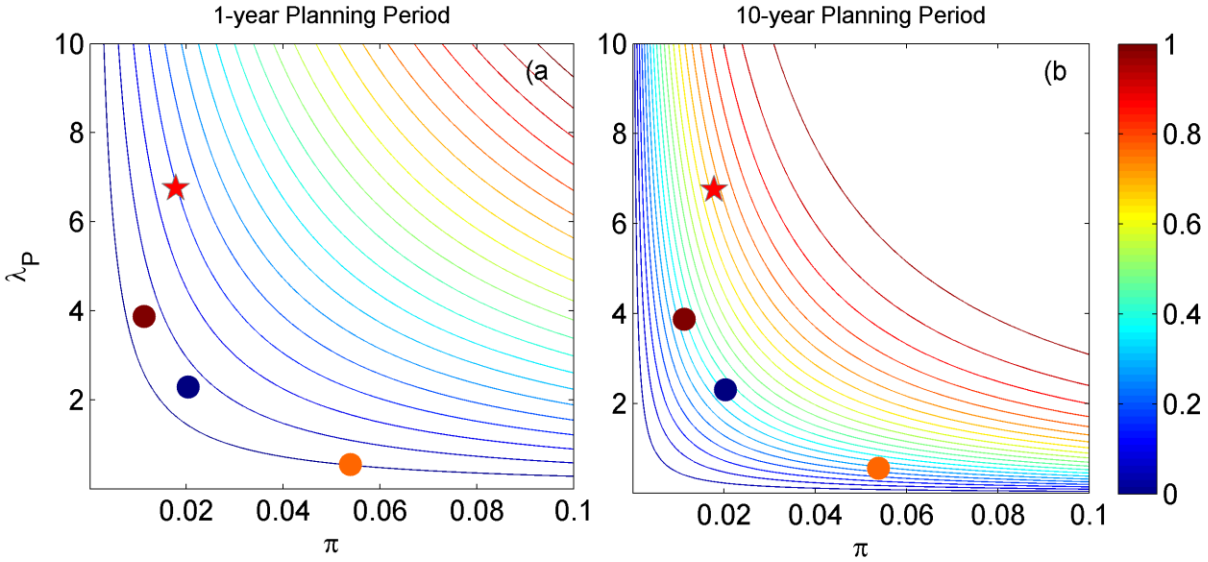

Figure 23 - Isoline mapping of Pr($N_Q \geq 1$) for a planning period of a) 1 year (n=1) and b) 10 year (n=10) across all λ_p and π. Point estimates of historical risk posed to Fall Creek are shown for spring precipitation (dark blue dot), late summer non-tropical precipitation (dark red dot), late summer tropical precipitation (orange dot), and the composite risk (based on $\lambda_p{}^c, \pi^c$) of all mechanisms (red star).

4.3 Updating Flooding Risk with Climate Projections

GCM-based climate projections are used to develop forecasts of future climate conditions and their influence on flood risk for Fall Creek. Here, we evaluate general changes to risk and how independent or joint updates to event frequency (λ_p), catchment antecedent conditions [$f_S(s)$], and extreme precipitation magnitude

$[f_P(p \mid P > p_c)]$ impact these changes. As mentioned previously, tropical and non-tropical summer events are grouped for the future climate analysis.

Figure 6 shows the climate and hydrologic changes projected by the ensemble of climate projections. During the spring season, the GCM simulations predict a uniform increase in air temperatures, which yield a higher probability of extreme precipitation occurring as rainfall. Increased spring air temperatures also result in reduced wintertime SWE, which decreases the runoff volume of snowmelt events. During the summer season, increased temperatures and decreased total seasonal precipitation leads to decreased soil moisture that reduces runoff risk. This result is consistent with the concept that future anticipated changes to hydrologic state variables such as reduced snowpack and unsaturated zone soil water content may impose a negative feedback on Fall Creek flood hydrology [Knighton et al., 2017].

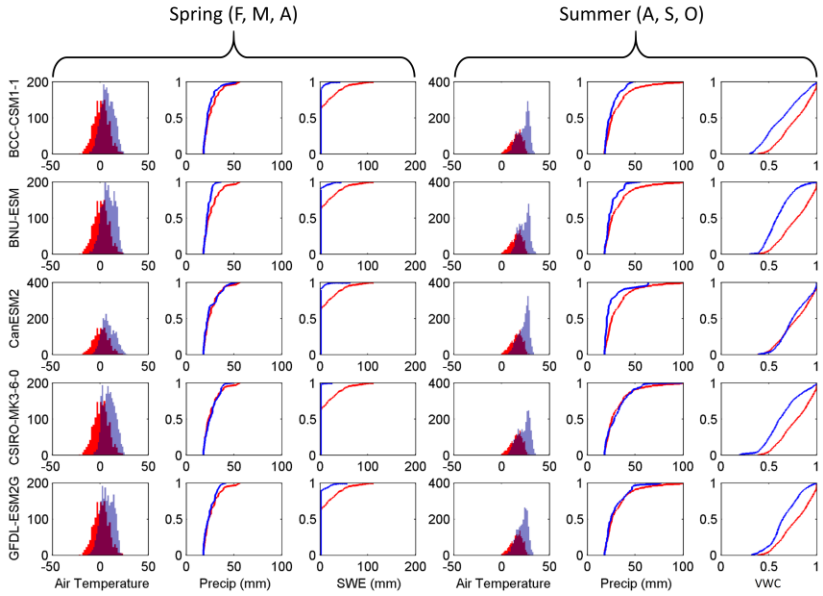

Figure 24– Estimated seasonal shifts in air temperature, extreme precipitation intensity (i.e., cdf of $P|P > p_c$), and estimated hydrologic state variables (i.e., cdfs of SWE and VWC, components of S), based on five downscaled GCM simulations from RCP8.5. Current conditions are shown in red, GCM estimates are shown in blue.

The downscaled GCM simulations predict either no substantial change in the cdf of extreme daily precipitation from current conditions during spring (CanESM2, CSIRO-MK3-6.0, BCC-CSM1-1, and GFDL-ESM2G), or a slight decrease (BNU-ESM). Similarly, the cdf of summer precipitation is predicted to remain relatively stationary (CSIRO-MK3-6.0, and GFDL-ESM2G) or decrease (CanESM2, BCC-CSM1-1 and BNU-ESM). These results are somewhat in disagreement with the annual extreme precipitation analysis of Ning et al. [2015] and the seasonal analysis of Shoof [2016]. Shoof [2016] estimates a slight increase in the frequency of extreme precipitation events greater than 10 and 20 mm^1day^{-1} for both spring and summer within the Northeast. This highlights how some climate information, like shifts in temperature and $f_S(s)$ may be more consistent than other projected changes, like those in $f_P(p \mid P > p_c)$ or $\lambda_{p,}$ particularly over small spatial scales.

In this example we consider three conceivable uses of GCM information: 1) to update characteristics of $f_S(s)$ which are sensitive to longer-term GCM projections of seasonal air temperatures and precipitation, 2) to update the seasonal characteristics of $f_S(s)$ and event frequencies λ_p, and 3) to update λ_p, $f_S(s)$, as well as the marginal pdf of extreme precipitation, $f_P(p \mid P > p_c)$. Other combinations of change are possible, but are not included for brevity of exposition. Figure 7 explicitly shows how these different combinations of change map directly onto a measure of system-relevant risk. We discuss in turn the results for spring and summer projections. All results are tabulated in the Supplementary Material.

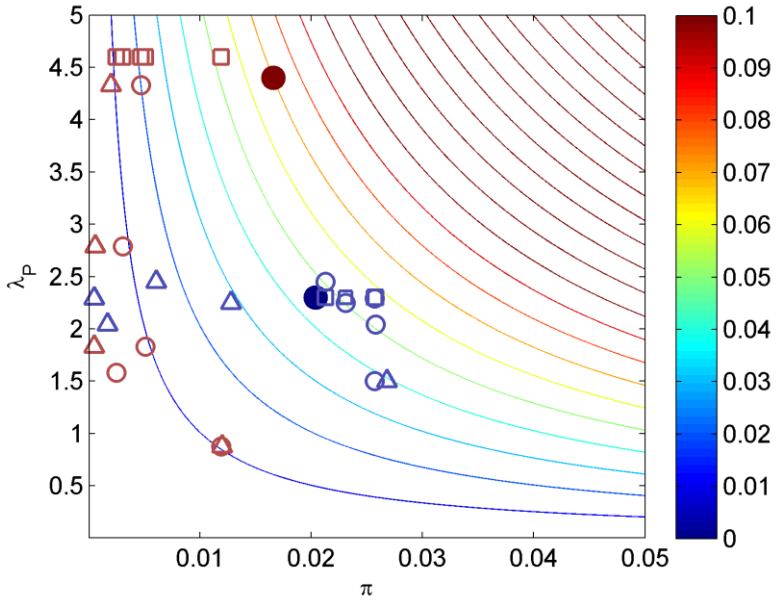

Figure 25– Isoline mapping of Pr($N_Q \geq 1$) for a planning period of 1 year (n=1) across all λ_p and π. Historic point estimates for spring precipitation (dark blue dot) and late summer precipitation (dark red dot) are shown, along with feasible future risk scenarios for spring (light blue) and summer (light red) precipitation derived from downscaled GCM RCP8.5 scenarios. Updates to different components of λ_p and π are shown using different shapes – (squares) $f_S(s)$ only; (open circles) $f_S(s)$ and λ_p; (triangles) $f_S(s)$, λ_p, and $f_P(p \mid P > p_c)$; each open symbol is based on a different GCM.

4.3.1 Spring Season Flooding Risk

Within the spring season, updates to $f_S(s)$ in isolation marginally increase the probability π that extreme rainfall triggers a flood (Figure 7, open blue squares), despite a significant change to the hydrologic state (Figure 6). Higher winter air temperatures lead to generally lower SWE accumulation, which lowers the risk of large melt events. However, high spring temperatures also increase the risk of precipitation falling as rain. These counteracting forces generally maintain overall flood risk for the season near its historical value. The similarity between historical and future projected risk in this case is particularly interesting because climate drivers of snow accumulation and melt dynamics are one of the more robust predictions of

hydrologic change under warming [Knutti and Sedlacek, 2013], but in isolation, the implications for Fall Creek flood risk are muted.

Next, we consider updates to the frequency of intense spring precipitation, λ_p. These values are not substantially different than the value estimated from the historical record, although there are some decreases for certain projections (Figure 7, open blue circles). This may be because extreme precipitation during the spring is linked to extratropical cyclones, and GCMs do not generally show a consistent and large signal of change in the frequency of these large-scale storms in the mid-latitudes of the Northern Hemisphere [Emori and Brown 2005; Chang et al., 2012]. We note that the GCM derived changes to spring λ_p are similar to the regionally expected precipitation patterns using more robust downscaling techniques [e.g., Schoof 2016], which suggests that the result is not an artifact of the BCSD downscaling.

When considering updates to the pdfs of intense precipitation magnitudes, $f_P(p \mid P > p_c)$, concurrently with changes to $f_S(s)$ and λ_p, the GCM projections suggest similar or decreasing spring flood risk (Figure 7, open triangles). This is caused primarily by a relatively high level of disagreement among predictions of π. Several GCMs predict a slight increase in moderate spring precipitation events (< 30 cm), but a decrease in the upper tail events that tends to drive the flood risk for Fall Creek (see Figure 6). This result runs somewhat counter to the expected physical relationship between warming air temperatures and atmospheric moisture holding capacity. Ning et al. [2015] demonstrate a large variance among the GCM predictions of extreme precipitation in the Northeast US, suggesting low predictive skill of the underlying models. Further, Tryhorn and DeGaetano [2011] and Ning et al [2015] suggest the BCSD downscaling technique may also influence the prediction of extreme precipitation within the region. Therefore, there may be considerable uncertainty associated with estimates of $f_P(p \mid P > p_c)$ derived from the downscaled

CMIP5 simulations used here. Shifts in flood risk that only consider changes to $f_S(s)$ and λ_p may be more informative in this case. This highlights the utility of the bottom-up based risk assessment approach, since it is easy to visualize the consequences from complex, coupled changes in hydrologic states, storm frequency, and intensity and discount certain projections if they are deemed unreliable.

4.3.2 Summer Season Flooding Risk

Considering only downscaled GCM updates to $f_S(s)$ suggests a decrease in summertime flood risk (Figure 7, open red squares). This effect is linked most strongly to decreased seasonal precipitation totals during a period of relatively high evaporation and transpiration losses. These hydrological processes lead to reduced soil water. Thibeault and Seth [2014] demonstrate the CMIP5 models provide generally reasonable estimates of summer season precipitation patterns in the Northeast US. Increased summer air temperatures, also a robust GCM prediction, cause a slight increase in atmospheric water demand from the land surface within the Priestly Taylor PET model. Similar to the spring season, relatively consistent predictions of future summer climate and hydrologic state variables have a limited effect on flood risk.

Updates to both $f_S(s)$ and the frequency of extreme summer precipitation events, λ_p, show a consistent decrease in the frequency of intense summer storms, but with a large variability among the projections (Figure 7, open red circles). Janssen et al. [2016] demonstrate that the CMIP5 GCMs tend to induce a slight anomalous shift in the frequency of extreme precipitation events from summer and fall to spring, which may be due to difficulty in reproducing convective precipitation processes. Accurately simulating the physical processes governing intense small-scale convective precipitation in climate models is a challenging task that exceeds the prediction skill of many existing models [Dai 2006; Pritchard et al., 2010; Kendon et al., 2012; Kysely et al., 2016]. As discussed previously, some of the summer risk is also related to tropical

moisture exports, sometimes in the form of tropical cyclones [Steinschneider and Lall, 2015, 2016; Lu and Lall, 2017]. Warmer tropical Atlantic sea-surface temperatures should facilitate increases in the frequency of land-falling tropical cyclones in the Northeast US [Emanuel, 2005], though this result is not consistently simulated by CMIP5 GCMs [Wuebbles et al., 2014]. Finally, as with spring extreme precipitation there are similar issues with downscaling summer rainfall events. The downscaling technique of Schoof [2016] predicts a slight increase to summer extreme precipitation frequency in the Northeast US, potentially indicating that the frequency decrease could be attributed at least in part to the BCSD downscaling approach.

Finally, incorporating updates to summer $f_P(p \mid P > p_c)$ does not provide a meaningful change in risk as compared to the case when only changes to $f_S(s)$ and λ_p are considered (Figure 7, red open triangles), despite the estimated changes in summertime precipitation intensity (Figure 6). This is likely due to the low risk already associated with these events. Further, warmer air temperatures should be a physical driver for greater precipitation intensities for both non-tropical and tropical moisture driven systems due to the Clausius-Clapeyron relationship. We suspect the decrease in the intensity of summer precipitation is due to anomalous numerical issues with both the GCMs and the BCSD downscaling methodology, but verifying this was outside the scope of our study.

4.4 Sensitivity to Climate Projections and Risk Threshold

Finally, we consider modifications to the stakeholder relevant risk threshold, q_c, to determine how changes in exposure would alter the interpretation of climate projections. Under present-day climate conditions, lowering the levee structure from elevation 2 m to 1.5 m (an effective channel capacity reduction from 120 m^3s^{-1} to 85 m^3s^{-1}) results in an expected general increase in the estimate of π and therefore the composite flood risk (λ_q = 0.22) above existing conditions (λ_q = 0.12) (Figures 8a, b).

The increase in flood risk is attributable most strongly to an increase in spring risk ($\lambda_p\pi$ = 0.110 under 1.5 m vs. $\lambda_p\pi$ = 0.046 under 2 m) with a less substantial increase in summer risk ($\lambda_p\pi$ = 0.110 under 1.5 m vs. $\lambda_p\pi$ = 0.0750 under 2 m). Such an increase in flooding risk (flooding at 5- vs. 9-year return period) may necessitate the construction of infrastructure to reduce flooding risk, or through financial risk management tools such as flooding insurance.

For the spring season, utilizing seasonal GCM predictions to only update $f_S(s)$ as well as $f_S(s)$ and λ_p produce more consistent increases in flood risk with a the lower risk threshold (Figure 8a) as compared to a higher risk threshold (Figure 7). This result is primarily attributable to an increase in the probability of moderate spring precipitation falling as rain that produce flow that exceeds the lower q_c threshold. For summer, we see uniform decreases in risk under 1.5 m levees, similar to what was seen for the 2m levees. Projections incorporating changes to $f_P(p \mid P > p_c)$ similarly show low agreement (Figures 8a, b).

Importantly, changes to $f_S(s)$ and $f_P(p \mid P > p_c)$ may involve a complex mapping onto a risk profile that is not only dependent on the climate mechanism of interest, but also on the threshold for risk that can be tolerated. At the higher risk threshold there is substantial variability in future projections of π. The spring estimates of π begin to converge as the threshold decreases to the lower q_c of 85 m^3s^{-1}, and at very low values of q_c differences between the GCMs become irrelevant (Figure 8b). This may not be apparent at the outset of analysis, and the results here demonstrate that accurately defining q_c is critical to developing estimates of vulnerability to future climate conditions.

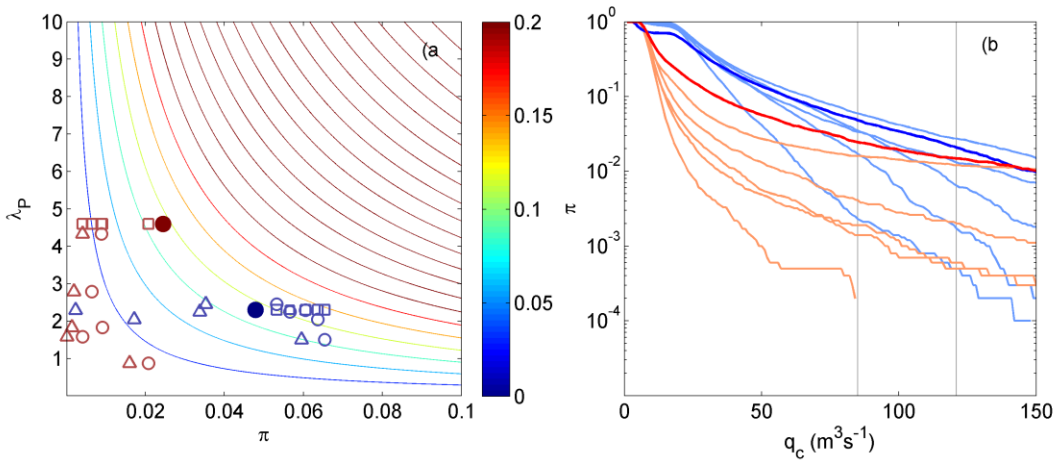

Figure 26– a) As in Figure 3.7, but demonstrating the effects of a lower stakeholder derived risk threshold; symbology is the same as Figure 3.7. b) Changes in π due to changes in q_c considering GCM updates to both $f_S(s)$ and, $f_P(p \mid P > p_0)$ (dark lines -current climate; light lines - GCM climate projections), (winter – blue, summer- red). q_c scenarios used in b shown by gray lines.

5. Methodology Extensions

While the approach presented here offers important innovations to existing flood risk assessment methodologies, our application does suffer from some important limitations that require further discussion, along with opportunities for future work to address these issues.

5.1. Extensions to other datasets and hydrologic regions

In the case study presented herein we defined q_c as a fixed threshold of a standard hydrologic variable as recommended by Ithaca, NY community stakeholders. Fixed thresholds for q_c are commonly used to define flooding (e.g., bank-full discharge), though it is possible to use fragility curves to express relationships between hazard and risk probabilistically [e.g. Stephenson and D'Ayala, 2014; De Bruijn et al., 2014; Schröter et al., 2014; Remo et al., 2016; Botto et al., 2014]. It is further possible to expand Q and q_c to consider the joint frequency of other hazards. For instance, water depths and velocities (Q) above 0.5 m and 0.5 m/s (q_c), respectively, may cause damage to local infrastructure [Kreibich et al., 2009]; the coincidence of phosphorus

and nitrogen concentrations (Q) greater than 0.5 mg^1L^{-1} and 20 mg^1L^{-1} (q_c), respectively, may threaten oligotrophic aquatic ecosystems [Dodds and Smith, 2016]; or inundation durations of agricultural fields (Q) for greater than 72 hours during the growing season (q_c) could significantly reduce the value of crops [Förster et al., 2008]. The meteorological and hydrologic forcing data analysis was tailored to our study catchment though we note that generalizations are possible. The pdf of extreme precipitation event characteristics, $f_P(p \mid P > p_c)$, could be defined over another accumulation period (e.g. hourly precipitation) or expanded to represent a vector of critical precipitation characteristics (e.g. duration, peak hourly intensity, etc.) if it is hydrologically relevant to reproduce multiple characteristics of extreme rainfall as in Knighton & Walter [2016]. Extreme precipitation characteristics $f_P(p \mid P > p_c)$ and λ_p could also be defined with other datasets such as remotely sensed products, climate reanalysis products [Fuka et al., 2014; Auerbach et al., 2016], or paleo data [Steinschneider et al., 2016]. Similarly, $f_S(s)$ could be estimated from long records of observed watershed hydrologic state variables, which affect runoff risk (e.g. soil moisture, snowpack) [e.g. Hoffmeister et al., 2016]. Finally, if correlations between $f_P(p \mid P > p_c)$ and $f_S(s)$ are found to be significant within a catchment, this dependency could be modeled explicitly with probabilistic approaches such as copula models [e.g. Genest & Favre, 2007].

Sampling uncertainty in λ_p and $f_P(p \mid P > p_c)$ was not considered in our application for brevity of exposition, but could be easily incorporated. Sampling uncertainty in the parameters of the pdfs of $f_P(p \mid P > p_c)$ and $f_S(s)$ could be propagated into the estimation of π with further adjustments to Eq. 5 to integrate over the sampling distributions of these parameters; whereas uncertainty in λ_p could be introduced in Eq. 3.

Our case study focused on a small catchment influenced by seasonal snow hydrology which discharges through a dense urban community. Application of this methodology to larger or more hydrologically distinct watersheds would require several considerations. First as in this case study a careful definition of q_c to represent stakeholder concerns. Next, this work would require further definition of the characteristics of flood causing precipitation events [$f_P(p \mid P > p_c)$] and the antecedent moisture conditions [$f_S(s)$] which are most relevant for simulations in the region and seasons of importance. Evaluating $f_Q(q \mid P = p, S = s)$ requires selection of a hydrologic model that captures the flood-relevant processes at the spatial and temporal scales of interest.

5.2. Fidelity of the physical hydrologic modeling

The case study incorporated a relatively simplistic hydrologic model [Archibald et al., 2014] to develop estimates of future flood risk. More physically-based or distributed hydrologic models could be utilized likely provide a more accurate or higher resolution evaluation of $f_Q(q \mid P = p, S = s)$. We further considered our hydrologic model structure and parameterization to be climate invariant. The temporal and spatial transferability of hydrologic models and parameterizations may be evaluated and considered explicitly when forcing simulations as in Broderick et al. [2016] and Knighton et al. [2014] respectively. Generally, the selected hydrologic model and simulation design must adequately reproduce the flood-relevant hydrology of the region of interest.

5.3. Treatment of Climate Mechanisms

Our case study necessitated an analysis of historical climate conditions that separated precipitation into three mechanisms: spring precipitation on snow, late summer non-tropical, and late summer tropical moisture related events. Each of these mechanisms could be further separated into convective and stratiform precipitation, as

these types of precipitation may have distinct precipitation characteristics, forecast lead times that may be a risk-relevant characteristic, and varied prediction reliability within climate models. Similarly, our analysis of future changes to atmospheric flood inducing mechanisms further aggregated all late summer precipitation events into one composite mechanism by grouping non-tropical and tropical events. Storm tracking algorithms allow for the separation of precipitation events by moisture source [e.g. Knippertz and Wernli, 2010]. Future research could employ a tracking algorithm to make clearer inferences on GCM-based predictions for specific flood-inducing storm types.

Finally, we qualitatively discussed the credibility in estimates of λ_p and π in the context of a bottom-up framework. Methods of objectively combining projections of varying credibility (e.g. Bayesian Model Averaging, Granger-Ramanathan averaging; Diks & Vrugt et al [2010]) to combine multiple estimates of λ_p and π may yield more robust predictions.

6. Conclusions

This study presents a vulnerability-based approach to estimating riverine flooding risk that accommodates a more direct linkage between decision-relevant metrics of risk and the dominant causal atmospheric mechanisms that drive riverine flooding. The approach is supported by a modified POT methodology that uses a semi-physical hydrologic model to quantify risk posed by individual flood inducing climate mechanisms. The methods presented in this work represent a significant step towards the development of a planning tool based on an understanding of climate-flood linkages [Blöschl et al., 2015; Merz et al., 2014]. We demonstrated this approach for Fall Creek in Ithaca NY, using a stakeholder derived flooding threshold and focusing on three storm types identified in the historical record: spring precipitation on snow, late summer non-tropical rainfall, and late summer tropical rainfall.

The analysis utilized a bottom-up approach to future flooding risk that can help facilitate decision-making under uncertainty. We incorporated information on structural changes to the atmosphere under a high emissions scenario from a series of downscaled GCM projections to demonstrate how future change in different underlying mechanisms, projected by the GCMs, map directly onto a risk profile tailored to a local context. When we only consider changes to seasonal antecedent conditions, which tend to be the most consistent across climate models, there is relatively little influence on projected risk from each storm type (or season). Changes to extreme precipitation event frequency and intensity, which are more variable across the GCMs and potentially less reliable, show an inconsistent influence on flooding risk among the GCMs considered. However, the analysis suggests that of all the mechanisms considered, changes in springtime extreme precipitation could potentially increase flood risk, highlighting that this mechanism may deserve additional attention in future analysis. Importantly, the bottom-up approach to risk analysis clearly demonstrates the degree to which flood risk will increase given complex changes to the frequency and intensity of extremes and antecedent conditions, regardless of whether the climate models are able to simulate such behavior well.

In addition, we demonstrate that vulnerability-based planning, particularly when incorporating highly uncertain climate projections, is sensitive to the stakeholder-relevant risk threshold. A hypothetical case of a lowered levee elevation, and therefore a reduced risk threshold, alters conclusions surrounding the expected shift in risk related to future spring storms but has little impact on the assessment of change in summer risk. This highlights the importance of carefully working with stakeholders to establish a reliable estimate of the threshold for societal risk before allocating substantial resources towards an assessment of all potential climate risks facing a system. An initial analysis may indicate that some climate risks do not pose

much of a threat given the existing level of exposure compared to others (flooding from summer vs. springtime storms), which could help determine how to allocate future resources for further analysis.

6. Annotation List

M – hydrologic model

n – number of years (planning period)

N_Q –the number of floods that exceed the threshold q_c within the planning period

N_P – the number of precipitation events that exceed the threshold p_c within the planning period

p_c – user defined threshold for critical precipitation characteristic

P –critical precipitation event characteristic

Q – hydrologic flooding variable of interest

q_c – critical threshold for floods

S – vector of antecedent watershed conditions

ε – hydrologic model error term

λ_q – rate parameter defining the frequency that Q exceeds q_c

λ_p – rate parameter defining the frequency that P exceeds p_c

π – conditional probability that Q exceeds q_c given that P exceeds p_c

Ω_s - the multivariate space of possible antecedent conditions

Θ - parameter space for hydrologic model and error model

REFERENCES

Aerts, J. C., Lin, N., Botzen, W., Emanuel, K., & de Moel, H. (2013). Low-Probability Flood Risk Modeling for New York City. Risk Analysis, 33(5), 772-788.

Agel, L., Barlow, M., Qian, J. H., Colby, F., Douglas, E., & Eichler, T. (2015). Climatology of daily precipitation and extreme precipitation events in the northeast United States. Journal of Hydrometeorology, 16(6), 2537-2557.

Alfonso, L., Mukolwe, M. M., & Di Baldasssarre, G. (2016). Probabilistic Flood Maps to support decision-making: Mapping the Value of Information. Water Resources Research.

Archibald, J. A., & Walter, M. T. (2014). Do Energy-Based PET Models Require More Input Data than Temperature-Based Models?—An Evaluation at Four Humid FluxNet Sites. JAWRA Journal of the American Water Resources Association, 50(2), 497-508.

Archibald, J. A., Buchanan, B. P., Fuka, D. R., Georgakakos, C. B., Lyon, S. W., & Walter, M. T. (2014). A simple, regionally parameterized model for predicting nonpoint source areas in the northeastern US. Journal of Hydrology: Regional Studies, 1, 74-91.

Auerbach, D. A., Easton, Z. M., Walter, M. T., Flecker, A. S., & Fuka, D. R. (2016). Evaluating weather observations and the climate forecast system reanalysis as inputs for hydrologic modeling in the tropics. Hydrological Processes.

Ben-Haim, Y. (2006). Info-gap decision theory: decisions under severe uncertainty. Academic Press.

Benavides, J. A., & Winter, H. M. (2013). Chapter 12. Severe Storm Impacts and Flood Management. IN (eds. Bendient, Huber, Vieux) Hydrology and Floodplain Analsysis, 5th ed. Pearson Education, Inc. 801 pages.

Berghuijs, W. R., Woods, R. A., Hutton, C. J., & Sivapalan, M. (2016). Dominant flood generating mechanisms across the United States. Geophysical Research Letters, 43(9), 4382-4390.

Beven, K. J., Aspinall, W. P., Bates, P. D., Borgomeo, E., Goda, K., Hall, J. W., ... & Stephenson, D. B. (2015). Epistemic uncertainties and natural hazard risk assessment–Part 1: A review of the issues. Natural Hazards and Earth System Sciences Discussions, 3, 7333-7377.

Beven, K. J., Almeida, S., Aspinall, W. P., Bates, P. D., Blazkova, S., Borgomeo, E., ... & Stephenson, D. B. (2016). Epistemic uncertainties and natural hazard risk assessment–Part 2: Different natural hazard areas.

Black, P.E. (2012). The U.S. flood control program at 75: Environmental issues. Journal of the American Water Resources Association, 48(2), 244-255.

Blöschl, G., Gaál, L., Hall, J., Kiss, A., Komma, J., Nester, T., ... & Salinas, J. L. (2015). Increasing river floods: fiction or reality?. Wiley Interdisciplinary Reviews: Water, 2(4), 329-344.

Botto, A., Ganora, D., Laio, F., & Claps, P. (2014). Uncertainty compliant design flood estimation. Water Resources Research, 50(5), 4242-4253.

Botzen, W. J. W., Aerts, J. C. J. H., & Van den Bergh, J. C. J. M. (2013). Individual preferences for reducing flood risk to near zero through elevation. Mitigation and Adaptation Strategies for Global Change, 18(2), 229-244.

Broderick, C., Matthews, T., Wilby, R. L., Bastola, S., & Murphy, C. (2016). Transferability of hydrological models and ensemble averaging methods between contrasting climatic periods. Water Resources Research, 52(10), 8343-8373.

Brown, C., Ghile, Y., Laverty, M., & Li, K. (2012). Decision scaling: Linking bottom-up vulnerability analysis with climate projections in the water sector. Water Resources Research, 48(9).

Brown, C., Werick, W., Leger, W., & Fay, D. (2011). A decision-analytic approach to managing climate risks: Application to the Upper Great Lakes. JAWRA Journal of the American Water Resources Association, 47(3), 524-534.

Chang, E. K. M., Y. Guo, and X. Xia (2012), CMIP5 multimodel ensemble projection of storm track change under global warming, J. Geophys. Res., 117, D23118, doi:10.1029/2012JD018578.

DeGaetano, A. T. (2009). Time-dependent changes in extreme-precipitation return-period amounts in the continental United States. Journal of Applied Meteorology and Climatology, 48(10), 2086-2099.

Diks, C. G., & Vrugt, J. A. (2010). Comparison of point forecast accuracy of model averaging methods in hydrologic applications. Stochastic Environmental Research and Risk Assessment, 24(6), 809-820.

Dixon, K. W., Lanzante, J. R., Nath, M. J., Hayhoe, K., Stoner, A., Radhakrishnan, A., ... & Gaitán, C. F. (2016). Evaluating the stationarity assumption in statistically downscaled climate projections: is past performance an indicator of future results?. Climatic Change, 135(3-4), 395-408.

Dodds, W., & Smith, V. H. (2016). Nitrogen, phosphorus, and eutrophication in streams. Inland Waters, 6(2), 155-164.

Emanuel, K. (2005). Increasing destructiveness of tropical cyclones over the past 30 years. Nature, 436(7051), 686-688.

Emori, S., and S. J. Brown (2005), Dynamic and thermodynamic changes in mean and extreme precipitation under changed climate, Geophys. Res. Lett., 32, L17706, doi:10.1029/2005GL023272

Fischer, E. M., & Knutti, R. (2016). Observed heavy precipitation increase confirms theory and early models. Nature Climate Change, 6(11), 986-991.

Fuka, D. R., Walter, M. T., MacAlister, C., Degaetano, A. T., Steenhuis, T. S., & Easton, Z. M. (2014). Using the Climate Forecast System Reanalysis as weather input data for watershed models. Hydrological Processes, 28(22), 5613-5623.

Förster, S., Kuhlmann, B., Lindenschmidt, K. E., & Bronstert, A. (2008). Assessing flood risk for a rural detention area. Natural Hazards and Earth System Science, 8(2), 311-322.

Genest, C., & Favre, A. C. (2007). Everything you always wanted to know about copula modeling but were afraid to ask. Journal of hydrologic engineering, 12(4), 347-368.

Halbert, K., Nguyen, C. C., Payrastre, O., & Gaume, E. (2016). Reducing uncertainty in flood frequency analyses: A comparison of local and regional approaches involving information on extreme historical floods. Journal of Hydrology.

Hadka, D., Herman, J., Reed, P., & Keller, K. (2015). An open source framework for many-objective robust decision making. Environmental Modelling & Software, 74, 114-129.

Hassanzadeh, E., Elshorbagy, A., Wheater, H., & Gober, P. (2016). A risk-based framework for water resource management under changing water availability, policy options, and irrigation expansion. Advances in Water Resources, 94, 291-306.

Haynes (2010), Dreary state of precipitation in global models, J. Geophys. Res., 115, D24211, doi:10.1029/2010JD014532.

Herman, J.D., Zeff, H.B., Lamontagne, J.R., Reed, P.M., and Characklis, G.W. (2016), Synthetic drought scenario generation to support bottom-up water supply vulnerability assessments, Journal of Water Resources Planning and Management, 142(11)

Hofmeister, K., Georgakakos, C., Walter, M. T. 2016. A runoff risk model based on topographic wetness indices and probability distributions of rainfall and soil moisture for central New York agricultural fields. Journal of Soil and Water Conservation 71(4), 289-300.

Janssen, E., Sriver, R. L., Wuebbles, D. J., & Kunkel, K. E. (2016). Seasonal and regional variations in extreme precipitation event frequency using CMIP5. Geophysical Research Letters, 43(10), 5385-5393.

Kasprzyk, J. R., Reed, P. M., Kirsch, B. R., & Characklis, G. W. (2009). Managing population and drought risks using many-objective water portfolio planning under uncertainty. Water Resources Research, 45(12).

Kendon, E. J., Roberts, N. M., Senior, C. A., & Roberts, M. J. (2012). Realism of rainfall in a very high-resolution regional climate model. Journal of Climate, 25(17), 5791-5806.

Kirby, W. (1969), On the Random Occurrence of Major Floods, Water Resour. Res., 5(4), 778–784, doi:10.1029/WR005i004p00778.

Kjeldsen, T. R., Macdonald, N., Lang, M., Mediero, L., Albuquerque, T., Bogdanowicz, E., ... & Gül, G. O. (2014). Documentary evidence of past floods in Europe and their utility in flood frequency estimation. Journal of Hydrology, 517, 963-973.

Knighton J, DeGaetano, A., Walter, M.T. (2017). Hydrologic State Controls on Riverine Flood Hazard: Negative Feedbacks on the Effects of Climate Change. Journal of Hydrometeorology. DOI: 10.1175/JHM-D-16-0164.1

Knighton J, Walter, M.T. (2016). Critical Rainfall Statics for Predicting Watershed Flood Responses: Rethinking the Design Storm Concept. Hydrological Processes. DOI: 10.1002/hyp.10888

Knighton, J., White, E., Lennon, E., & Rajan, R. (2014). Development of probability distributions for urban hydrologic model parameters and a Monte Carlo analysis of model sensitivity. Hydrological processes, 28(19), 5131-5139.

Knippertz, P., & Wernli, H. (2010). A Lagrangian climatology of tropical moisture exports to the Northern Hemispheric extratropics. Journal of Climate, 23(4), 987-1003.

Knutti, R., & Sedláček, J. (2013). Robustness and uncertainties in the new CMIP5 climate model projections. Nature Climate Change, 3(4), 369-373.

Kreibich, H., Piroth, K., Seifert, I., Maiwald, H., Kunert, U., Schwarz, J., ... & Thieken, A. H. (2009). Is flow velocity a significant parameter in flood damage modelling?. Natural Hazards and Earth System Sciences, 9(5), 1679.

Kron, W. (2005). Flood risk= hazard• values• vulnerability. Water International, 30(1), 58-68.

Kysely, J., Z. Rulfova, A. Farda, and M. Hanel (2015), Convective and stratiform precipitation characteristics in an ensemble of regional climate model simulations, Climate Dynamics, 1-17, doi: 10.1007/s00382-015-2580-7.

Lempert, R., Nakicenovic, N., Sarewitz, D., & Schlesinger, M. (2004). Characterizing climate-change uncertainties for decision-makers. An editorial essay. Climatic Change, 65(1), 1-9.

Lempert, R. J. (2003). Shaping the next one hundred years: new methods for quantitative, long-term policy analysis. Rand Corporation.

Lu, M., and Lall, U. (2017), Tropical moisture exports, extreme precipitation and floods in the Northeast US, Earth Science Research, 6(2), doi: 10.5539/esr.v6n2p91

McDaniels, T. L., Gregory, R. S., & Fields, D. (1999). Democratizing risk management: Successful public involvement in local water management decisions. Risk analysis, 19(3), 497-510.

Mei, X., Dai, Z., Tang, Z., & Gelder, P. H. A. J. M. (2016). Impacts of historical records on extreme flood variations over the conterminous United States. Journal of Flood Risk Management.

Merz, B., Kreibich, H., Schwarze, R., & Thieken, A. (2010). Review article" Assessment of economic flood damage". Natural Hazards and Earth System Sciences, 10(8), 1697.

Merz, B., Aerts, J. C. J. H., Arnbjerg-Nielsen, K., Baldi, M., Becker, A., Bichet, A., ... & Delgado, J. M. (2014). Floods and climate: emerging perspectives for flood risk assessment and management. Natural Hazards and Earth System Sciences, 14(7), 1921.

Morss, R. E., Wilhelmi, O. V., Downton, M. W., & Gruntfest, E. (2005). Flood risk, uncertainty, and scientific information for decision making: lessons from an interdisciplinary project. Bulletin of the American Meteorological Society, 86(11), 1593.

National Climatic Data Center (NCDC) (2016). Land-Based Station Data. Available Online: http://www.ncdc.noaa.gov/data-access/land-based-station-data

Neal, J., Keef, C., Bates, P., Beven, K., & Leedal, D. (2013). Probabilistic flood risk mapping including spatial dependence. Hydrological Processes, 27(9), 1349-1363.

Ning, L., Riddle, E. E., & Bradley, R. S. (2015). Projected changes in climate extremes over the northeastern United States. Journal of Climate, 28(8), 3289-3310.

Obama, B (2015), Establishing a Federal Flood Risk Management Standard and a Process for Further Soliciting and Considering Stakeholder Input, United States Executive Order 13690, The White House, Wash. [Available at https://www.whitehouse.gov/the-press-office/2015/01/30/executive-order-establishing-federal-flood-risk-management-standard-and-]

Parent, E., Favre, A. C., Bernier, J., & Perreault, L. (2014). Copula models for frequency analysis what can be learned from a Bayesian perspective?. Advances in Water Resources, 63, 91-103.

Pappenberger, F., Stephens, E., Thielen, J., Salamon, P., Demeritt, D., Andel, S. J., ... & Alfieri, L. (2013). Visualizing probabilistic flood forecast information:

expert preferences and perceptions of best practice in uncertainty communication. Hydrological Processes, 27(1), 132-146.

Pritchard, M.S., M.W. Moncrieff, and R.C.J. Somerville (2011), Orogenic propagating precipitation systems over the United States in a global climate model with embedded explicit convection, Journal of Atmospheric Sciences, 68, 1821-1840, doi: http://dx.doi.org/10.1175/2011JAS3699.1

Prudhomme, C., N. Reynard, and S. Crooks, 2002: Downscaling of global climate models for flood frequency analysis: where are we now? Hydrol. Process., 16, 1137-1150, doi: 10.1002/hyp.1054.

Prudhomme, C., Wilby, R. L., Crooks, S., Kay, A. L., & Reynard, N. S. (2010). Scenario-neutral approach to climate change impact studies: application to flood risk. Journal of Hydrology, 390(3), 198-209.

Remo, J. W., Pinter, N., & Mahgoub, M. (2016). Assessing Illinois's flood vulnerability using Hazus-MH. Natural Hazards, 81(1), 265-287.

Rogger, M., Viglione, A., Derx, J., & Blöschl, G. (2013). Quantifying effects of catchments storage thresholds on step changes in the flood frequency curve. Water Resources Research, 49(10), 6946-6958.

Roth, David M; Weather Prediction Center (2012). "Tropical Cyclone Rainfall in the Mid-Atlantic United States". Tropical Cyclone Rainfall Point Maxima. United States National Oceanic and Atmospheric Administration's National Weather Service. Retrieved June 23, 2012.

Sarhadi, A., Burn, D. H., Concepción Ausín, M., & Wiper, M. P. (2016). Time varying nonstationary multivariate risk analysis using a dynamic Bayesian copula. Water Resources Research.

Schoups, G., & Vrugt, J. A. (2010). A formal likelihood function for parameter and predictive inference of hydrologic models with correlated, heteroscedastic, and non-Gaussian errors. Water Resources Research, 46(10).

Schoof, J. T., & Robeson, S. M. (2016). Projecting changes in regional temperature and precipitation extremes in the United States. Weather and Climate Extremes, 11, 28-40.

Schröter, K., Kreibich, H., Vogel, K., Riggelsen, C., Scherbaum, F., & Merz, B. (2014). How useful are complex flood damage models?. Water Resources Research, 50(4), 3378-3395.

Shepherd, T. G. (2014). Atmospheric circulation as a source of uncertainty in climate change projections. Nature Geoscience, 7(10), 703-708.

Shin, J. Y., Lee, T., & Ouarda, T. B. (2015). Heterogeneous Mixture Distributions for Modeling Multisource Extreme Rainfalls*. Journal of Hydrometeorology, 16(6), 2639-2657.

Singh, R., Reed, P. M., & Keller, K. (2015). Many-objective robust decision making for managing an ecosystem with a deeply uncertain threshold response. Ecology and Society, 20(3), 1-32.

Srinivasan, T. N., & Rethinaraj, T. G. (2013). Fukushima and thereafter: Reassessment of risks of nuclear power. Energy Policy, 52, 726-736.

Stedinger, J. R., & Tasker, G. D. (1985). Regional hydrologic analysis: 1. Ordinary, weighted and generalized least squares compared. Water Resources Research, 21(9), 1421-1432.

Stedinger, J. R., & Cohn, T. A. (1986). Flood frequency analysis with historical and paleoflood information. Water Resources Research, 22(5), 785-793.

Stedinger, J. R., Vogel, R. M., Lee, S. U., & Batchelder, R. (2008). Appraisal of the generalized likelihood uncertainty estimation (GLUE) method. Water resources research, 44(12).

Steinschneider, S., and C. Brown (2013), A semiparametric multivariate, multi-site weather generator with low-frequency variability for use in climate risk assessments, Water Resour. Res., 49, 7205-7220, doi: 10.1002/wrcr.20528.

Steinschneider, S., & Lall, U. (2015). A hierarchical Bayesian regional model for nonstationary precipitation extremes in Northern California conditioned on tropical moisture exports. Water Resources Research, 51(3), 1472-1492.

Steinschneider, S, Wi, S, and Brown, C (2015a), The integrated effects of climate and hydrologic uncertainty on future flood risk assessments. Hydrol. Process., 29, 2823–2839. doi:10.1002/hyp.10409

Steinschneider, S., McCrary, R., Wi, S., Mulligan, K., Mearns, L. O., & Brown, C. (2015b). Expanded decision-scaling framework to select robust long-term water-system plans under hydroclimatic uncertainties. Journal of Water Resources Planning and Management, 141(11), 04015023.

Steinschneider, S., M. Ho, E. R. Cook, and U. Lall (2016), Can PDSI inform extreme precipitation?: An exploration with a 500 year long paleoclimate reconstruction over the U.S., Water Resour. Res., 52,3866–3880, doi:10.1002/2016WR018712.

Steinschneider, S., and U. Lall (2016), Spatiotemporal structure of precipitation related to tropical moisture exports over the eastern United States and its relation to climate teleconnections, Journal of Hydrometeorology, doi: http://dx.doi.org/10.1175/JHM-D-15-0120.1

Steinschneider, S. and U. Lall (2015), Daily Precipitation and Tropical Moisture Exports across the Eastern United States: An Application of Archetypal

Analysis to Identify Spatiotemporal Structure. J. Climate, 28, 8585–8602. doi: http://dx.doi.org/10.1175/JCLI-D-15-0340.1

Stephenson, V., & D'Ayala, D. (2014). A new approach to flood vulnerability assessment for historic buildings in England. Natural Hazards and Earth System Sciences, 14(5), 1035-1048.

Sun, X., Lall, U., Merz, B., & Dung, N. V. (2015). Hierarchical Bayesian clustering for nonstationary flood frequency analysis: Application to trends of annual maximum flow in Germany. Water Resources Research, 51(8), 6586-6601.

Taylor, K. E., Stouffer, R. J., & Meehl, G. A. (2012). An overview of CMIP5 and the experiment design. Bulletin of the American Meteorological Society, 93(4), 485-498.

Thibeault, J. M., & Seth, A. (2014). A framework for evaluating model credibility for warm-season precipitation in northeastern North America: A case study of CMIP5 simulations and projections. Journal of Climate, 27(2), 493-510.

Tryhorn, L., & DeGaetano, A. (2011). A comparison of techniques for downscaling extreme precipitation over the Northeastern United States. International Journal of Climatology, 31(13), 1975-1989.

United States Geological Survey (USGS). 2016. USGS 04233300 Fall Creek Near Ithaca NY. Available Online: http://waterdata.usgs.gov/usa/nwis/uv?site_no=04234000

Viglione, A., Merz, R., Salinas, J. L., & Blöschl, G. (2013). Flood frequency hydrology: 3. A Bayesian analysis. Water Resources Research, 49(2), 675-692.

Villarini, G., & Smith, J. A. (2010). Flood peak distributions for the eastern United States. Water Resources Research, 46(6).

Vittal, H., Singh, J., Kumar, P., & Karmakar, S. (2015). A framework for multivariate data-based at-site flood frequency analysis: Essentiality of the conjugal

application of parametric and nonparametric approaches. Journal of Hydrology, 525, 658-675.

Wachinger, G., Renn, O., Begg, C., & Kuhlicke, C. (2013). The risk perception paradox—implications for governance and communication of natural hazards. Risk analysis, 33(6), 1049-1065.

Walter, M. T., Brooks, E. S., McCool, D. K., King, L. G., Molnau, M., & Boll, J. (2005). Process-based snowmelt modeling: does it require more input data than temperature-index modeling?. Journal of Hydrology, 300(1), 65-75.

White, I., Kingston, R., & Barker, A. (2010). Participatory geographic information systems and public engagement within flood risk management. Journal of Flood Risk Management, 3(4), 337-346.

Winsemius, H. C., Van Beek, L. P. H., Jongman, B., Ward, P. J., & Bouwman, A. (2013). A framework for global river flood risk assessments. Hydrology and Earth System Sciences, 17(5), 1871-1892.

Wuebbles, D., Meehl, G., Hayhoe, K., Karl, T. R., Kunkel, K., Santer, B., ... & Goodman, A. (2014). CMIP5 climate model analyses: climate extremes in the United States. Bulletin of the American Meteorological Society, 95(4), 571-583.

Yan, H., & Moradkhani, H. (2016). Toward more robust extreme flood prediction by Bayesian hierarchical and multimodeling. Natural Hazards, 81(1), 203-225.

Yan, H., & Moradkhani, H. (2015). A regional Bayesian hierarchical model for flood frequency analysis. Stochastic Environmental Research and Risk Assessment, 29(3), 1019-1036.

CONCLUSIONS

The utilization of mechanistic hydrologic models allows for evaluation land surface responses to future climate conditions, projections of which are often highly uncertain. The research presented in this dissertation outlines methods which can be extended further study both the physical changes to ecohydrologic systems and to evaluate the utility of current generation hydrologic models for answering such questions.

Within this dissertation I have described several challenges in the utilization of synthetically generated precipitation datasets, as both 1) local stochastic weather generation and 2) BCSD downscaled global GCM estimates. Future studies of land surface responses to climate change would directly benefit from improvements in future weather forecasts. I intend to apply similar methods to those presented in these chapters to refine predictions of regional precipitation extremes relevant for the study of land surface responses under a changing climate. As was demonstrated in Chapter 3, BCSD downscaled current generation GCMs provide relatively poor estimates of future precipitation extremes, limiting their utility for the study of discharge extremes. However, these GCMs provide relatively reliable estimates of synoptic-scale climate variables (surface air temperatures, geopotential height fields, integrated vapor transport [IVT]) and the structure of some synoptic-scale weather systems, though potentially with some regional heterogeneity. Recent studies have demonstrated the viability of relating synoptic-scale climate patterns to local weather as an alternative methodology for downscaling. These approaches avoid some of the issues of climate transferability in the explicit consideration of future changes to the frequency of synoptic-scale climate states. I intend to extend my research into the development of new methods of predicting precipitation extremes under a changing climate.

Estimates of eastern USA forest composition response to climate change are similarly uncertain, but possibly less controversial though they have received limited attention in flood frequency analysis. Trees exert a fundamental control on the hydrologic cycle through soil shading, canopy interception and storage, root water uptake of soil and groundwater, partitioning of latent heat losses between evaporation and transpiration, and root modification of soil pore size distributions. Researchers have long considered active forest management as a path towards controlling the distribution of catchment water, yet the viability of forest conservation practices as a means of flood management has been questioned. Research has suggested that the influence of forest cover on flooding frequency may be better estimated with methodologies that isolate the physical mechanisms by which land cover partitions infiltration and surface runoff. Hydrological land surface model development for prediction of hydrologic extremes typically maintains a strong focus on infiltration mechanisms with less emphasis on capturing the complexity of plant dynamics, often neglecting to properly represent the functional traits that govern plant hydraulic regulation. I intend to perform a regional exploration of plant hydraulic regulation by root water uptake and canopy interception in the Northeast US within a popular catchment-scale hydrologic modeling framework to understand the importance of these potentially neglected ecohydrologic processes.

This proposed research faces several challenges in the form of data limitation, and uncertain hydrologic model structures. I intend to use emerging measurement techniques involving stable water isotopes to track root hydraulic regulation through the shallow soils. I intend to objectively estimate the value of isotopic measurements for understanding RWU with the ech2o-iso model, developed the track water fluxes and isotopic exchanges at the catchment scale. I will determine if the additional information provided by plant stem water isotopes is useful, given the additional

model complexity (i.e. tree storage dynamics) required to incorporate these measurements in a formal model calibration.

I intend to merge the concepts described above to study the joint effects of shifting atmospheric forcing and plant species succession at the continental scale. Hydraulic regulation of evapotranspiration (ET) is perhaps a dominant control on catchment ET, yet current generation hydrologic and land surface models (LSM) do not resolve this physical process. I intend to modify several popular LSMs to include plant hydraulic regulation. I then intend to study the spatial similarities in the native ranges of tree species and the ranges of extreme seasonal precipitation to better understand where reforestation may provide a viable means of flood risk mitigation.